MAY. - AUG. 1997
Volume III Number II

ISSN 0859 144X

THE ASEAN JOURNAL OF RADIOLOGY

Published by The Radiological Society and
The Royal College of Radiologists of Thailand,
Bangkok, Thailand

Supported through an educational grant from

MAY. - AUG. 1997
Volume III Number II

ISSN 0859 144X

THE ASEAN JOURNAL OF RADIOLOGY

Published by The Radiological Society and
The Royal College of Radiologists of Thailand,
Bangkok, Thailand

Supported through an educational grant from

BRACCO
INTERNATIONAL

ASDIR

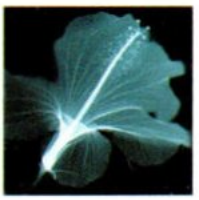

EDUCATION

Asian-Oceanian Seminars on Diagnostic and Interventional Radiology

1 9 9 7

Imaging and Interventional Radiology of the Hepatobiliary System
February 19-21
Khon Kaen, Thailand
Programme Leader:
B. Sitisara

Urogenital Imaging
April 25-27
Bombay, India
Programme Leader:
R. Sukthankar

Radiology of Cerebrovascular Disease, including interventional neuroradiology
October 23-24
Melbourne, Australia
Programme Leader:
B. Tress

Chest Radiology
November 1-2
Kuala Lumpur, Malaysia
Programme Leader:
Joginder Singh

BRACCO
INTERNATIONAL

For further information please contact:
Bracco International B.V.
47 Hill Street
S.C.C.C.I. Building
#06-05 Singapore 179365
Tel: ++65-337 1880
Fax: ++65- 337 7576

1. The AAR Journal of Radiology publishes the papers on Radiological Sciences, such as research work, review articles, case reports, innovations in Medical Sciences related to all branches of Radiology, and letters to the editor. The aforementioned materials can be written in English only.

2. The authors have to submit 2 copies of the manuscript and a diskette: **to Prof. Dr. Kawee Tungsubutra,** 318 Kaweevej Hospital, Tarksin Road, Dhonburi, Bangkok 10600, Thailand. **or to the Associate Editors** at the Radiological Society of Malaysia, Indonesia, Philippine, Singapore and Brunei. The names and adresses of the Associate Editors in each country were published in the front page of this Journal.

3. The original copy to be submitted must be typed in a double space on one side of the page of 8" x 11" paper.

4. The format of the article must include :
   a. Title page and address of the author (s)
   b. Abstract
   c. Introduction (Background)
   d. Material and Method
   e. Results and discussion (Tables and Illustrations)
   f. Acknowledgement (if any)
   g. References (Follow the Vancouver style developed by ICMJE)

5. We will provide 25 copies of reprints for the author (s) who submit (s) and article for publication in the AAR Journal.

6. The illustrations and tables must be clearly prepared with legends in English as they are the art works to be reproduced.

7. The authors are responsible for the contents of the article as to its facts and findings.

8. Ethics.

Paper reporting studies which might be interpreted as human experimentation (e.g. controlled trials) should conform to the standards of the Declaration of Helsinki (see British Medical Journal 1964:2:177) and should indicate that, approval that such studies may proceed, has been granted by the local or hospital Ethics Committee.

When reporting experiments on animals indicate whether the institution's or the National Research Council's guide for, or any national law on, the care and use of laboratory animals was followed.

THE ASEAN JOURNAL OF RADIOLOGY

Volume III Number II MAY-AUG. 1997

CONTENTS

THE ASEAN JOURNAL OF RADIOLOGY

Volume III Number II MAY-AUG. 1997

SPIRAL CT SCAN OF THE THYMIC CYST

Patchrin PEKANAN[1,2], Chirote SUCHATO[2], Vibul CHOTESKULRAT[3], Chingyium PANJAPIYAKUL[3], Charoen SUWANWILAI[4].

ABSTRACT

A case of uncomplicated thymic cyst was demonstrated by plain films and spiral CT scan. The patient was 58 years old, having chronic cough. Images of simple cyst at anterior mediastinum extending to left perihilar area were shown.

INTRODUCTION

Cystic lesions of the thymus gland are acquired lesions of thymic tissue that may be found anywhere along lines of the thymic descent, from the angle of the mandible to the body of the sternum. Thymic cysts are distinguished from other cysts by the presence of thymic tissue in their walls. These simple cysts are lined by epithelium that may be flattened, columnar, squamous, or ciliated and are filled with accumulated fluid, cellular debris and hemorrhagic extravasation. Leakage of these contents into the surrounding tissues may simulate infectious granulomatous inflammation. Although some may be developmental in origin and derived from the third branchial pouch, the origin of most thymic cysts-whether mediastinal or cervical in location-appears to be degenerating or enlargement of the Hassall's corpuscles. It is probable that most are derived from remnants of the fetal thymopharyngeal duct.[4,15,16] An unusual intrathoracic thymic cyst that has been described in a 2 year old girl contained not only thymic tissue in its walls but also parathyroid and salivary gland tissue, all tissues of pharyngeal origin. Thymic cysts are uncommon mediastinal lesions that account for only 1 to 2 per cent of all tumors in the anterior compartment.[1-3] The apparent association of some cysts with infection (e.g. syphilis or tuberculosis), neoplasms, radiation therapy and trauma suggest that local disruption of thymic tissue can induce the formation or growth of the cysts.[5]

CASE REPORT

A 58-year old male patient, presented with chronic cough and syncope attack. Routine chest films for the insurance showed a lobulated left perihilar anterior mediastinal mass (Fig.1). The patient has no systemic abnormal physical examination. Spiral CT scan of the thorax was performed. It showed a well defined border cystic mass (H.U. 4.4-25.4) at anterior mediastinum, extending from midline area to paramedian and left perihilar region. The mass showed no increased enhancement. The surrounding structures were not invaded. There was no enlarged intrathoracic nodes (Fig. 2). The thoracoscopic thymectomy was performed. A large cystic mass was seen in left lobe of the thymus gland by surgery and pathology.

[1] Department of Radiology, Ramathibodi Hospital, Rama 6 Street, BKK 10400, Thailand.
[2] Department of Radiology, Samitivej Hospital.
[3] Department of Surgery, Samitivej Hospital.
[4] Department of Pathology, Samitivej Hospital.

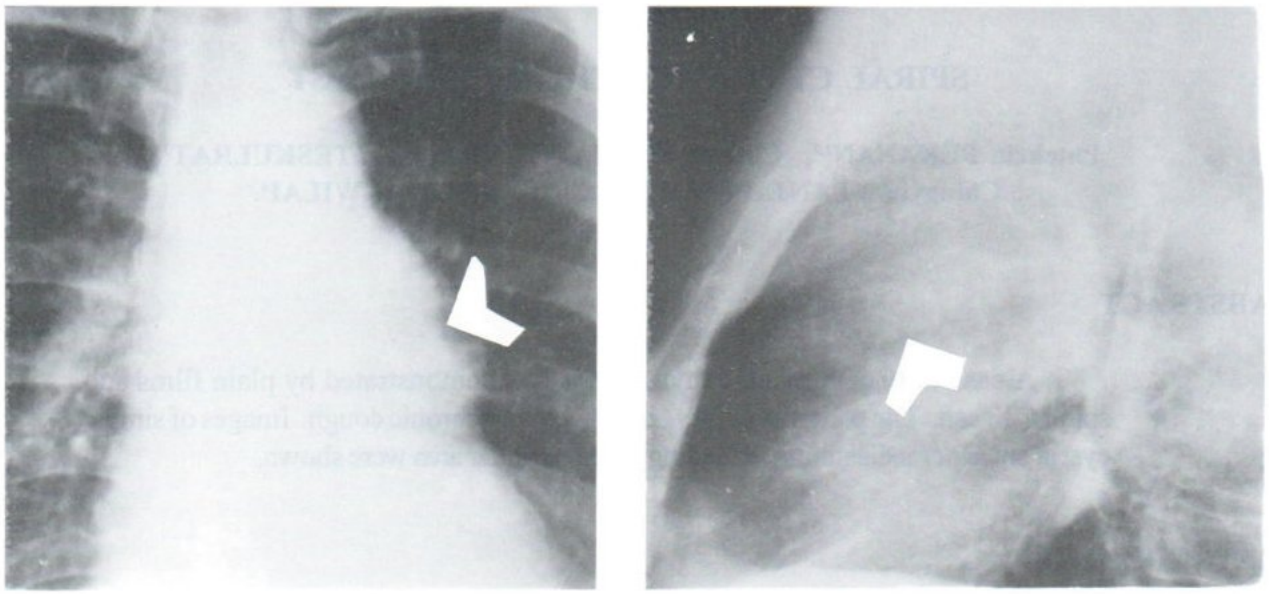

Fig. 1. PA and left lateral chest films showed a lobulated mass at left perihilar area, obscuring the left heart border and in lateral view, the soft tissue density filled the usually radiolucent anterior mediastinal region, indicating that the soft tissue mass was at the left anterior mediastinum.

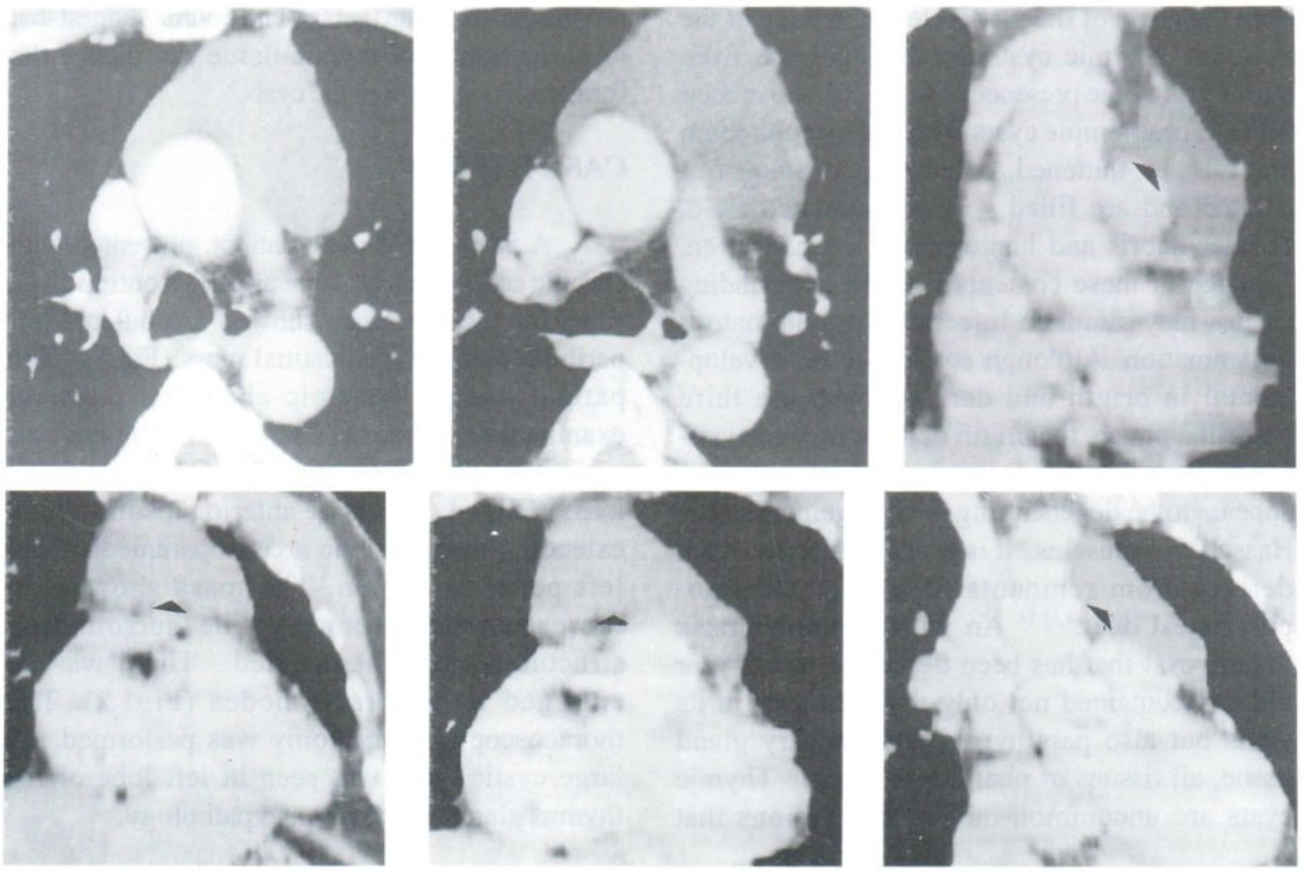

Fig.2. Axial, coronal and oblique coronal and oblique sagittal views spiral CT scan of the thymic cyst showed a sharply well defined border cystic lesion at the anterior mediastinum, extending to the left perihilar area without invasion of the nearby structures.

DISCUSSION

Pathologically, the thymic cysts are unilocular or multilocular and range in size from microscopic to 18 cm in maximun diameter.[1,4] They can contain straw-colored fluid or, if hemorrhage has occurred, brown-green gelatinous or grumous material. Histologically, the cyst wall is lined by squamous, transitional, or simple cuboidal or columnar epithelium; ulceration with underlying fibrosis and chronic inflammation is fairly common as is evidence of remote hemorrhage (hemosiderin-laden macrophages and cholesterol clefts). Thymic tissue can be identified focally in the cyst wall and its presence is necessary to make the diagnosis.

An important point in the pathologic differential diagnois is the observation that some malignant tumors, particularly thymoma, Hodgkin's disease, and seminoma, can show prominent cystic change, occasionally associated with neoplastic tissue that is relatively small in amount; consequently thorough sampling of every "thymic cyst" must be carried out to exclude the possibility of neoplasia, especially if the "cyst" wall is thickened by fibrous tissue. In addition to such degenerative changes in a primary neoplasm, it has been suggested that Hodgkon's disease can occasionally develop in the wall of a true thymic cyst.[1,6] Although rare, carcinoma also has been reported to arise from cyst epithelium.[7]

The appearance of the thymic cysts on conventional roentgenograms is no way characteristic or diagnostic[1,2,3] although their cystic nature should be readily apparent on CT or MR images. Most patients are asymptomatic. In one patient, obstruction of the pulmonary artery by the cyst resulted in chest pain, dyspnea, and a systolic thrill and murmur on physical examination; the patient was originally misdiagnosed as having stenosis of the pulmonary valve.[1,8]

The patient with a thymic cyst may be symptom-free and a routine chest radiograph may reveal a mass in the anterior mediastinum. When symptoms do occur, they are probably related to hemorrhage into the cyst leading to increase in size and pressure on adjacent structures. The most frequent symptoms are pain or fullness in the chest and dyspnea, which may be more severe when the patient is supine. Other less frequent symptoms are dysphagia, choking, non-productive cough, weight loss and tachypnea. Thymic cysts may also present with acute cardiorespiratory distress,[9] Horner's syndrome,[10] vocal cord paralysis,[11] loculated pneumomediastinum,[12] simulation of cardiomegaly with haemodynamic abnormalities.[13]

CT shows the cysts to be rounded and fluid-filled. These cysts may undergo hemorrhage or calcification. The CT density of these cysts is usually near that of water, it can be confused with solid masses because of the hemorrhagic or proteinaceous content.[5,14]

Cystic lesions of other derivations arising in the thymus or in the same locations as thymic cysts include developmental cysts of the respiratory, gastrointestinal, pericardial and lymphatic systems.[15,16]

REFERENCES

1. Fraser, Pare, Pare, Fraser, Genereux. Diagnosis of diseases of the chest. 3rd ed. Philadelphia: W.B. Saunders Company, 1991:1820.
2. McCafferty MH, Bahnson HT. Thymiccyst extending into the pericardium: A case report and review of thymic cysts. Ann Thorac Surg 1982;33:503
3. Indeglia RA, Shea MA, Grage TB. Congenital cysts of the thymus gland. Arch Surg 1967;94:149.
4. Bieger RC, McAdams AJ. Thymic cysts. Arch Pathol 1966;82:535
5. Jaramillo D, Perez-Atayde A, Griscom NT. Apparent association between thymic cysts and prior thoracotomy. Radiology 1989;172:207.

6. Smith PLC, Jobling C, Rees A. Hodgkin's disease in a large thymic cyst in a child. Thorax 1983;38:392.
7. Leong AS-Y, Brown JH. Malignant transformation in a thymic cyst. Am J Surg Pathol 1984;8:471.
8. Soorae AS, Stevenson HM. Cystic thymoma simulating pulmonary stenosis. Br. H Dis Chest 1980;74:193.
9. Greipp PR, Gay GT, Dockerty MB, Westbrook P, Pluth JR. Thymic cyst presenting as an acute mediastinal mass. Chest 1973;64:125.
10. Sarma OA. Horner's syndrome due to intrathoracic thymic cyst. J Ind Med Ass 1974;-63:98.
11. Bailey LL, Hilde RL, Smith TR, Thompson RJ. Cervico-mediastinal thymic cyst with vocal cord paralysis. Cancer 1977;39:347.
12. Raila FA, McKerchar B. Thymic cysts simulating loculated pneumomediastinum in the newborn. Br J Radiol 1977;50:286.
13. Schluger J, Scarpa WJ, Rosenblum DJ, Pinck RL, Giustra FX. Thymic cyst simulating massive cardiomegaly : Report of a case and review of the literature. Dis Chest 1968;53:365.
14. Baron RL, Sagel SS, Baglan RJ. Thymic cysts following radiation therapy for Hodgkin disease. Radiology 1981;141:593-597.
15. Breckler IA, Johnston DG. Choristoma of the thymus. Am J Dis Child 1956;92:175.
16. Kissane JM. Anderson's Pathology. 8th ed. St. Louis: C.V. Mosby Company,1985:1381.

CERVICAL CORD COMPRESSION IN A PATIENT WITH FLUOROSIS

Patchrin PEKANAN, Sashilekha BALACHANDRA, Kamolporn LIMCHAOVALIT, Chompoonuch VIJITSANGUAN, Chanika SRITARA.

ABSTRACT

A 61 year-old male patient from Chiangrai province (northern part of Thailand) who presented with cervical cord compression. Bone survey, CT and MR scan shows diffuse sclerosis of the vertebrae, ribs, and pelvic bones. Calcified ligaments at multiple sites are shown and ossified posterior longitudinal ligament as the cause of the cervical cord compression. Though the fluorine level in the blood of the patient was normal at the admission time, fluorosis is obvious by images.

INTRODUCTION

Fluorosis or chronic fluorine intoxication arises when the drinking water contains fluoride in concentrations higher than 4 parts per million (ppm).[1,2] It occurs as an endemic problem in certain regions of the world; in Thailand the patients usually come from the northern part. It was first described in the 1930's and sporadically in almost a worldwide distribution.[1,3] Industrial workers who are exposed to fluorine compounds over a period of years,[4] laboratory personnel who have inhaled fluorine vapors, patients who received medications containing high doses of fluorine [5] and individuals who habitually drink fluorine-containing wine [6] also developed this entity. Fluoride concentration in 1 ppm can reduce dental caries, in 2 ppm or more can lead to mottled enamel, 8 ppm can produce osteosclerosis in 10 per cent of individuals and greater than 100 ppm may induce growth disturbances, kidney damage, or death.[7]

Approximately 50 per cent of the absorbed fluoride is excreted mainly in the urine and approximately 99 per cent of the fluoride retained in the body is deposited in the calcified tissue.[8] The biologic half-life for bone fluoride is about 8 years, owing to the slow rate of turnover of skeletal tissues. With cessation of the exposure to fluoride and with continued, although slow, metabolism of bone tissue, excretion of fluoride can lead to an improvement in the pulmonary and skeletal manifestations of the disease. Radiographic improvement has been documented.[9]

Cervical cord compression could occur in this disease due to ossified / calcified posterior longitudinal ligament.

CASES REPORT

A 61-year-old man from Chiangrai province, developed progressive weakness of all extremities for 4 months. Physical examination was compatible with C6-7 cord compression. The patient consumed drinking water from a well and regulary chew the tea leaves. The urine fluoride was within normal limit. Renal function was mildly impaired.

Plain films of the bones showed diffuse

Department of Radiology, Ramathibodi Hospital, Rama 6 Street, Bangkok 10400, Thailand.

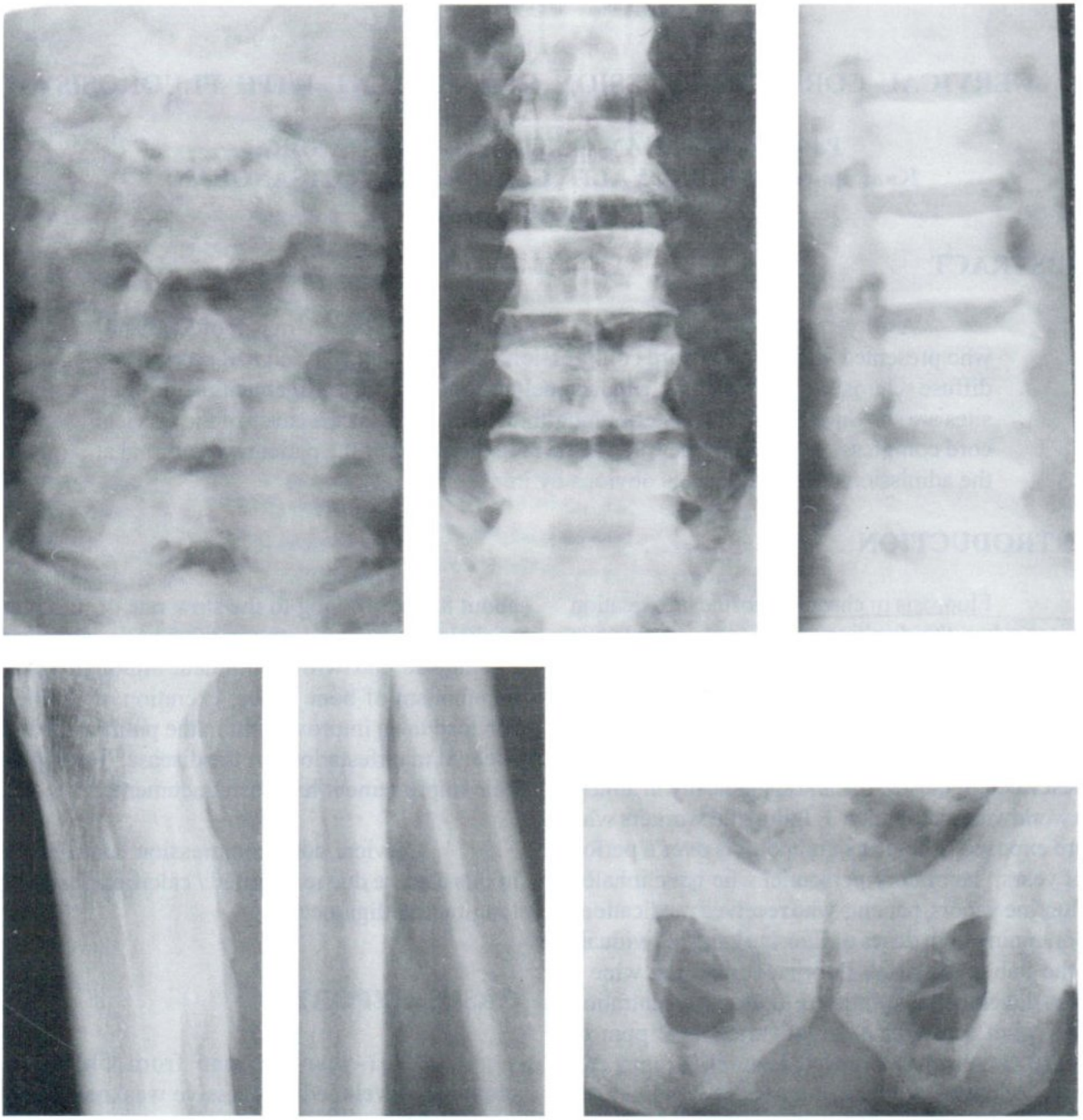

Fig. 1 Radiographic images of axial skeleton, ribs and pelvic bones and limbs which showed diffuse osteosclerosis, osteophytosis, periostitis and ligamental calcification.

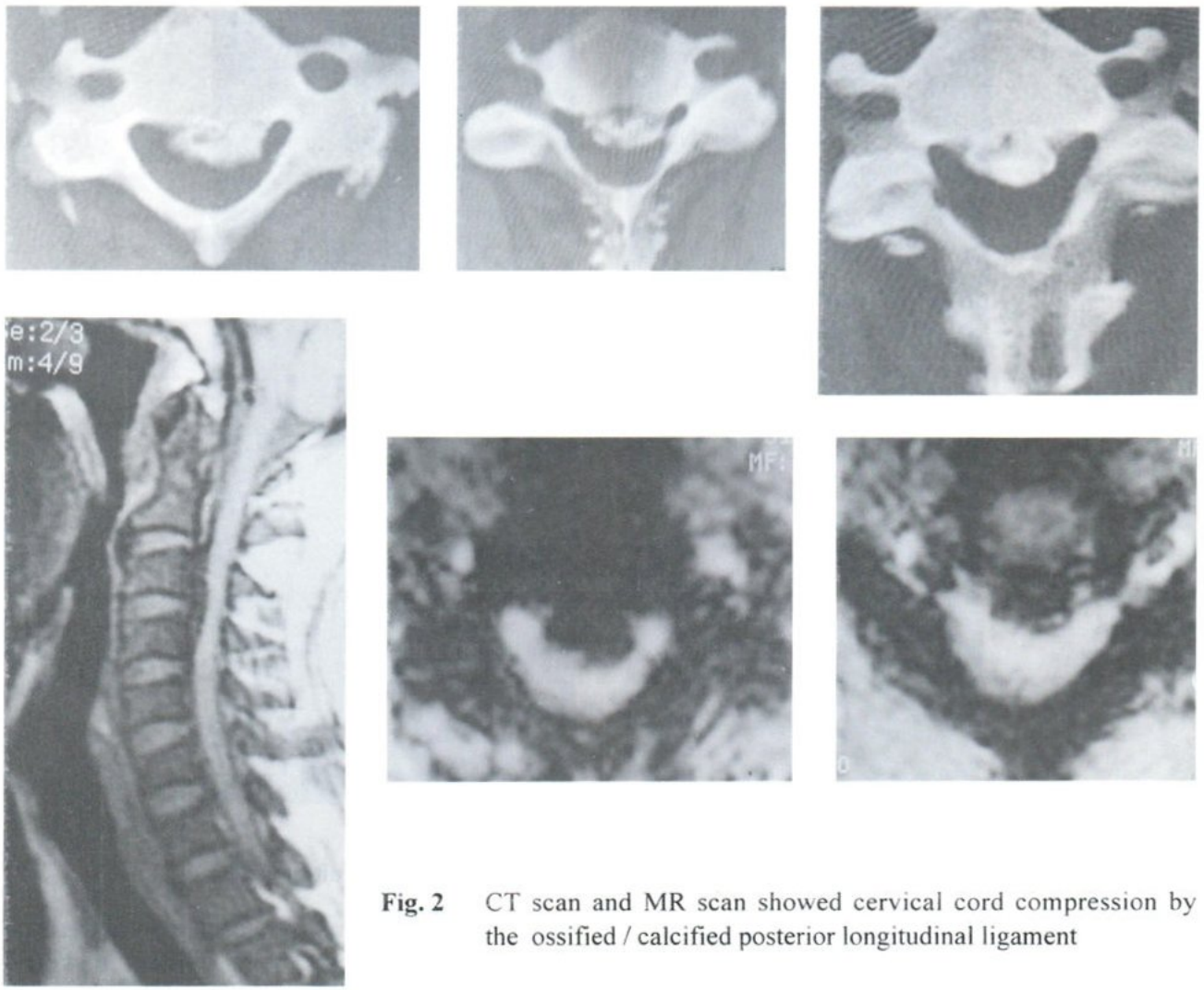

Fig. 2 CT scan and MR scan showed cervical cord compression by the ossified / calcified posterior longitudinal ligament

osteosclerosis of the axial skeleton, ribs and pelvic bones, vertebral osteophytosis, periostitis and multiple sites of ligamentous calcification (Fig.1). CT scan and MRI study showed ossified or calcified posterior longitudinal ligament with cord compression at C2-4 (Fig.2). Corpectomy of C3-4 and was performed. The 99m Tc-MDP bone scan revealed increased uptake along the axial skeleton, both shoulders, ribs and pelvic bones, left tip of the calcaneous indicating increased bone formation (Fig.3).

DISCUSSION

Clinical manifestations of chronic fluoride exposure include joint pain and restriction of motion, back stiffness, restriction of respiratory movements, functional dyspnea, dental alterations, paraplegia, and palpable thickening of the bones, including the clavicle, tibia and ulna.[8] Involvement of the axial skeleton is characteristic. Changes are most marked in the spine, the pelvis, and the ribs. Osteosclerosis usually appears first. Increasing trabecular condensation eventually creates a radiodense or chalky appearance throughout the thorax, vertebral column, and pelvis with obscuration of bony architecture. The skull and tubular bones of the appendicular skeleton are relatively spared in this sclerotic process.[1]

Vertebral osteophytosis can lead to encroachment on the spinal canal and intervertebral foramina. In the axial skeleton, hyperostosis and

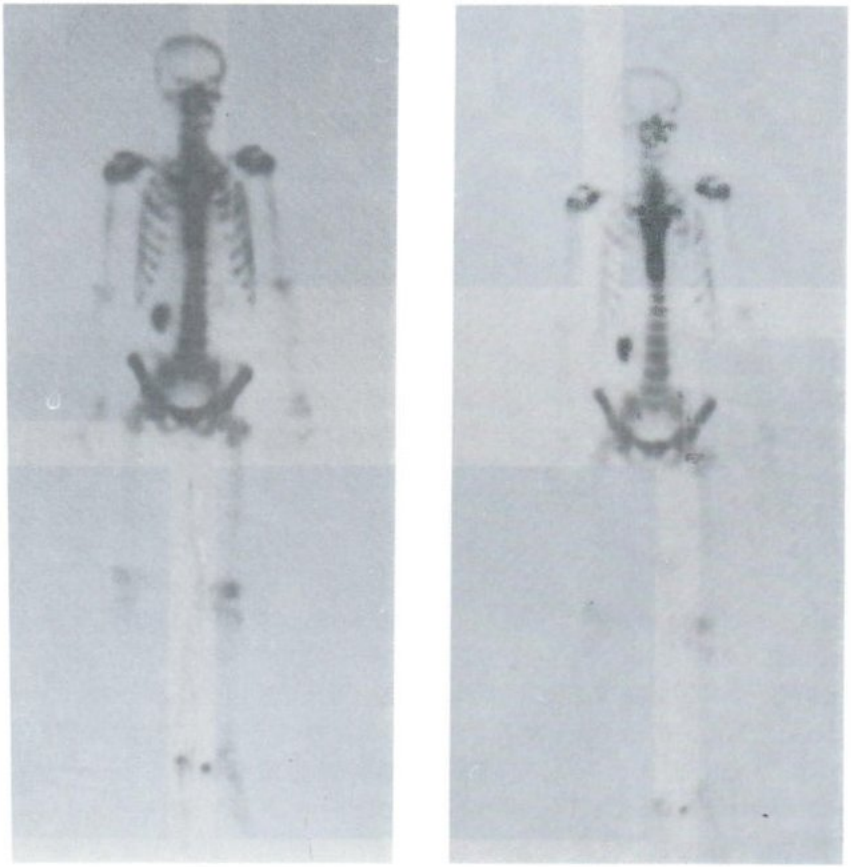

Fig. 3 Bone scintigraphy revealed increased uptake at multiple sites.

bony excrescences develop at sites of ligamentous attachment, especially in the iliac crests, ischial tuberosities, an inferior margins of the ribs. Calcification of paraspinal ligaments as well as sacrotuberous and iliolumbar ligaments can be noted.

In the appendicular skeleton, periosteal thickening, calcification of ligaments, and excrescences at ligamentous and muscular attachments to bone can be seen at one or more sites, particularly near the interosseous membranes of the forearm and leg, the calcaneus, the posterior surface of the femur, the tibial tuberosity and the proximal humerus. Soft tissue ossification resembling myositis ossificans and cartilaginous atrophy and ulceration have been noted .[11]

Osteosclerosis, osteophytosis, and ligamentous calcification represent a useful triad of abnormalities that are evident on pelvis and spine roentgenograms. Osteosclerosis alone is not diagnostic of fluorosis, being evident in skeletal metastasis, myelofibrosis, mastocytosis, certain hemoglobinopathies, renal osteodystrophy, Paget's disease, congenital disor-ders and other conditions. Likewise, vertebral osteo-phytosis or similar outgrowths can accompany many diseases, including fluorosis, spondylosis deformans, diffuse idiopathic skeletal hyperostosis, ankylo-sing spondylitis, the spondylitis of psoriasis, Reiter's syndrome, and inflammatory bowel disorders, acromegaly, neuroarthropathy, and alkaptonuria.[1] Proliferative changes at ligamen-tous and tendinous insertions in bones are apparent not only in fluorosis but also in diffuse idiopathic skeletal hyperostosis, hypoparathyroidism, X-linked hypophosphatemic osteomalacia and certain plasma cell dyscrasias. Periostitis similar to that which may be seen in fluorosis can be detected in hypertrophic osteoarthropathy,

pachydermoperiostosis, and thyroid acropathy. Thus, each individual radiographic finding of skeletal fluorosis can be apparent in other disorders as well: it is the combination of findings in fluorosis that is diagnostic.[1]

Ossification of the posterior longitudinal ligament (OPLL) is a dense, ossified strip or plaque of variable thickness along the posterior margins of the vertebral bodies and intervertebral disks.[12] It is most common in the midcervical (C3-5) and the midthoracic (T4-T7) spine. Multilevel involvement is characteristic. On NCE CT scans, the ossified strip that characterizes OPLL is typically separated from the vertebral body by a thin radiolucent zone. Sagittal T1- or proton-density weighted MR scans show increased signal intensity from the fatty marrow of thickly ossified lesions; axial imaging is necessary to demonstrate thinly ossified OPLL.[13] The differential diagnosis of OPLL includes calcified HNP and calcified meningioma, although the shape and multilevel involvement of OPLL are characteristic. Calcified/ ossified OPLL in this case was a part of disease process of fluorosis.

REFERENCE

1. Resnick & Niwayama. Diagnosis of bone and joint disorders. 2nd ed. Philadelphia: W.B. Saunders Company, 1988:3068-78.
2. Singh A, Jolly SS. Endemic fluorosis. Q J Med 1961;30:357.
3. Shortt HE, McRobert GR, Barnard TW, Nayar ASM. Endemic fluorosis in the Madras residency. Ind J Med Res 1937;25-553.
4. Boillat MA, Carcia J, Velebit L. Radiological criteria of industrial fluorosis. Skel Radiol 1950;5:161.
5. Meunier PJ, Courpron P, Smoller JS, Briancon D. Niflumic acid-induced skeletal fluorosis: Iatrogenic disease of therapeutic perspective for osteoporosis? Clin Orthop Rel Res 1980;148:304.
6. Soriano M. Periostitis deformans (un nuevo tipo de fluorosis osea en el hombre) la fluorosis vinica. Rev Clin Esp 1965;97:375.
7. Smith FA, Hodge HC. Fluoride toxicity. In JC Muhler, MK Hine (Eds). Fluorine and Dental Health. Bloomington, Indiana University Press,1959.
8. Grandjean P. Ocupational fluorosis through 50 year:Clinical and epidemiological experiences. Am J Industr Med 1982;3:227.
9. Grandjean P, Thomsen G. Reversability of skeletal fluorosis. Br J Indust Med 1983; 40:456.
10. Singh A, Jolly SS, Bansal BC, Mathur CC. Endemic fluorosis. Epidemiological, clinical and biochemical study of chronic fluorine intoxication in Panjab (India). Medicine 1963;42:229.
11. Soriano M, Manchon F. Radiological aspects of a new type of bone fluorosis, periostitis deformans. Radiology 1966;87:1089.
12. Resnick D. Degenerative diseases of the vertebral column. Radiol 1985;156: 3-14.
13. Otake S, Matsuo M, Nishizawa S, et al. Ossification of the posterior longitudinal ligament: MR evaluation. AJNR 992;13: 1059-67.

NCE CT = Non-contrast enhancement CT.
HNP = Herniated Nucleus Pulposus.

SIRENOMELIA

Rutchanee SINSAWATJAREON[1], Patchrin PEKANAN[1], Yaowalak BOONPASART[2], Satit HOTRAKIT[3], Vasana PONGJAPOE[2], Banchuen BENJASUWANTHEP[3].

ABSTRACT

A case of sirenomelia was presented in a new born with perinatal death. The fetus had abnormal appearance of the head and face, single lower extremity, enlarged ears, small eyes and flattened nose. The external genitalia and anus was absent. The lungs were hypoplastic; the kidneys were agenetic. There was a single umbilical artery. A blind pouch was noted at the sigmoid colon and imperforate anus was present. The genitalia was absent; the tubes and fimbria was noted and the uterus could not be well identified. Babygram revealed malformed ischium and pubic bones. Asymmetric femurs, single tibia, and single fibula was noted.

INTRODUCTION

Sirenomelia or the mermaid syndrome of lower extremity fusion or sympus apus, is a severe manifestation of the caudal regression syndrome and has a reported incidence of about 1 in 60,000.[1,2] Sirenomelia is uniformly fatal due to its association with other major anomalies including (a) rotation and fusion of the lower limb; medial position, fusion, or absence of the fibulas; (b) pelvic bone anomalies; (c) renal agenesis; (d) absence of an anus and external genitalia, blind - ending colon; (e) oligohydramnios; (f) single umbilical artery; (g) vascular steal has been proposed as the pathogenic mechanism producing sirenomelia and associate visceral and soft tissue defects.[3]

CASE REPORT

The patient was a product of term pregnancy with unremarkable antenatal period. It was delivered by Caesarian section due to breech presentation and fetal distress. Perinatal death was encountered. At physical examination, the fetus had abnormal appearance of the head and Potter's facies, central cyanosis and a single lower extremity. The ears were enlarged, the eyes were smaller and the nose was flattened. The chest and abdomen appeared normal. There was no external genitalia, nor anus. The hip joints were constantly flexed and knees were extended. Varus deformity of both feet was observed. At autopsy, the lungs were hypoplastic; both kidneys were agenetic. There was a single umbilical artery. A blind pouch was noted at the sigmoid colon and imperforate anus was present. The genitalia was absent; the tubes and fimbria were noted and the uterus was not well identified. The appearance of the fetus was shown on figure 1. Roentgenography was performed shortly after death (Fig. 2).

DISCUSSION

Caudal regression syndrome (CRS) was termed by Duhamel[4] as a spectrum of congenital

[1]Department of Radiology, Ramathibodi Hospital, Rama 6 Street, Bangkok 10400, Thailand.
[2]Department of Pathology, Ramathibodi Hospital.
[3]Department of Pediatrics, Ramathobodi Hospital.

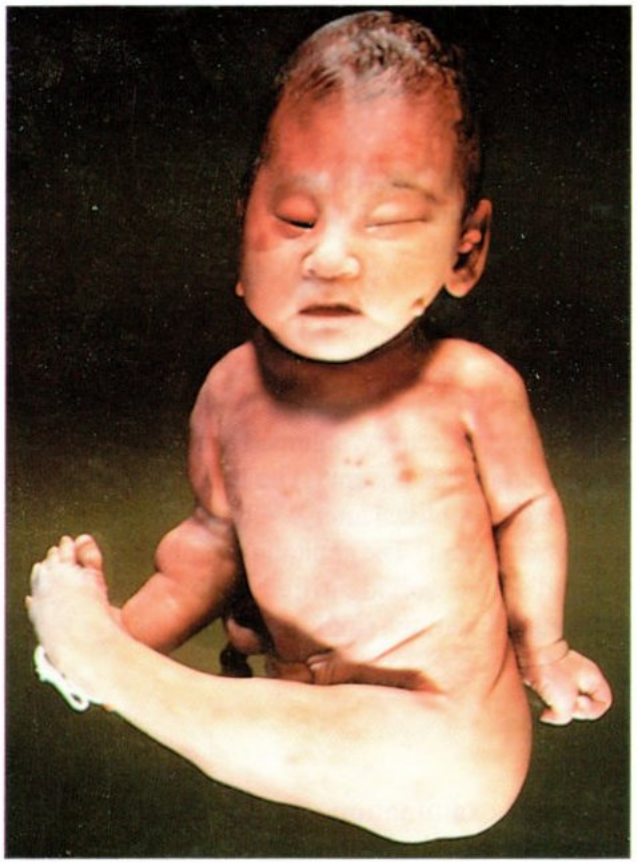

1 (a)

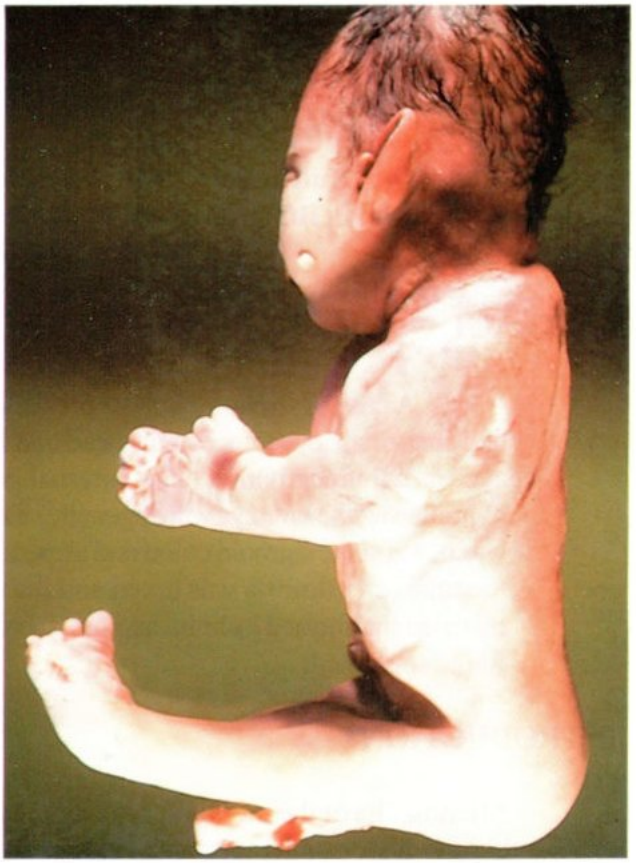

1 (a)

Fig. 1 (a). general appearance of the whole fetus
(b). facial and cranial part

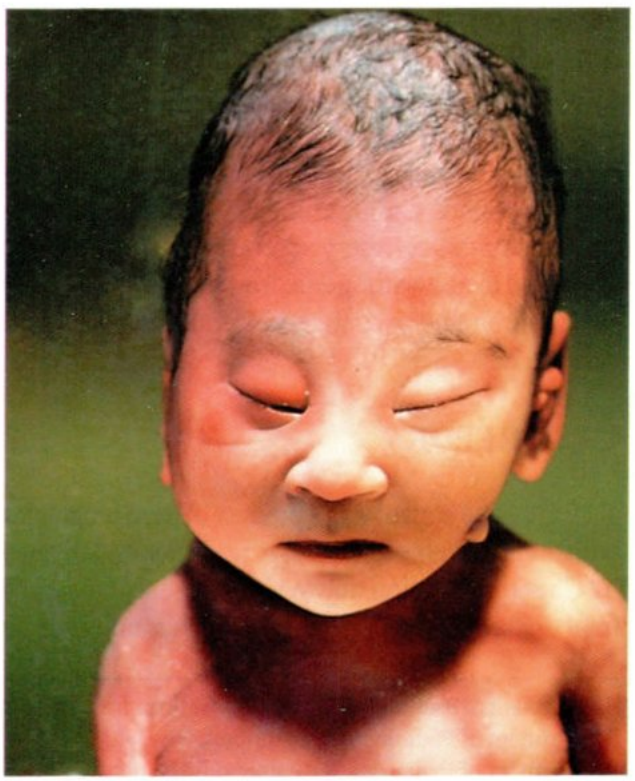

1 (b)

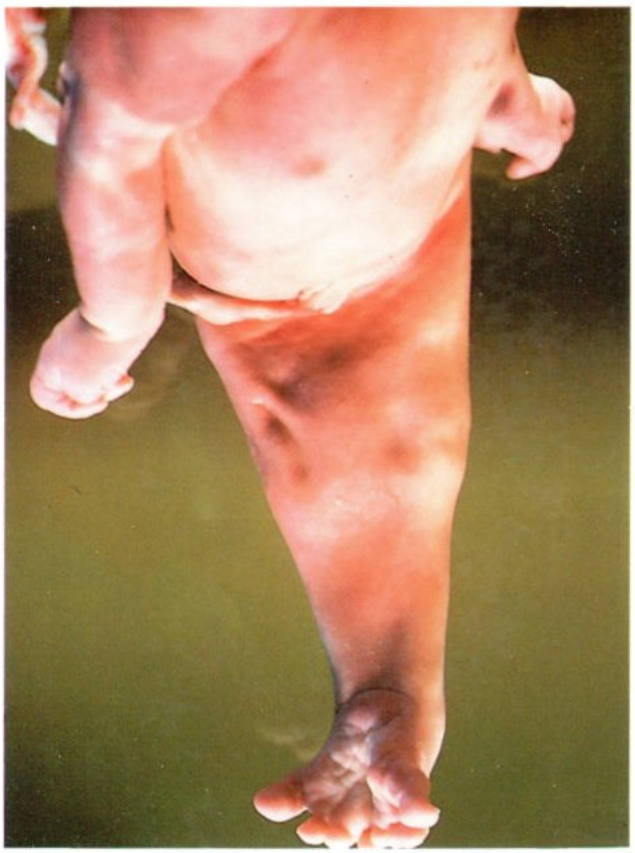

1 (c)

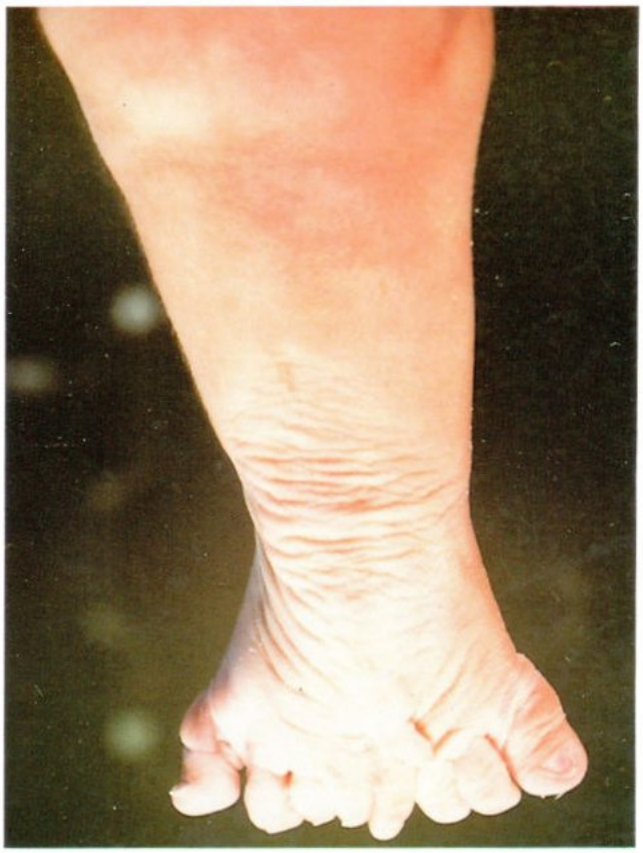

1 (d)

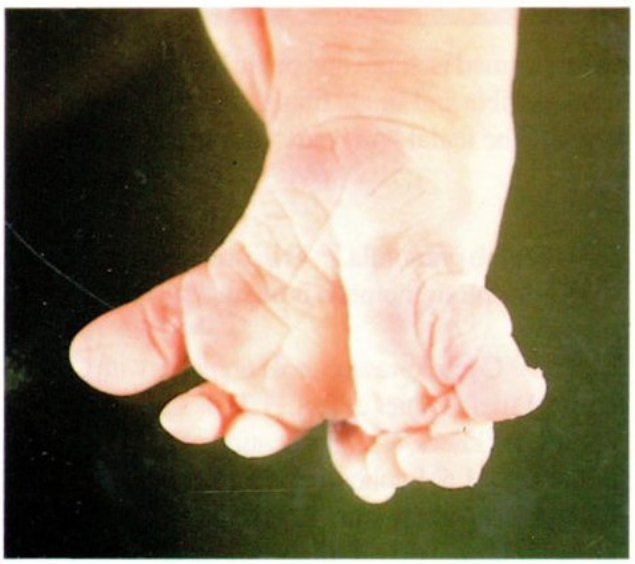

1 (e)

Fig. 1 (c). trunk and lower extremity
(d). lower limb
(e). feet

malformations ranging from simple anal atresia, to absence of the sacrum, lumbar and lower thoracic vertebrae (caudal aplasia/dysgenesia), to the most severe form with fusion of the lower extremities and major visceral malformations known as sirenomelia.[5]

The embryologic insult occurs at the mid-posterior axis mesoderm and/or caudal blastema,[5] but the etiology remains unclear. Factors influencing caudal vertebral development operate before 4 weeks of gestation.[7] Association between maternal diabetes mellitus and CRS was described.[8-11] Although a wide spectrum of vertebral and limb malformations similar to caudal regression were produced in animal models by different teratogens, the only agents associated with this syndrome in humans included organic fat solvents and the appetite suppressant diethylpropion.[12-16] CRS may result from the combination of maternal diabetes and a genetic predisposition.[17]

Vascular hypoperfusion is favored in the pathogenesis of the extreme form of CRS,

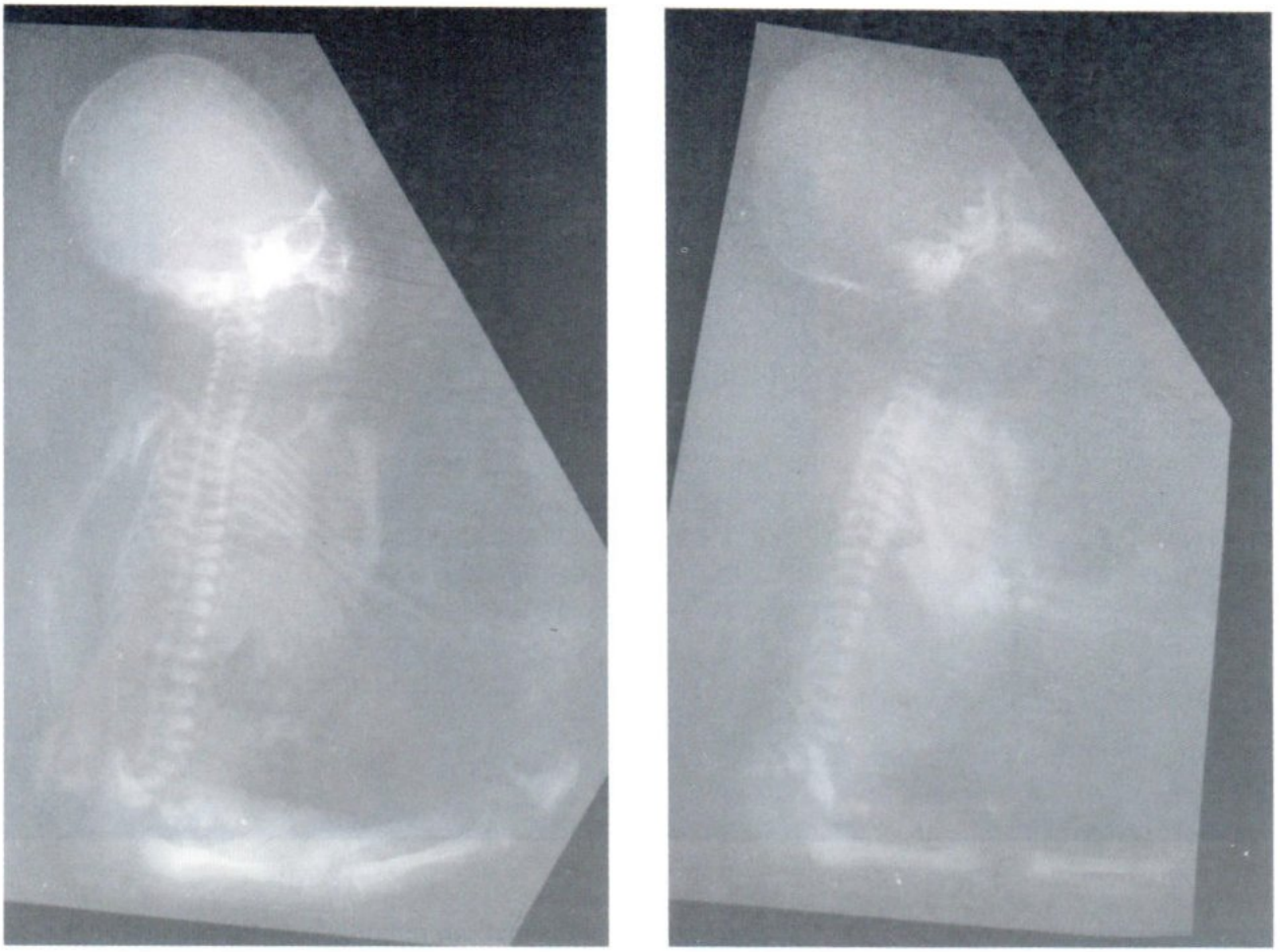

Fig. 2 Babygram immediate post perinatal death showed malformed ischium and pubic bones. Two femurs were noted and with asymmetric size. There were single tibia and single fibula. The bony parts of the feet was difficult to evaluate. The head was enlarged. The facial bony parts, the spinal column, the ribs and the upper extremities appeared normal.

sirenomelia.[18] The nutritional deficiency theory was proposed and supported based on the findings at dissection of the abdominal vasculature in cases of sirenomelia.[19,20] The vascular steal theory indicates that a single large artery assumes the function of the umbilical arteries and diverts blood flow from the caudal portion of the embryo to the placenta, producing nutritional deprivation and maldevelopment of the caudal structures. Examination of umbilical cords in 95 infants with sirenomelia revealed a single umbilical artery in all cases.[21]

The single lower extremity seen in sirenomelia results either from failure of cleavage of the lower limb bud [20] or from the posterior fusion of the hindlimb primordia. [22] The association of maternal diabetes with sirenomelia is much less pronounced .[21]

Common associated anomalies with CRS [23-26] are: (1.1) deformities of feet, (1.2) flexion contractures of hips and knees, (1.3) dislocation of hip, (1.4) pelvic deformity, (1.5) kyphoscoliosis, (1.6) absence of ribs; (2.1) anorectal atresia, (2.2) inguinal hernia, (2.3) abdominal wall defect, (2.4) malrotation of gut, (2.5) tracheoesophageal fistula, rectovaginal fistula, rectourethral fistula; (3.1) vesicoureteral reflux, (3.2) hydronephrosis, (3.3) fused kidneys, (3.4) renal agenesis, (3.5) ectopic ureters, (3.6) transposition of external genitalia, (3.7) mullerian duct agenesis; (4.1) neural tube defects, (4.2) congenital heart disease,

(4.3) midline facial cleft, (4.4) strabismus.

To correlate sonographic with pathologic findings, two distinct groups exist within the continum of CRS [27] Caudal regression would be diagnosed if there is lumbosacral agenesis of the spine, associating with normal amniotic fluid volume and a three-vessel umbilical cord. The diagnosis of sirenomelia was confirmed in the presence of oligohydramnios, bilateral renal agenesis, and lower extremities fusion and a two-vessel cord is usually seen. Amniofusion enables a more accurate sonographic evaluation of fetal anatomy in severe oligohydramnios.[28] MRI was said to be helpful in detecting anomaly with cases of oligohydramnios.[29] Lower extremity abnormalities in caudal aplasia range from hypoplasia to the complete fusion seen in sirenomelia. The persistent side by side relationship of fetal femurs, that does not change over time, during sonographic examination is suggestive of this abnormality.[5]

Obstetric management depends on gestational age at diagnosis, severity of the lesion, associated malformations, and parental wishes. The chromosomes in CRS are usually normal;[30] however, there are isolated reports of pericentric inversion.[31] Recurrence risk with a positive family history of the anomaly are about 3 to 5 per cent.

REFERENCE

1. Van Zalen-Sprock MM, Van Vugt JMG, Van der Harten JJ, Van Geun HP. Early second-trimester diagnosis of sirenomelia. Prenatal Diagnosis 1995;15:171-7.
2. Nyberg Da, Mahoney BS, Pretorius DH. Diagnostic ultrasound of fetal anomalies. Text and atlas. Chicago: Year book medical publishers 1989;187-190.
3. Taybi H, Lachman RS. Radiology of syndromes, metabolic disorders, and skeletal dysplasias. 3rd ed. Chicago: Year book medical publishers, inc 1990:301.
4. Duhamel B. From the mermaid to anal imperforation: The syndrome of caudal regression. Arch Dis Child 1961;36:152.
5. Adra A, Cordero D, Mjides A, Yasin S, Salman F, O'Sullivan MJ. Caudal regression syndrome: Etiopathogenesis, prenatal diagnosis, and perinatal management. Obstetrical and Gynecological Survey 1994;49:508-15.
6. Perrot LJ, Williamson S, Jimenez JF. The caudal regression syndrome in infants of diabetic mothers. Ann Clin Lab Sci 1987;17:211.
7. Betti RJ, Traisman HS,. Sirenomelia: A spectrum of related syndromes. Clin Pediatr 1971;238:10.
8. Pedersen LM, Tygstrup I, Pedersen J. Congenital malformations in newborn infants of diabetic women: Correlation with maternal diabetic complications. Lancet 1964;1:1124.
9. Rusnak SL, Driscoil SG. Congenital spinal anomalies in infants of diabetic mothers. Pediatrics 1965;36:989.
10. Passarge E, Lenz W. Syndrome of caudal regression in infants of diabetic mothers: Observation of further cases. Pediatrics 1966;37:672.
11. Gabbe SG. Congenital malformations in infants of diabetic mothers. Obstet Gynecol Surv 1977;125:32.
12. Abraham E. Sacral agenesis with associated anomalies (caudal regression syndrome). Clin Orthop 1979;145:168.
13. Ziva SS, Golding J, Drummond JC, et al. The relation of the fat-soluble factor to rickets growth in pigs. Biochem J 1921;427:15.
14. Baldwin WM. The action of ultra-violet rays upon the frog's egg. The artificial production of spina bifida. Anat Rec 1915;365-9.
15. Warkany J, Nelson RL, Schraffenberger E. Congenital malformations induced in rats by maternal nutritional deficiency. Malformations of the extremities. J Bone Joint Surg 1943;261:25.
16. Kucera J. Exposure to fat solvents. A possible cause of sacral agenesis in man. J Pediatr 1968;72:857.
17. Welch JP, Aterman K. The syndrome of caudal dysplasia: A review, including etiologic considerations and evidence of heterogeneity. Pediatr Pathol 1984;2:313.
18. Hoyme HE. The pathogenesis of sirenomelia: An editorial comment. Teratology 1988;38:485.

19. Kampmeier OF. On sireniform monsters, with a consideration of the causation and the predominance of the male sex among them. Anat Rec 1927;34:365.
20. Stevenson RE, Jones KL, Phelan MC, et al. Vascular steal: The pathogenetic mechanism producing sirenomelia and associated defects of the viscera and soft tissues. Pediatrics 1986;78:451.
21. Stocker JT, Heifetz FSA. Sirenomelia. Perspect Pediatr Pathol 1987;10:7
22. Davies J, Chazen E, Nance WE. Symmelia in one of monozygotic twins. Teratology 1971;4:367.
23. White RI, Klauber GT. Sacral agenesis. Analysis of 22 cases. Urology 1976;8:521.
24. Blumel J, Evans EB, Eggers GWN. Partial and complete agenesis or malformation of the sacrum with associated anomalies. J Bone Joint Surg 1959;41A:497.
25. Sparnon AL, Ahmed S. Urological anomalies in the caudal regression syndrome. Aug NZ J Surg 1984;54:365.
26. Sirtori M Ghidini A, Romero R, et al. Prenatal diagnosis of sirenomelia. J Ultrasound Med 1989;8:83.
27. Twickler D, Budorick N, Pretorius D, et al. Caudal regression versus sirenomelia: Sonographic clues. J Ultrasound Med 1993;12:323.
28. Quetal TA, Mejides AA, Salman FA, et al. Amnioinfusion: An aid in the ultrasonographic evaluation of severe oligohydramnios in pregnancy. Am J Obstet Gynecol 1992;167:333.
29. Savader SJ, Savader BL, Clark RA. Sirenomelia without Potter syndrome: MR characteristics. J Comput Assist Tomogr 1989;13:689.
30. Sarnat HB, Case ME, Graviss R. Sacral agenesis. Neurologic and neuropathologic features. Neurology 1976;26:1124.
31. Chenoweth CK, Kellogg SJ, Abu-Yousef M. Antenatal sonographic diagnosis of sirenomelia. JCU 1991;19:167.

A HUGE MEDIASTINAL GERM CELL TUMOR

Panpen UTTAMAKUL[1,2], Patchrin PEKANAN[2], Mana ROJANAVUTHINON[3], Pakorn JIARAKONOMUN[2].

ABSTRACT

A case of a huge mediastinal endodermal sinus tumor was shown in a 22-year-old male who presented with chronic cough and dyspnea. The mediastinal mass extends from right anterior mediastinum to the right posterior mediastinum. The tumor was a mixture of solid and cystic tissue. The airway was severely compressed. The sternum was destroyed and the anterior chest wall was invaded. The right pleural effusion was massive and multiple pleural nodules were found. The alpha feto-protein was markedly elevated and the beta HCG was zero. The patient passed away due to profound shock immediately after the procedure of intercostal drainage.

INTRODUCTION

Germ cell tumors encompass a group of tumors histologically identical to certain testicular and ovarian neoplasms, all of which are believed to be derived from primitive germ cell elements.[1] It includes benign and malignant teratoma, seminoma, endodermal sinus tumors, choriocarcinoma, and embryonal carcinoma. In the majority of cases, the neoplasm becomes manifest in adolescence or early adulthood, the mean age at diagnosis is around 30-31 years old;[2,3] the age incidence of benign and malignant tumors is similar.[4] For unexplained reasons, benign lesions are more common in females and malignant tumors in males. The vast majority of mediastinal germ cell neoplasms were located in the anterior compartment [4] (94%) and the rest were found in the posterior mediastinum. The most common form of mediastinal germ cell tumor is benign teratoma, particularly the cystic form[5] The most common malignant tumor is seminoma. Many malignant tumors have a mixed histologic appearance.

CASE REPORT

A 22-year-old male patient from Chaiyapum province, was admitted to Ramathibodi Hospital due to dyspnea for 10 days. He had chronic cough for 3 months and was worse for one month. The symptom was aggravated in the supine position. The mass was palpated at the upper chest without tenderness. Weight loss was detected for 5 kgs in 3 months. He had no known chronic illnesses. He smoked regularly for 6 years. At physical exami-nation, the patient had tachycardia and tachypnea, orthopnea, engorged external jugular vein. PMI was at 5th ICS, 4 FB lateral to the MCL. An ill defined, irregular surface mass was noted at the upper midline part of the chest wall, about 3 inches in the diameter. The superficial vein was detected on the mass with intact skin. Hypoalbuminemia was present.

AP chest film showed haziness of the whole right hemithorax with mediastinal shift to the left and depression of the right hemidiaphragm

[1]Department of Radiology, Prince of Songkla University Hospital, Haadyai, Songkla, Thailand.
[2]Department of Radiology, Ramathobodi Hospital, Bangkok.
[3]Department of Pathology, Ramathibodi Hospital, Bangkok.

PMI = Point of Maximum Intensity

(Fig. 1). Thoracocentesis was performed yielding serosanguinous fluid about 1100 cc. Cytology of the fluid revealed cells that were similar to the adeno Ca. Serum alpha fetoprotein was elevated and measured 10,240 ng/ml. Beta - HCG level = 0. CT scan of the thorax (Fig.2) showed a large mixed density mediastinal mass which was located more at right side, extending from the anterior mediastinum to the posterior mediastinum. The mass contained no calcification and enhanced inhomogeneously. The invasion was seen to the sternum and midline anterior chest wall. Right pleural fluid was noted in massive amount with numerous pleural nodules. The thoracic trachea, carina and main bronchi of both sides were compressed and the lumens were obliterated. Later the bloody fluid was obtained from the ICD and the patient was hypotensive and finally passed away. The necropsy tissue was obtained. Alpha fetoprotein monoclonal antibody was positive; the placenta alkaline phosphatase was negative. Presence of yolk sac tumor or endodermal sinus tumor was noted in the specimen. The seen tumor cells were highly malignant.

DISCUSSION

Mediastinal germ cell tumors are generally considered to arise from cell rests whose journey along the urogenital ridge to the primitive gonad is interrupted in the mediastinum.[1,6-8] Occasionally, clinical or pathological examination of a testicle reveals either viable tumor or focal scarring consistent with regressed tumor [9] indicating that the mediastinal neoplasm represents a metastais. Although careful clinical examination must be performed in every case of mediastinal germ cell tumor to exclude this possibility, the relatively large number of negative pathologic examinations at autopsy[2] and the usual lack of emergence of a gonadal primary during prolonged clinical follow up indicate that this is in fact a rare event. From a diagnostic point of view, metastatic testicular cancer usually involves the retroperitoneal lymph nodes first and can bypass the mediastinum to affect the supraclavicular nodes; when the mediastinum is involved, it is seldom in the anterior compartment.

About 8 per cent showed the association between mediastinal germ cell neoplasms and Klinefelter's syndrome.[10-12] The reason for the increased risk of germ cell neoplasia in these patients is unclear but may be related to the abnormal androgen and gonadotropin secretion that is characteristic of the syndrome or to intrinsically abnormal germ cell tissue in patients with Klinefelter's syndrome (or to both).

Because mediastinal germ cell neoplasms have a varied histologic appearance, pathologic diagnosis can be difficult, especially when the amount of tissue submitted for examination is limited, such as may be obtained by mediastinoscopy or TTNA .[1,13] Although this diagnostic problem may not be very important in relation to specific typing of the tumors, particularly since many of the neoplasms are of mixed histology in any event, current advances in chemotherapy make the distinction from metastatic carcinoma of some importance. It seems reasonable to suggest, therefore, that the possibility of a primary germ cell neoplasm be considered in any young patient with an anterior mediastinal mass in whom a diagnosis of metastatic carcinoma is made in the absence of an obvious primary focus. In this situation, review of histologic material and testing for the presence of serum and tissue alphafetoprotein may alter the diagnosis; if the results of these investigations are equivocal.

Endodermal sinus tumors are highly malignant germ cell neoplasms believed to show differentiation toward yolk sac endoderm. The mediastinal form is rare.[14] The tumor also occurs occasionally in association with other germ cell neoplasms. Histologically, the neoplasm is quite variable in appearance, showing reticular, tubulopapillary, cystic and solid patterns. Perivascular structures resembling the rat endodermal sinus (shiller-Duval bodies) and small intra-and extracellular globules of PAS-positive material are

TTNA = Tran Thoracic Needle Aspiration

characteristic features. Immunohistochemical studies have shown a positive reaction in most cases for alphafetoprotein and alpha antitrypsin;[14] occasionally tumors also show CEA and keratin positivity. Extracellular basement membrane-like material is often present on ultrastructural examination.[1,15] Most endodermal sinus tumors present in young adults, the mean age was 22.6 years; [14] the majority occurs in male. Roentgenographic findings are nonspecific, consisting of an anterior mediastinal mass. Symptoms related to local mediastinal compression or invasion are present in most cases at the time of diagnosis; systemic symptoms (anorexia, weight loss, and fever) are often present as are those related to metastases.[14] Serum levels of alphafetoprotein are elevated in virtually all patients and can be a useful indicator of disease progression or remission with therapy. Although the prognosis is generally poor, prolonged survival and even cure have been documented in some patients treated aggressively.[16-18]

The presence of high serum beta-HCG would suggest seminoma, seminoma with syncytiotrophoblastic giant cells (STGC), embryonal carcinoma with STGC, yolk sac tumor with STGC, and choriocarcinoma. The presence of high serum alphafetoprotein would suggest embryonal carcinoma, embryonal carcinoma with STGC, yolk sac tumor with STGC, and choriocarcinoma. Presence of high serum levels of both alphafetoprotein and beta-HCG were seen in embryonal carcinoma with STGC, chorio Ca and yolk sac tumor with STGC.[19]

The most common malignant germ cell tumor is seminoma, which makes up 40% of the malignant subset. Teratoma with embryonal cell carcinoma (teratocarcinoma) is the next most subtype, with pure endodermal sinus tumor, choriocarcinoma, and embryonal carcinoma being much less common. Most patients with malignant germ cell tumors present with symptoms. Symptoms include chest pain, cough, dyspnea, weight loss, and fever. Primary mediastinal seminoma may be associated with low level of HCG, but significant elevation of AFP indicates that a nonseminomatous component of the tumor exists. In nonseminomatous germ cell tumors, 80% have an elevated AFP and 30% have an elevated HCG.[20]

CT shows seminomas as homogeneous bulky masses with small cystic areas, and nonseminomas contain larger cystic areas, calcifications, and fat plane invasion indicative of invasion. MRI may have a role in imaging these tumors with its ability to display multiplanar images, which may help in tumor surgery. Seminomas are sensitive to radiotherapy, and with this treatment alone, cure rates of 80% are obtained. Because of the success in treating gonadal seminomas, cisplatin-based chemotherapy is being used in patients with mediastinal seminoma. After treatment, there may be a small residual mass, which usually represents scar tissue and rarely harbors seminoma or teratoma if the mass is less than 3 cm. Nonseminomatous mediastinal tumors are treated with cisplatin-based chemotherapy followed by surgery to remove residual tumor. These patients have a worse prognosis than do the seminoma patients with only 50% survival rate.[20]

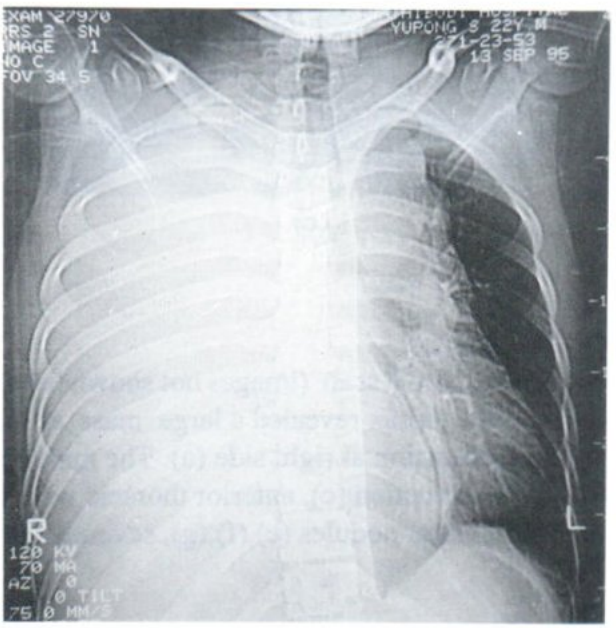

Fig. 1 Plain AP chest film shows total haziness of the right hemithorax with mediastinal shift to the left, inferiorly displaced right hemidiaphragm.

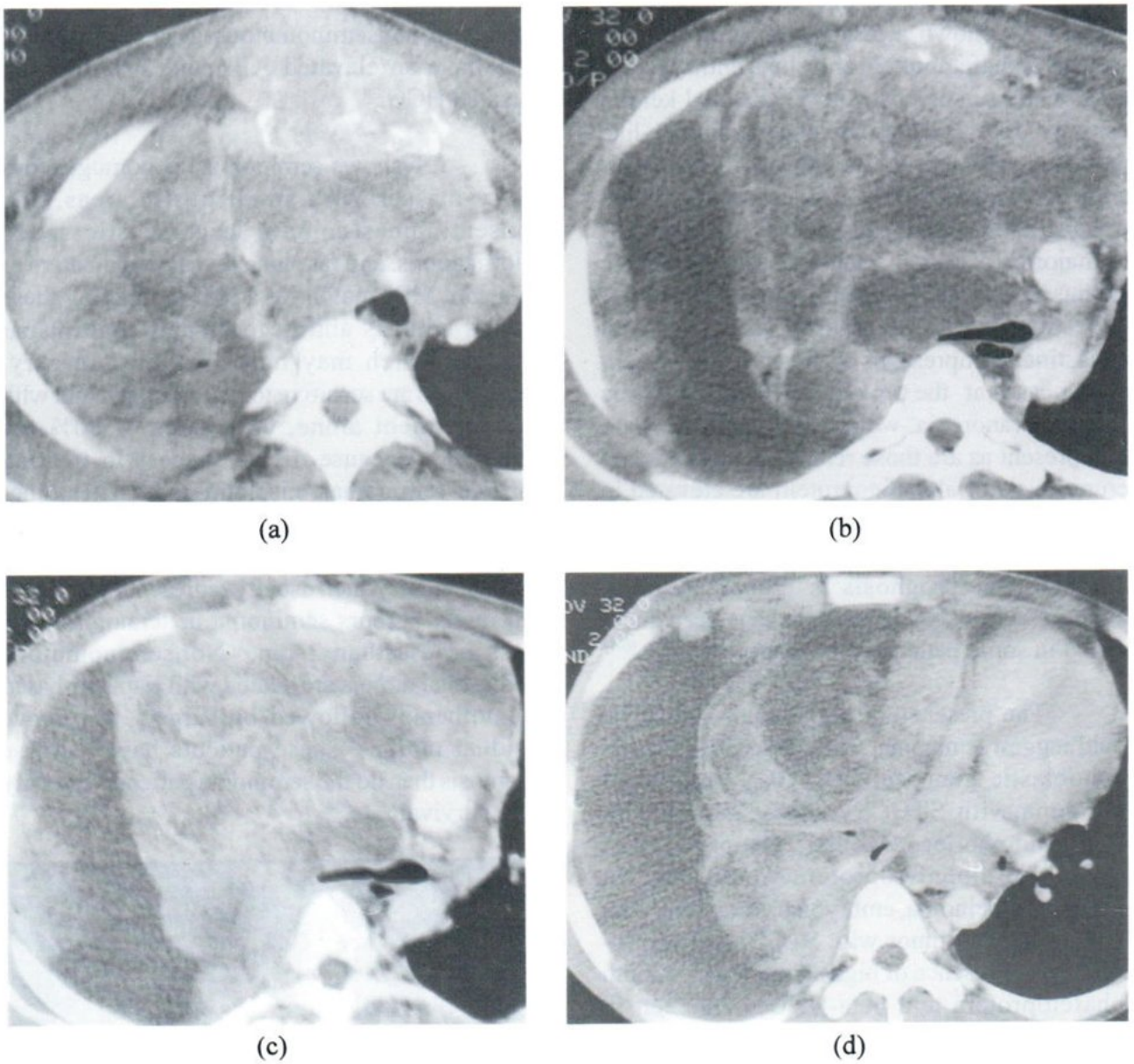

(a) (b)

(c) (d)

Fig. 2: a,b,c,d.
NCE CT scan (images not shown here) showed no calcification in the mass. CE CT scan of the thorax revealed a large mass at the anterior mediastinum with posterior mediastinal extension at right side (a). The mass showed predominantly cystic component (b). Sternal destruction (c), anterior thoracic wall invasion (d), massive right pleural fluid and right pleural nodules (e),(f),(g), severely air way compression were obviously observed (h).

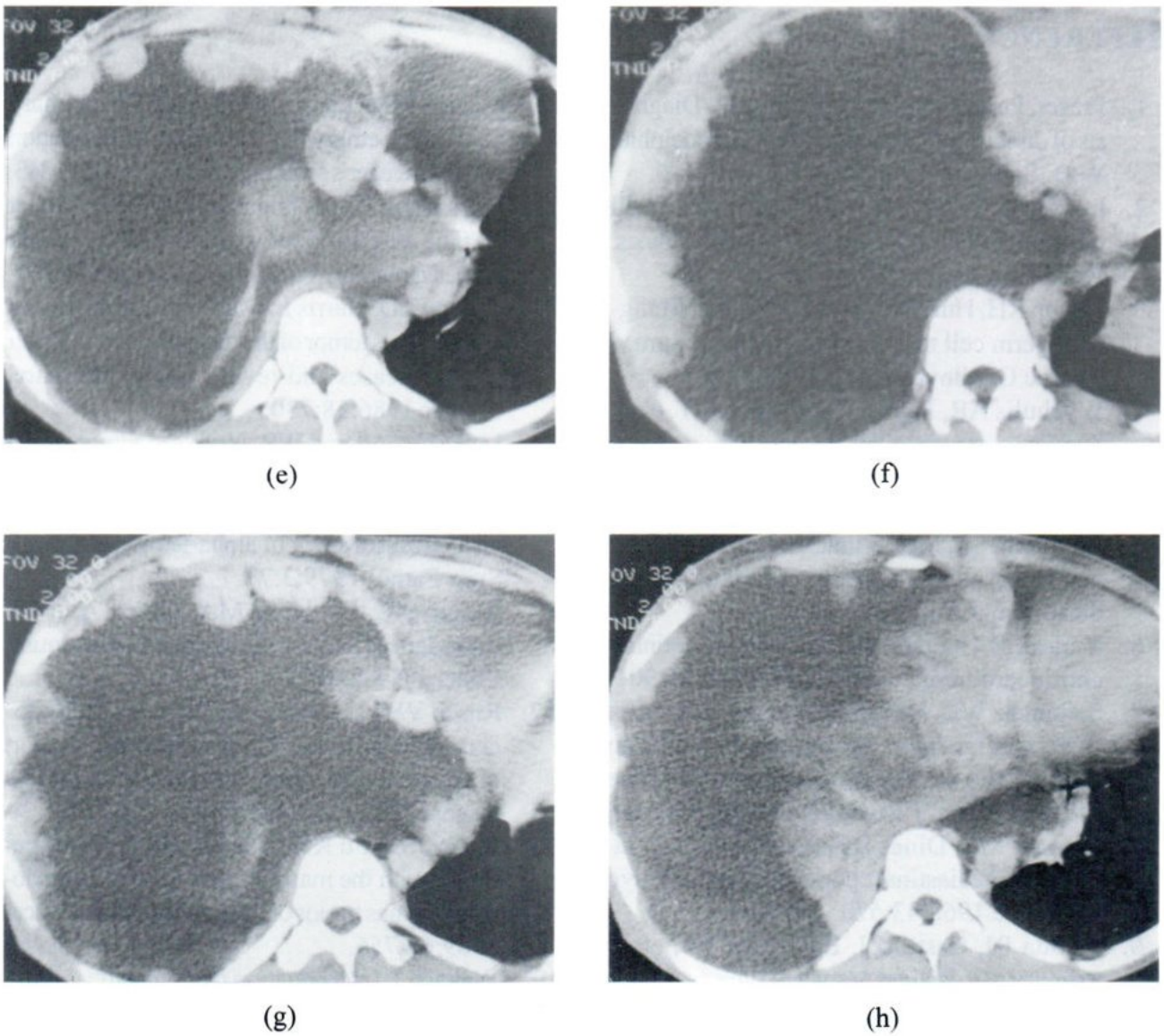

Fig. 2: e,f,g,h.
NCE CT scan (images not shown here) showed no calcification in the mass. CE CT scan of the thorax revealed a large mass at the anterior mediastinum with posterior mediastinal extension at right side (a). The mass showed predominantly cystic component (b). Sternal destruction (c), anterior thoracic wall invasion (d), massive right pleural fluid and right pleural nodules (e),(f),(g), severely air way compression were obviously observed (h).

REFERENCE

1. Fraser, Pare, Pare, Fraser, Genereux. Diagnosis of diseases of the chest. 3rd ed. Philadelphia: W.B. Saunders Company, 1991:2835-6.
2. Luna MA, Valenzuela - Tamariz J. Germ-cell tumors of the mediastinum; postmortem findings. Am J Clin Pathol 1976;65:450.
3. Knapp RH, Hurt RD, Payne WS, et al. Malignant germ cell tumors of the mediastinum. J Thorac Cardiovasc Surg 1985;82:9.
4. Wychulis AR, Payne WS, Clagett OT, et al. Surgical treatment of mediastinal tumors. A 40-year experience. J Thorac Cardiovasc Surg 1971;62:379.
5. Benjamin SP, McCormack LJ, Effler DB, et al. Critical review- Primary tumors of the mediastinum. Chest 1972;62:297.
6. Yurick BS, Ottoman RE. Primary mediastinum choriocarcinoma. Radiology 1960;75:901.
7. Steinmetz WH, Hays RA. Primary seminoma of the mediastinum. Report of a case with an unusual site of metastasis and review of the literature. Am J Roentgenol 1961;86:669.
8. Wenger ME, Dines DE, Ahmann DL, et al. Primary mediastinal choriocarcinoma. Mayo Clin Proc 1968;43:570.
9. Aliotta PJ, Castillo J, Englander LS, et al. Primary mediastinal germ cell tumors. Histologic patterns of treatment failures at autopsy. Cancer 1988;62:982.
10. Sogge MR, McDonald SD, Cofard PB. The malignant potential of the dysgenetic germ cell in Klinefelter's syndrome. Am Med 1979;66:515.
11. Lachman MF, Kim K, Koo B-C. Mediastinal teratoma associated with Klinefelter's syndrome. Arch Pathol Lab Med 1980;110:1067.
12. McNell MM, Leong AS-Y, Sage RE. Primary mediastinal embryonal carcinoma in association with Klinefelter's syndrome. Cancer 1981;47:343.
13. Richardson RL, Schoumacher BS, Fer MF, et al. The unrecognized extragonadal germ cell cancer syndrome. Ann Intern Med 1981;94:181.
14. Truong LD, Harris L, Mattioli C, et al. Endodermal sinus tumor of the mediastinum. A report of seven cases and review of the literature. Cancer 1986;58:730.
15. Mukai K, Adams WR. Yolk sac tumor of the anterior mediastinum. Case report with light and electron microscopic examination and immunohistochemical study of alpha-fetoprotein. Am J Surg Pathol 1979;3:77.
16. Kuzur ME, Cobleigh MA, Greco A, et al. Endodermal sinus tumor of the mediastinum. Cancer 1982;50:776.
17. Rusch VW, Logothetis C, Samuels M. Endodermal sinus tumor of the mediastinum. Report of apparent cure in two patients with extensive disease. Chest 1984;86:745.
18. Sham JST, Fu KH, Chiu CSW, et al. Experience with the management of primary endodermal sinus tumor of the mediastinum. Cancer 1989;64:756.
19. Wallach J. Interpretation of diagnostic tests: A synopsis of laboratory medicine. 5th ed. Boston; Little, Brown and Company, 1992:539.
20. Haaga JR, Lanzieri CF, Sartoris DJ, Zerhouni EA. Computed tomography and magnetic resonance imaging of the whole body. 3rd ed. St. Louis; Mosby, 1994:753.

ELEPHANTIASIS NEUROMATOSA : IMAGING FINDINGS

Suphaneewan JAOVISIDHA[1], Sansanee WONGWAISAYAWAN[2], Patchrin PEKANAN[1], Pimjai SIRIWONGPAIRAT[1].

ABSTRACT

A 26-year-old woman with numerous Cafe-au-lait spots at the left leg since birth was presented. Plain radiographs of left leg revealed lobulated enlargement of the soft tissue of left leg from knee to foot, containing no internal calcification. Undertubulation and thickening of the cortex and the periosteum of the tibia and fibula were observed. Osteopenia with multiple extrinsic bone erosions of the tarsal bones was noted. MR imaging showed generalized thickening of the subcutaneous tissue and enlargement of the muscles of left leg, except the tibialis anterior muscle, the tibialis posterior muscle and the extensor hallucis longus muscle. Low signal intensity on T1W sequence and increased signal intensity on T2W sequence of the involved muscles were demonstrated.

INTRODUCTION

Type 1 neurofibromatosis, the peripheral form of the disease, is carried on chromosome 17.[1,2] It is a hereditary hamartomatous condition characterized by cutaneous lesions, skeletal abnormalities, and multiple nerve sheath tumors, usually neurofibromas.[1,3,4] Multiple nerve roots may be involved in a plexiform manner, being a multilobulated, tortuous entanglement or interdigitating network of tumor along a nerve and its branches.[2,3] Eventhough it is an autosomaldominant disease, about half of these cases are due to spontaneous mutation.[4]

Recent articles have described the magnetic resonance (MR) appearances of plexiform neurofibroma (PN) affecting the spine and paraspinal regions, larynx, mediastinum, and intra-abdominal organs [1,3,5,6] and one article described MR findings of PN involving the extremity.[7] This article described MR appearance of PN affecting a lower extremity with pathologic and histologic correlation.

CASE REPORT

In December 1993, a 26-year-old Thai woman presented at the surgical clinic because she had a large, lobulated-contour left leg since birth which was gradually enlarged. This enlargement was rapid and painful in the last 3 years. She still could walk and run normally. Physical examination revealed a female patient with good consiousness and good cooperation. She had numerous Cafe-au-lait spots on both anterior and posterior aspects of her trunk. The left lower extremity was enlarged and lobulated without varus or valgus deformity. The lesion involved the entire left lower leg and foot. Other physical examination was unremarkable. The family history was obtained and disclosed that her

[1]Department of Radiology, Ramathibodi Hospital, Rama 6 Street, Bangkok 10400, Thailand.
[2]Department of Pathology, Ramathibodi Hospital.

three first-degree relatives and other three second-degree relatives had Cafe-au-lait spots, but to a lesser extent. Plain radiographs of left leg revealed lobulated enlargement of the soft tissue of the left leg from knee to foot without internal calcification. Undertubulation and cortical/ periosteal thickening of the tibia and fibula was shown. Osteopenia and multiple varied-size extrinsic bone erosions were noted at the tarsal bones (Fig.1). MR imaging of left leg (Fig.2,3) demonstrated generalized thickening of the subcutaneous tissue and enlargement of the muscles of left leg, except of the tibialis anterior muscle, tibialis posterior muscle, and extensor hallucis longus muscle. The signal intensity (SI) of the involved muscles were abnormal with less SI than normal muscle on T1W images (T1WI) and increased SI on T2WI and gradient recalled echo images (GREI). The exceptional muscle groups showed normal size and signal intensity. Marrow compartment appeared normal. Bone erosions at the tarsal bones on plain radiographs were produced by the soft tissue mass. The diagnosis was compatible with neurofibromatosis. No scoliosis or intrathoracic lesion seen on chest film.

The patient was undergone contouring procedure, and the excisional biopsy was taken from the left foot. The specimen consisted of elongated elliptical shaped skin with underlying mass, measuring 25 X 5 X 4 cm. The epidermis was brown and wrinkle. The underlying mass showed shiny white, soft appearance with an infiltrative border into the adjacent dermis and subcutaneous adipose tissue. Microscopically, the mass was composed of diffuse proliferation of compactly arranged spindle cells with scanty but extensively elongated cytoplasm which were lightly eosinophilic and fibrillary (Fig. 4a). Their nuclei were wavy or comma-shaped (Fig. 4b). Several expanded nerves were seen as the result of infiltration by the neoplasm. Dense eosinophilic rim representing the remnant of the original nerve was also present and it appeared as a small nodule at the low-power field. The diagnosis of plexiform neurofibroma was given. All surgical margins were not free. The patient had necrotic skin over the posterior ankle post operatively and was treated medically. She had an appointment for the second surgery in June 1994, but lost follow up.

DISCUSSION

Peripheral nerve tumors in neurofibromatosis most frequently involve neural supporting tissue. The two most common benign forms are solitary or multiple neurofibromas and neurilemmomas (schwannoma). The latter are encapsulated lesions that lie on the surface of the nerve. They are more common than neurofi-bromas, which infiltrate involved nerves diffusely and incorporate all nerve elements (i.e. Schwann cells, nerve fibers, and fibroblasts). Tumors of nerves may appear as focal fusiform enlargement or diffuse, multinodular, or coalescent sheetlike masses.[4,8] Benign plexiform or cirsoid neurofibromas, observed only in neurofibromatosis, appear as bizarre soft tissue networks that interdigitate imperceptibly with adjacent fat and muscle, recur after resection,[3,6] and have a potential for malignant degeneration. They are recognized most easily in massively enlarged extremities (i.e. elephantiasis neuromatosa), although the face, head and trunk also may be involved. Such lesions may occur anywhere along the course of central or peripheral nerves,[4] or within deep or superficial tissues.

The MR signal characteristics of PN has been described to be isointense or slightly greater than muscle on T1WI, and markedly increased on T2WI.[1,3,5-7] Previously, the low attenuation of neurofibromas on CT has been attributed to increased amount of endoneural myxoid matrix .[1,5,9] This matrix contains acid mucopoly-saccharides and a large amount of tissue fluid. The residual axons are spread by the matrix to produce the fusiform shape or the neurofibroma.[10] The lengthened T2 of the neurofibroma is probably due

to increased water content of the matrix. The slightly greater SI of the neurofibroma on T1WI can be attributed to relative shortening of T1 by the interaction of the large mucopolysaccharides molecules with the tissue water. Large protein molecules have been demonstrated to slow the tumbling rates of water molecules resulting in accelerated relaxation rates.[5,11]

Our case with elephantiasis neuromatosa exhibited slightly lower signal intensity than muscle on T1WI which could be attributed to cystic degeneration,[1] and to the increased fluid content within the lesion. The myxoid matrix found in histological examination as well as the high fluid content may account for the increased SI on T2WI. We did not find the central area of decreased SI on T2WI described in paraspinal lesions[5] in our case. The lesion in our study had infiltrative margins that blended imperceptibly with adjacent fat and muscles but still showed benignity histologically; this finding corresponds to what were described by other authors.[6] The low-SI linear or serpentine structures within the lesion, obviously seen on T2WI and GREI, representing separated muscle bundles. The dysplastic change of the tibia and fibula included undertubulation and thickening / hypertrophy of the cortex. The latter occured partly as result of the incooperation of the overgrowing periosteum which was a reactive change to the adjacent soft tissue tumor. The extrinsic erosive change of the tarsal bones reflected the aggressive pattern of the tumor growth.

In conclusion, we report imaging findings of a case of elephantiasis neuromatosa of left lower extremity which showed less SI than muscle on T1WI and high SI on T2WI. The selective involvement of particular muscle groups and preserved other groups characterized the plexiform manner of involvement along the course of peripheral nerves.

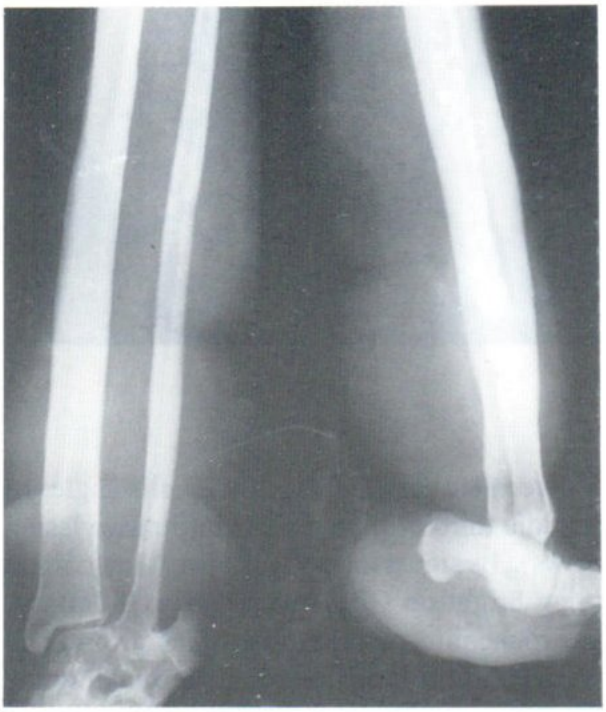

Fig. 1. Plain radiograph of left leg reveals multi-lobulated enlargement of soft tissue as well as skeletal abnormalities onsisting of cortical thickening and hypertrophy which are partly incorporated by the overgrowing periosteum.

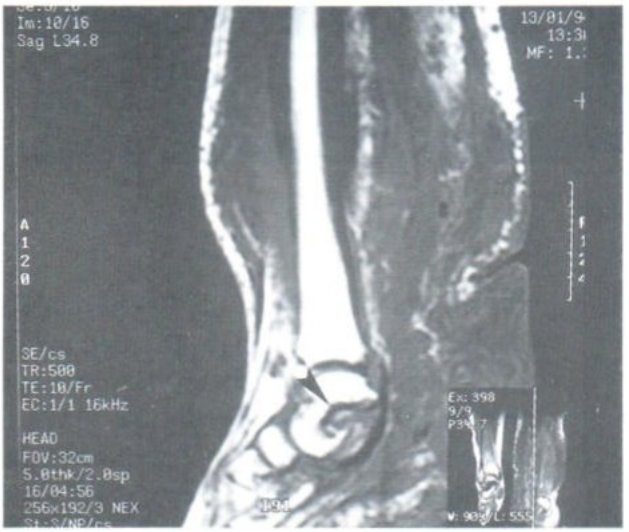

Fig. 2. T1- weighted (500/10 [TR/TE]) sagittal MR image reveals an infiltrating soft tissue PN showing lower-than-muscle SI and causing bone erosion of the tarsal bones (black arrowhead).

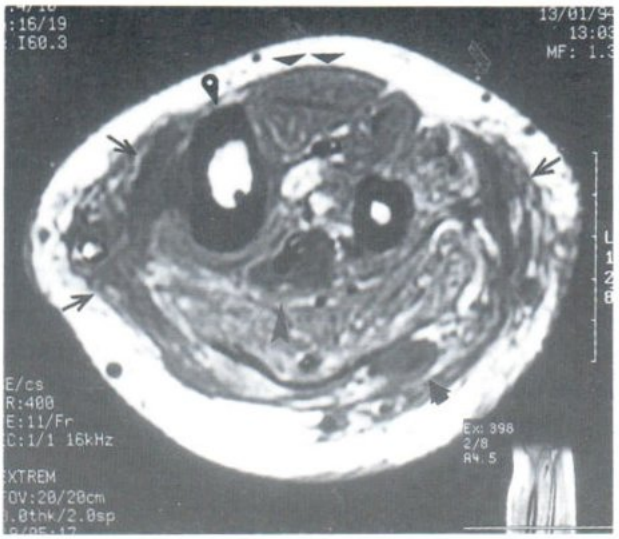

3(a)

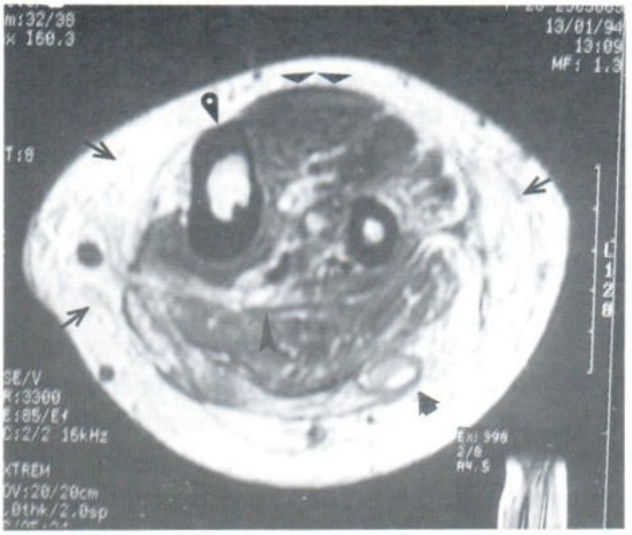

3(b)

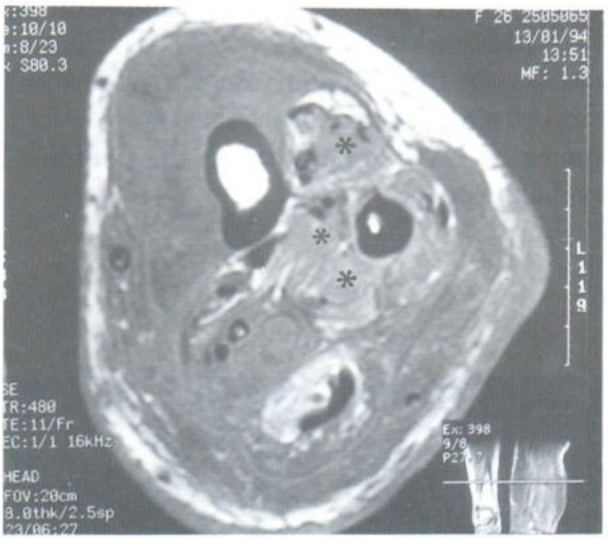

3(c)

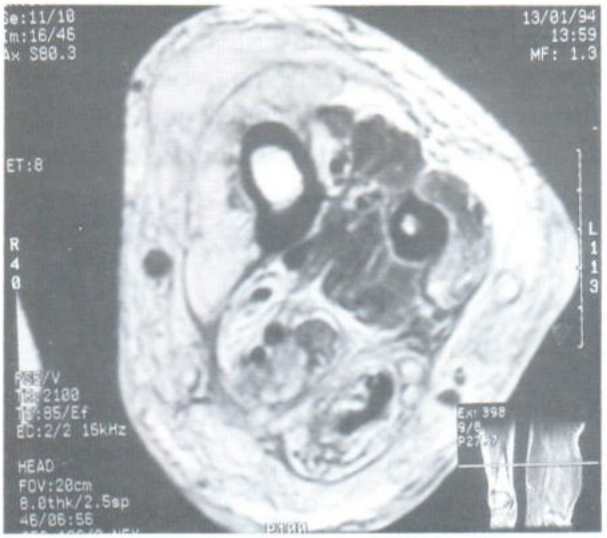

3(d)

Fig.3 **(a)** T1-weighted (400/11 [TR/TE]) and **(b)** gradient recalled echo (GRE)(600/20; flip angle, 15 degrees) axial MR images through the level of middle third of tibia reveals infiltrative lesion involving both subcutaneous fat and muscles (arrows). Its signal intensity is lower than normal muscles (broad arrowheads) on T1W1 and turning bright on GRE image. A well-defined, focal neurofibroma is observed within lateral gastrocnemius muscle (short thick arrow) and having internal cystic component. Another focal plexiform lesion is noted surrounding the posterior tibial neurovascular bundle (arrowhead). Abnormal thickening of bony cortex is also observed (round arrowhead.) **(c)** T1- weighted (480/11) and **(d)** GRE (680/20; flip angle, 15 degrees) axial MR images 20 mm below a) and b) exhibit more extensive lesion. On T1WI (c) the signal intensity of the lesion is lower than normal muscles (asterisks). The low-SI linear or serpentine structure seen within the lesions on GRE image represent muscle bundles and fascia separated by the tumor.

4(a)

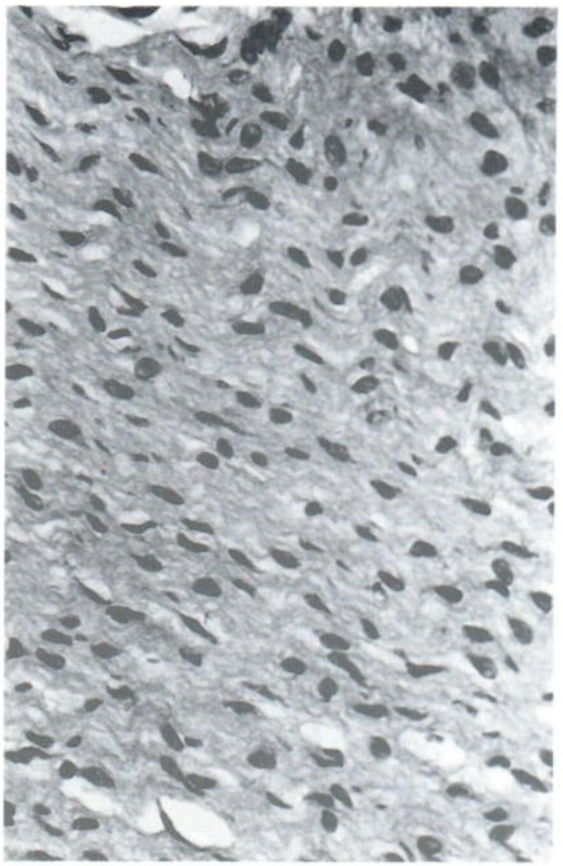

4(b)

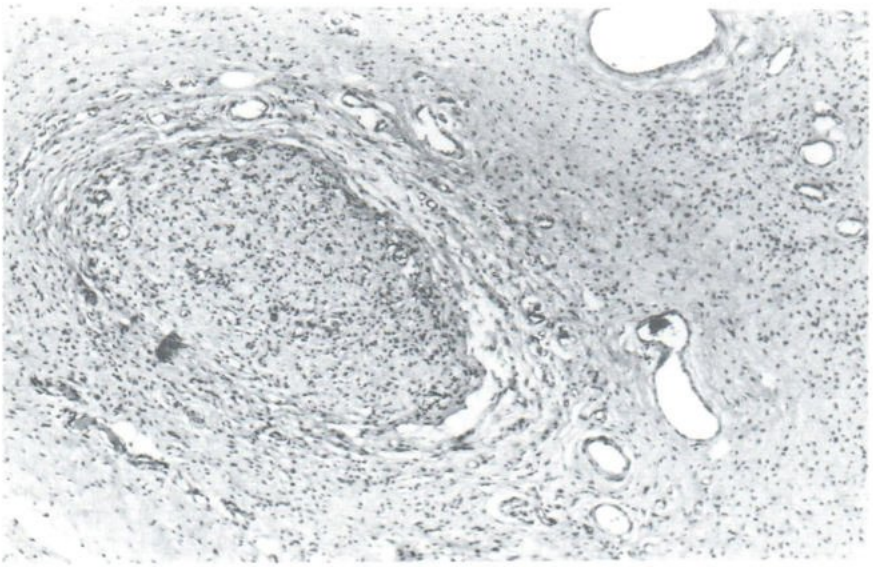

4(c)

Fig. 4. **(a)** (x40) The plexiform neurofibroma involves the dermis. Its border was well-defined but unencapsulated. The mass composed of spindle cells. **(b)** (x200) The cellular area of the plexiform neurofibroma shows proliferation of wavy, fibrillary elongated spindle cells. The nuclei are oval, wavy or comma-shaped. **(c)** (x40) One of a number of expanded nerves in plexiform neurofibroma. Its perineurium was thickened and extended into the adjacent tissue.

REFERENCES

1. Gossios KJ, Guy RL. Case report: Imaging of widespread plexiform neurofibromatosis. Clin Radiol 1993;47:211-3.
2. Harle TS, Carrol CL, Leeds NE, et al. Image interpretation session:1994. RadioGraphics 1995;15:223-5.
3. Feldman F. Tuberous sclerosis, neurofibromatosis, and fibrous dysplasia. In:Resnick D. ed. Diagnosis of Bone and Joint Disorders. 3rd ed. Philadelphia, PA: WB Saunders, 1995;4361-79.
4. Allan BT. Plexiform neurofibroma. AJR 1985;144:1300-2.
5. Burk DL Jr. Brunberg JA, Kanal E, Latchaw RE, Wolf GL. Spinal and paraspinal neurofibromatosis: Surface coil MR imaging at 1.5 T. Radiology 1987;162:797-801.
6. Martin DS, Stitch J, Awwad EE, Handler S. MR in neurofibromatosis of the larynx. AJNR 1995;16:503-6.
7. Sullivan TP, Seeger LL, Doberneck SA, Eckardt JJ. Case report 828: Plexiform neurofibroma of the tibial nerve invading the medial and lateral gastrocnemius muscles and plantaris muscle. Skeletal Radiol 1994;-23:149-52.
8. Holt JF, Wright EM. Radiologic features of neurofibromatosis. Radiology 1948;51:647-63.
9. Daneman A, Mancer K, Sonley M. CT appearance of thickened nerves in neurofibromatosis. AJR 1983;141:899-900.
10. Harkin JC, Reed RJ. Tumors of the peripheral nervous system: Atlas of tumor pathology. Series 2, fascicle 3. Washington D.C.: Armed Forces Institute of Pathology, 1969;67-96.
11. Koenig SH, Brown RD. The importance of the motion of water for magnetic resonance imaging. Invest Radiol 1985;20:297-304.

CRANIAL AND FIBULA CHONDROSARCOMA:A CASE REPORT

Nitat KIATHIRANNON[1], Patchrin PEKANAN[2], Thirasak PUENNGARM[3], Suchart PHUDHICHAREONRAT[4].

ABSTRACT

Cranial chondrosarcomas were discovered in a 62-year-old female patient who presented with neurological symptoms. CT scan showed a large mass at right temporal fossa, extending to near-by structures and another smaller lesion at left temporal fossa. The masses were invasive and destructive, containing no calcification. T1W MRI study showed low to iso-signal mass and on T2WI, the signal was iso to the gray matter and the contrast enhancement was dense. There was no neovasculature at angiography. Bone survey was later performed after obtaining histology of the mass from craniotomy. The primary lesion was detected at the left fibula with classic appearance of of chondrosarcoma.

INTRODUCTION

Chondrosarcomas comprise a group of tumors that have a broad spectrum of clinical and pathologic findings. The feature common to all is the production of neoplastic cartilage. It morphologically subclassified into conventional, intramedullary and juxtacortical, clear cell, dedifferentiated, and mesenchymal variants.[1] Chondrosarcomas commonly arise in the central portions of the skeleton, including the pelvis, shoulder and ribs. The clear cell variant is unique in that it originates in the epiphyses of long tubular bones. Chondrosarcoma rarely involves the distal extremities. These tumors usually present as painful, progressively enlarging masses. 70% of grade 3 tumors disseminated. When chondrosarcomas metastasize, they preferentially spread to the lungs and skeleton.

The reported patient had predominated neurological problems and intracranial lesions were earlier detected than the primary site.

CASE REPORT

A 62-year-old female patient admitted to Prasat neurological institute due to intermittent headache, right temporal mass, decreased visual acuity of right eye and progressive weakness of left extremities for three months. On physical examination, a 5 cm-solid mass at right temporal area was detected. Left lower extremity showed mild swelling. The patient was drowsy and confused. Right pupil was 3.5 mm and fixed while left pupil was 2 mm and reacted to light. Right optic atrophy and left papilledema was noted. Right total ophthalmoplegia and left lateral rectus palsy was seen. Left hemiparesis, grade I and right sided motor power was grade IV.

Cranial CT scan was performed and revealed two inhomogeneous enhanced masses. The first mass was at right temporal area, extending to the right orbit, squamosal temporal bone, medially to obliterate right lateral ventricle and cause 2 cm midline shift to the left, to the middle cranial fossa and destroy the sphenoid bone (Fig.

[1]Department of Neuroradiology, Prasat Neurological Institute, Rama 6 Street, Bangkok 10400, Thailand.
[2]Department of Radiology, Ramathibodi Hospital.
[3]Department of Neurosurgery, Prasat Neurological Institute.
[4]Department of Neuropathology, Prasat Neurological Institute.

1). The second mass was at the left temporal area with extension inferiorly to destroy the sphenoid bone. No intratumoral calcification was detected (Fig.1).

Signal of the mass on T1W MRI study showed low to iso-signal and on T2WI study showed iso-signal to the grey matter. Marked enhancement of the lesion by Gd-DTPA was noted (Fig.2).

Intracranial angiography showed no neovasculature from both internal and external carotid arteries (Fig.3).

The right fronto-temporal craniotomy with subtotal tumor removal was then performed. The gross specimen revealed light brown, firm tissue which was measured to be 8 cm in diameter. The microscopic examination showed moderately cellular tumor with fragments of bone, dense fibrous tissue and striated muscle. The tumor cells were round in shape, medium to large in size and were in cartilage lacunae. Multinucleated tumor cells and mitotic figures were frequently noted. The pathological diagnosis was chondrosarcoma.

The bone survey was later performed and the lesion of extensive chondrosarcoma of left fibula was detected (Fig. 4).

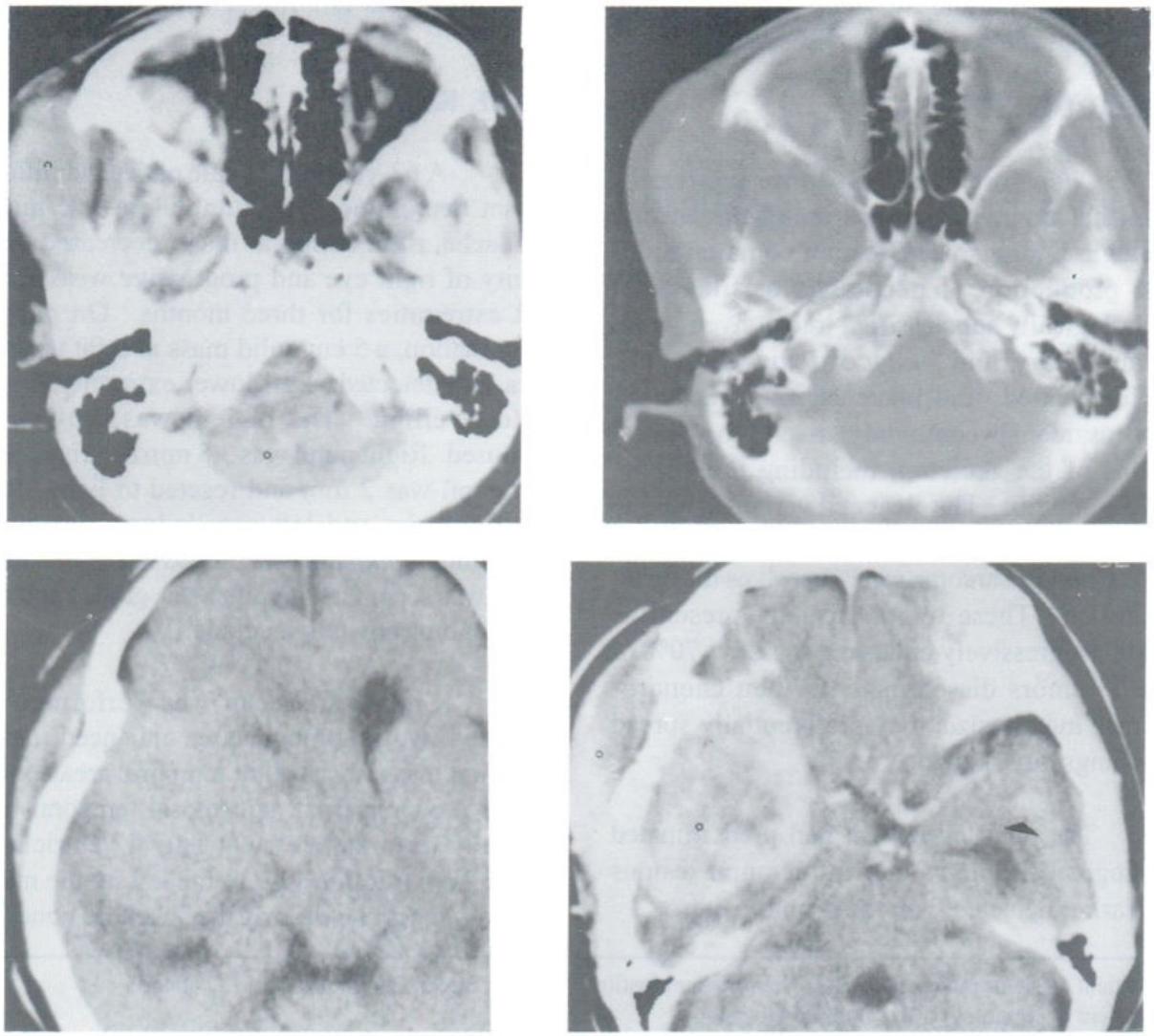

Fig.1 CT scan showed metastatic chondrosarcomas at both temporal fossae with invasive nature.

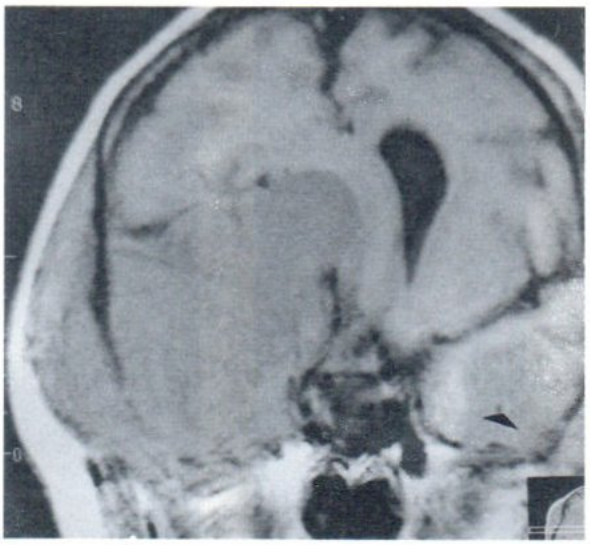

(2a)

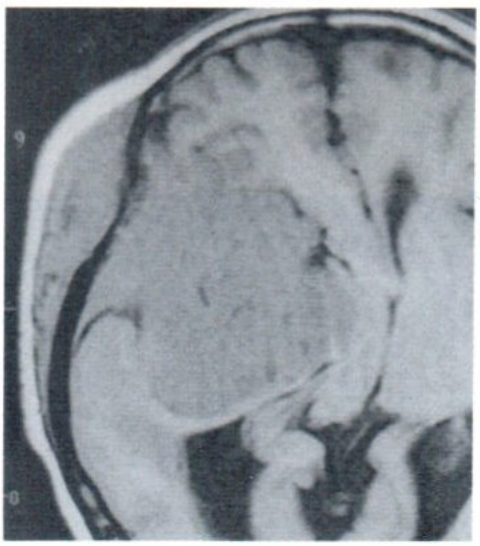

(2a)

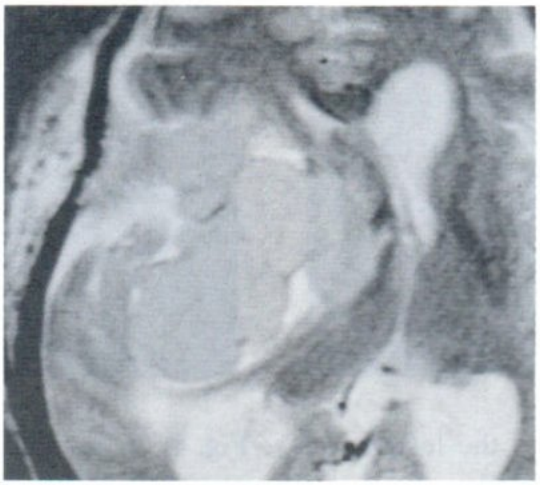

(2b)

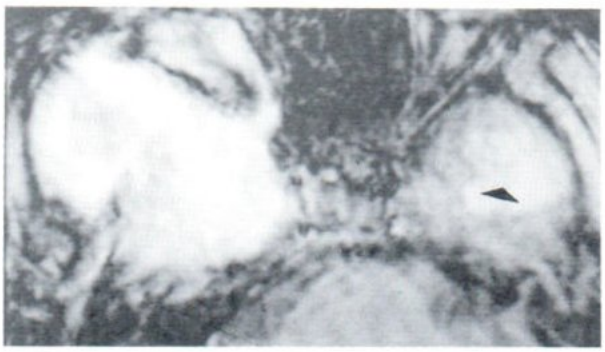

(2c)

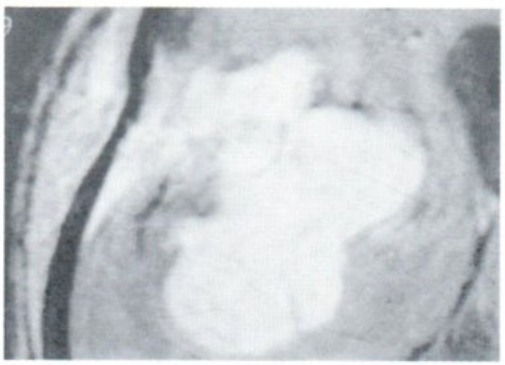

(2c)

Fig. 2 MRI images of the lesion
(a) T1WI, (b) T2WI, (c) post gadolinium enhancement

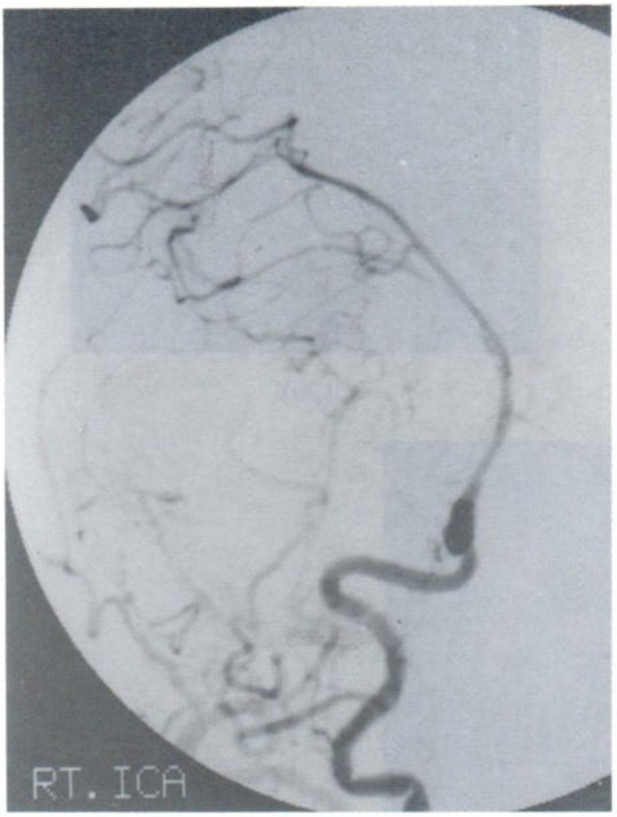

Fig. 3 No neovasculature to the lesion was noted at angiography

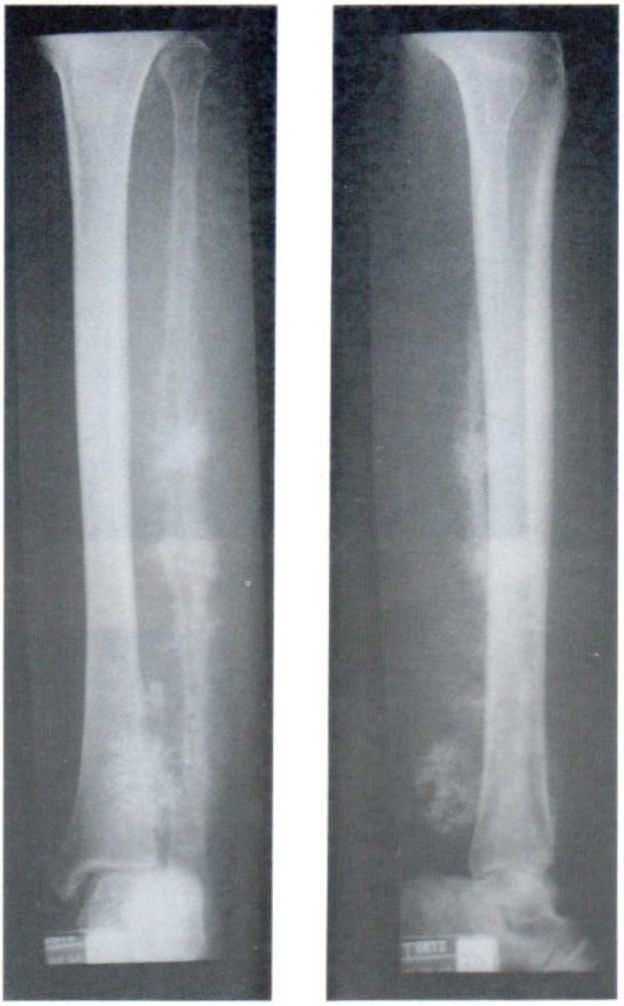

Fig. 4 Classical chondrosarcoma at the left fibula was shown by radiography

DISCUSSION

Chondrosarcomas of the bone represent a range of malignant tumors of cartilage that includes the classic or conventional chondrosarcoma, dedifferentiated chondrosarcoma, clear cell chondrosarcoma, mesenchymal chondrosarcoma, and malignant chondroblastoma.[1]

Classic or simply chondrosarcoma is the second most common malignant neoplasm of bone after osteosarcoma. It is subclassified as central (medullary) if it is located within the medullary cavity or peripheral (juxtacortical) if its origin is on the surface of the bone. It may arise de novo or secondarily from preexisting benign cartilage lesions such as the osteochondromas in multiple osteochondromatosis or the enchondromas of Ollier's disease. Chondrosarcoma is a malignant tumor of hyaline cartilage that arises in the medullary cavity or on the surface of a bone. It is a tumor of adults generally between 20 and 70 years of age. Males are affected more often than females. The most common sites of involvement are the pelvis, femur, scapula, humerus, and the ribs. Radiographic findings indicate the cartilaginous nature of a tumor when typical calcifications are present. Matrix calcifications have been variously described as annular, punctate, popcorn-like, ringlet-like, stippled, or small ill defined radiodense formations. These features do not discriminate benign from malignant tumors.

Dedifferentiated chondrosarcoma has the worst prognosis. Postulation was formed that low grade cartilaginous lesions may transform into a high-grade sarcoma[2] or that these tumors are formed by synchronous differentiation of two separate clones of cells.[3] Most cases occur in the sixth decade of life.[4] The patient distribution by sex is about equal. The site of tumor is most often the bones of the pelvis, followed by the femur.[5] Radiologically, these tumors may show foci of typical cartilaginous calcifications, denoting the low-grade component, and a large lytic component, which usually has a significant soft-tissue mass component. However, a good number of tumors do not present the calcification of the low-grade component, but only the large noncacified mass. Glossly these tumors are large infiltrative lesions that not only involve the bone but also extend into the adjacent soft tissues. Foci of cartilage may be seen on gross inspection.

Mesenchymal chondrosarcoma is rare, accounting for 0.33% of all primary malignant neoplasms of bone. Eighty per cents of cases are diagnosed before 40 years of age. The peak incidence is in the second decade of life. Radiologically there is nothing characteristic for this tumor. If calcified cartilage matrix is present, the tumor may look like a conventional chondrosarcoma. Any bone may be involved. Huvors reported 31% of it in the lower extremity, 17% in the pelvic girdle, and 14% in the cranial bones.

Clear cell chondrosarcoma has a relatively good prognosis and is extremely rare. The patients ages ranged from 14 to 84 years, with a slight peak in the third and fourth decades of life. There was a male predominance; the male-to female ratio was 2.5 to 1.[6] Radiologically this lesion is seen in the epiphysis of the long bones, especially the head of the femur which is the most common location; most of these tumors contain typical cartilaginous calcifications. Some small tumors may be difficult to differentiate from chondroblastoma.[7]

Chondrosarcomas of the skull occur from childhood to old age. No sex predilection has been noted. They are locally aggressive but grow slowly with tumor frequently leading to death five or more years after onset of symptoms.[8,9] Metastases have been reported[10] but are uncommon. Chondrosarcomas occur most often along the base of the skull, the most frequent site being parasellar.[11] The predilection of intracranial chondrosarcomas for the base of the skull is not surprising since embryologically the base arises from a cartilaginous

matrix. Atypically located chondrosarcoma may arise from cartilaginous rests other than at the base of the skull or from multipotential cells within the meninges.

On MR images obtained with short TR/TE sequences, chondrosarcomas generally had low to intermediate signal intensity and were slightly hyper-or isointense to muscle and iso-or hypointense to gray matter. On MR images obtained with long TR/short TE and long TR/TE sequences, chondrosarcomas of the skull base generally had high signal intensity and were predominantly hyperintense to muscle and gray matter.[11] Chondrosarcomas showed a marked degree of contrast enhancement.

Cranial involvement in our case was most probably metastatic lesions due to multiplicity of the lesions. Though the primary site contained abundant typical cartilaginous calcifications, the metastatic components had absent calcification. The signal on T2WI in our case was not similar to those reported.

REFERENCES

1. Damjanov I, Linder J. Anderson's pathology. 10th ed. St. Louis: Mosby, 1996:2546-7.
2. Dahlin DC, Beabout JW. Dedifferentiation of low-grade chondrosarcoma. Cancer 1971; 28:461.
3. Johnson S, Tetu B, Ayala AG, Chawla SP. Chondrosarcoma with additional mesenchymal component (dedifferentiated chondrosarcoma): A clinicopathologic study of 26 cases. Cancer 1986;58:278.
4. Frassica FI, Unni KK, Beabout JW, Sim FH. Dedifferentiated chondrosarcoma: a report of the clinicopathologic features and treatment of seventy eight cases. J Bone Joint Surg 1986;68A:1197.
5. Campanacci M, Bertoni F, Capanna R. Dedifferentiated chondrosarcomas. Ital J Orthop Traumtol 1979;3:331.
6. Bjornsson J, Beabout JW, Unni KK, et al. Clear cell chondrosarcoma of bone: observations in 47 cases. Am J Surg Pathol 1984; 8:223.
7. Wang LT, Liu TC. Clear cell chondrosarcoma of bone: a report of three cases with immunohistochemical and affinity histochemical observations. Pathol Res Pract 1993; 189:411.
8. Bahr AL, Gayler BW. Cranial chondrosarcomas: report of four cases and review of the literature. Radiology 1977;124:151-6.
9. Berkmen YM, Blatt ES. Cranial and intracranial cartilaginous tumours. Clin Radiol 1968;19:327-33.
10. Leedham PW, Swash M. Chondrosarcoma with subarachnoid dissemination. J Pathol 1972;107:59-61.
11. Acquaviva R, Tamic PM, Thevenot C, et gal. Los condromas intracraneales.Revision de la literatura a proposito de dos casos. Rev Esp. Otoneurooftal 1965;24:15-34.

HEPATIC FASCIOLIASIS

Janjira JATCHAVALA[1], Patchrin PEKANAN [1], Paisal PONGCHAIRUEK [2], Suphaneewan JAOVISIDHA[1]

ABSTRACT

A case of hepatic fascioliasis without peripheral eosinophilia is presented. CT scan revealed a cluster of small abscesses in subhepatic area of the liver with tract like fashion. The adjacent subhepatic cyst was noted as a complication of the disease.

INTRODUCTION

Fascioliasis, caused by the trematode Fasciola hepatica or less common by the Fasciola gigantica, is a common parasitic disease in cattle and sheep. Humans are accidental hosts during the life cycle of the parasites.[1,2] They are infected by ingesting contaminated watercress,[3] water,[4] raw fish [5] or infected raw sheep or cattle livers.[3]

In human fascioliasis, two stages of disease have been distinguished; an acute phase, which coincides with hepatic invasion, and a chronic phase caused by persistence of adult flukes in the bile ducts.[2] Triad of fever, hepatomegaly and high peripheral eosinophilia was known as characteristic of the disease. Ultrasonographic and CT findings of the disease had been reported.[6-9] However, radiologic findings of complicated cases were seldom demonstrated.

We report a case of hepatic fascioliasis with no peripheral eosinophilia and a large subhepatic cyst.

CASE REPORT

A 48-year-old man was admitted to the hospital because of severe epigastric pain and syncope for 2 hours. He had experienced abdominal discomfort for 1 year, anorexia and weight loss for 4 kgs in 2 months. Physical examination revealed fever (T 38-39 degree celsius), and no jaundice. During the examination, mild hepatomegaly and tenderness at epigastrium and right upper abdomen were noted. Laboratory findings showed Hct 47.5%, mild leukocytosis (WBC 11,900/mm,[3] N 80, L16, M3, B1). Urine and stool examination were within normal limit. Liver enzymes were slightly elevated; alkaline phosphatase 104 (20-90) U/L, alkaline Am. trans 37 (6-36) U/L, G.Glutamyl trans 67 (5-38). Lipase and amylase were within normal limit. HIV antibody and AFP were negative. CEA was 3-31 mg/ml. Ultrasound revealed multiple small hypoechoic lesions in the left lobe of liver and a large cystic mass between left lobe of liver and the pancreatic head region (Fig.1).

CT scan showed a cluster of small, low attenuation lesions in the periphery of the medial segment of the left lobe. They were arranged in linear fashion. A large cystic mass about 7.5 X 5 X 5 cm. is noted containing few septations protruding from the subhepatic area to the peripancreatic region (Fig. 2). Inflammatory thickening

[1]Department of Radiology, Ramathibodi Hospital, Rama 6 street, Bangkok 10400, Thailand.
[2]Department of Surgery, Ramathibodi Hospital.

of the surrounding fat and the gallbladder was noted (Fig. 3). Explore-laparotomy was performed, a large hepatic abscess was found about 8 cm. in diameter, protruding from the liver surface (segment IV) with a liver fluke 1 X 1.5 cm in this abscess. Intraoperative cholangiography was normal. Draining of the abscesses and cholecystectomy were performed. Pus culture showed no growth after 3 days. Histologic analysis showed a parasitic cyst, Fasciola specie in the liver tissue. Gall Bladder specimen showed evidence of cholecystitis.

After medical treatment with Albendazole, improvement was seen clinically. Sonography obtained at 3 weeks later showed multiple small hypoechoic areas in the medial segment of left lobe with mild hepatomegaly (Fig. 4).

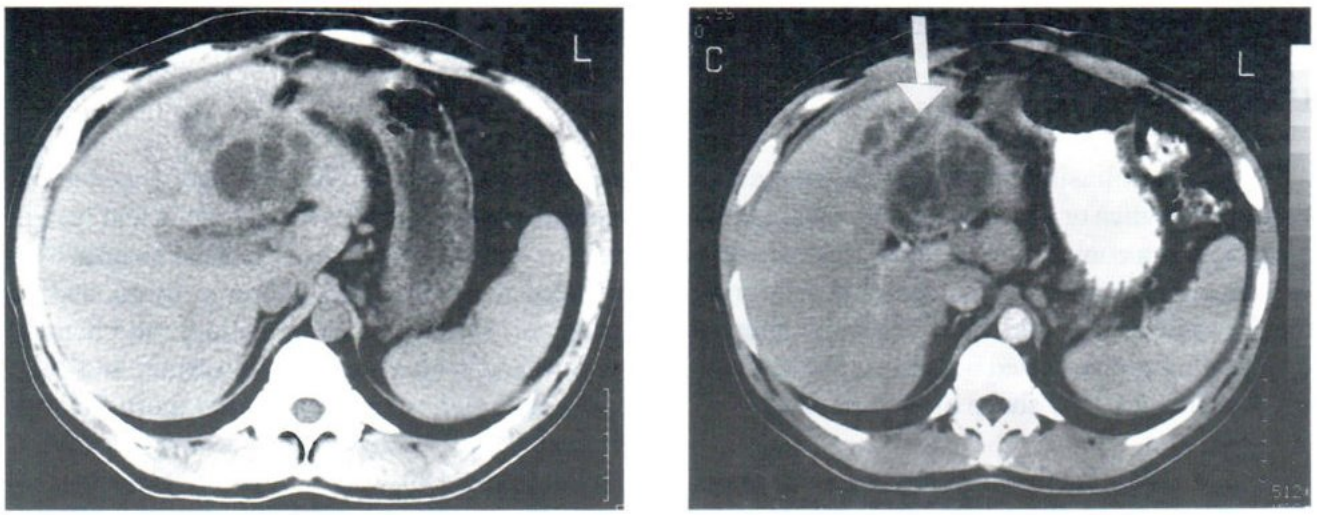

Fig.1 CT scan of the liver revealed a cluster of small, low density areas in subhepatic region of left lobe with tract like fashion (arrow). Minimal free fluid was seen at anterior aspect of the liver (arrowhead).
A. unenhanced B. contrast enhanced study

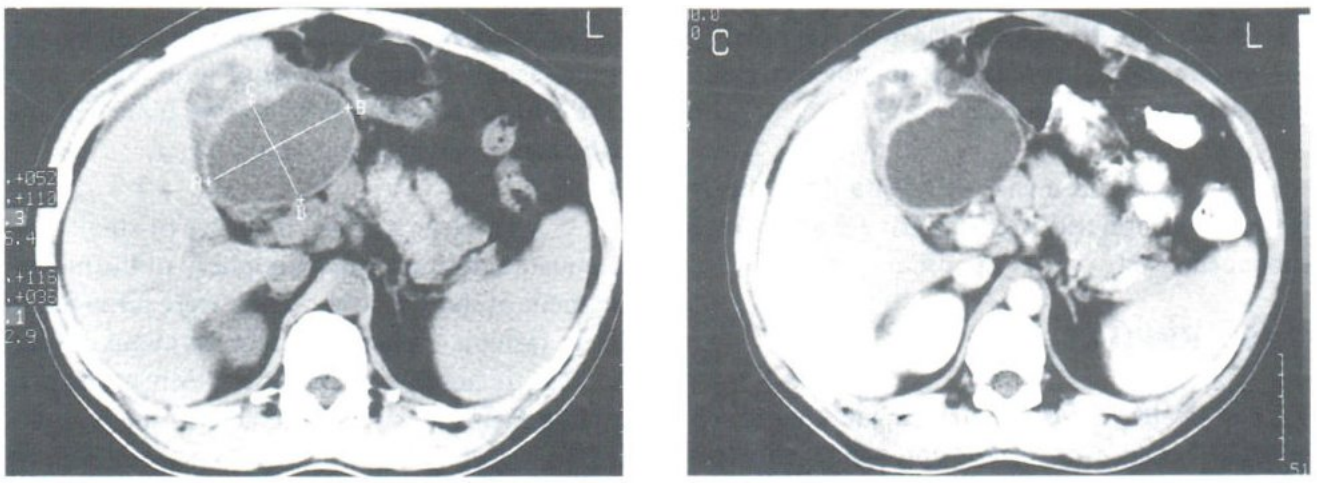

Fig. 2 Large cystic mass containing few septations protruded from the subhepatic area to pancreatic head region
A. unenhanced B. contrast - enhanced study

DISCUSSION

Human fascioliasis results from the ingestion of metacercaria contaminated plants and water. The clinical course has two stages. The first stage or acute stage is the stage of hepatic invasion. When the metacercaria hatches in the digestive tract, the immature fluke penetrates the intestinal wall and enters the abdominal cavity. It then penetrates Glisson's capsule and enters the liver parenchyma. This stage usually lasts 1-3 months, is characterized by fever, pain in the right upper abdomen, hepatomegaly and eosinophilia. No eggs or flukes are detected, but the results of serologic tests are usually positive.[7] In the second or chronic stage begins after the immature flukes migrate throughout the liver until they reach the bile ducts. The immature flukes

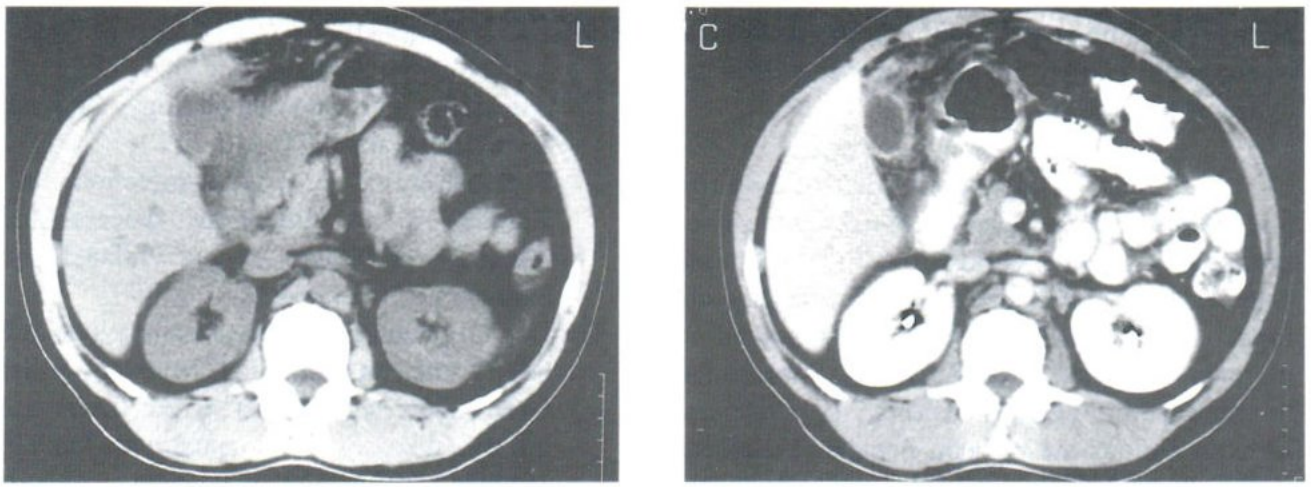

Fig. 3 Inflammatory thickening of the surrounding fat and the gallbladder (arrowhead)
A. unenhanced B. contrast enhanced study

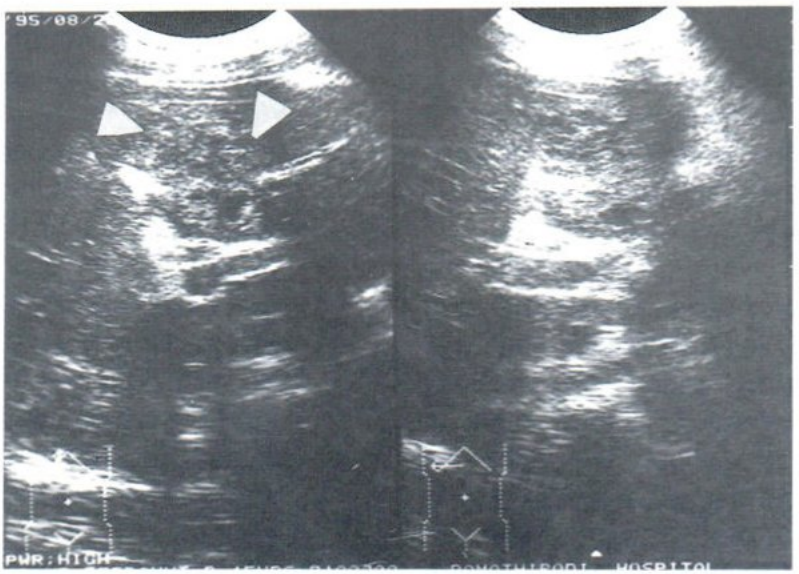

Fig. 4 Sonogram taken 3 weeks later showed ill defined hypoechoic areas in the left lobe of the liver (arrowheads).

mature in the bile ducts after 2 months and produce eggs and metabolites which irritated the bile duct mucosa. The symptoms are caused by the obstruction of the bile ducts such as recurrent episode of biliary colic, angiocholitis and cholecystitis.[1,8-10] The diagnosis is enabled by identification of flukes or eggs in the bile fluid or feces.

Complications of hepatic fascioliasis are invasion of the gallbladder, hepatic subcapsular hemorrhage, hemobilia and ectopic migration causing pulmonary infiltration, lung mass or hydropneumothorax.[11]

The CT characteristics of hepatic fascioliasis [8,12] are 1). clusters of microabs-cesses arranged in tract-like fashion. The tortuous channels have also been described at surgery and laparoscopy[13] and probably correspond to migratory tracts left by the flukes. 2). Subcapsular location of the hepatic lesions. If peripheral tortuous lesions are present, hepatic fascioliasis should be the primary consideration. 3). Very slow evolution of the lesion on follow up examination.

In our patient, he had clinical symptom of fever, right upper abdominal pain and mild abnormal liver biochemical test. The initial diagnosis was difficult because of no peripheral eosinophilia. CT scan showed clusters of small abscesses with nodular and tract-like fashion, located at subcapsular area of the liver, corresponded to previous reports.[6-9] Small perihepatic fluid could be secondary from the penetration of Glisson's capsule by the liver flukes. The large cystic mass with thin enhancing wall containing internal septations suggested complicated cyst or abscess. This finding occurred because the immature flukes were trapped in the immediate subcapsular tissue of the liver where they died leaving a cavity filled with necrotic debris. Therefore, most of the hepatic lesions were confined to a depth less than 2 cm, beneath the capsule.[14] However, the CT findings may be impossible to differentiate from the cluster appearance of small pyogenic abscesses.[15]

In summary, hepatic fascioliasis may be presented without peripheral eosinophilia. CT characteristics of cluster of microabscesses arranged in tract like fashion and subcapsular location may be helpful in the diagnosis. Perihepatic cysts may be the complications of the disease.

REFERENCES

1. Suh BS. Clinical parasitology, 2nd ed. Seoul:Ilchokak, 1978: 217-219.
2. Barrett-Connor E. Fluke infection. In: Braude AI ed. Infectious disease and medical microbiology. 2nd ed. Philadelphia: Saunders, 1986:979-982.
3. Ong GB. Helminthic disease of the liver and biliary tract. In: Wright R, Millward-Saller GH, Albert KGMM, et al, eds. Liver and biliary disease. London:Balliere Tindall, 1985:1523-1545.
4. Rajab M, Farag HF. On human fascioliasis in Egypt. J Egypt Med Assoc 1978;61:773-780.
5. Wong RKH, Peura DA, Mutter ML, et al. Hemobilia and liver flukes in a patient from Thailand. Gastroenterology 1985;88:1958-1963.
6. De Miguel F, Carrasco J, Garcia N, et al. CT findings in human fascioliasis. Gastrointest Radiol 1984;9:157-159.
7. Goebel N, Markwalder K, Siegenthaler W. Fascioliasis hepatis: computed tomography appearance. Radiology 1985;156:863.
8. Takeyama M, Okumura N, Sakai Y, et al. Computed tomography findings in hepatic lesions in human fascioliasis: report of two cases. Am J Gastroenterol 1986;81:1078-1081.
9. Serrano M., Vega A, Ortega E, Gonzalez A. Computed tomography of hepatic fascioliasis. J Comput Assist Tomogr 1987;11:-269-272.

10. Joon Koo Han, Byung Ihn Choi, Jae Min Cho, et al. Abdom Imaging 1983;18:264-264.
11. Acuna-Solo R, Braun-Roth G. Bleeding ulcer in the common bile duct due to Fasciola hepatica. Am J Gastroenterol 1987;82:560-562.
12. Beus Van Bernard, Jacques P, Andre G, et al. Hepatobiliary Fascioliasis: noninvasive imaging findings. Radiology 1990;174:-809-810.
13. Moreto M, Barron J. The laparoscopic diagnosis of the liver fascioliasis. Gastro-intest Endosc 1980;25:147-149.
14. Acosta-Ferreira W, Vercelli-Retta J, Falconi LM. Fasciola hepatica Human Path Anat Histol 1979;383:319-327.
15. Brokk JR, Corito TS, Frank CC, Michael FP. CT of small pyogenic hepatic abscesses: the cluster sign. AJR 1988;151:487-489.

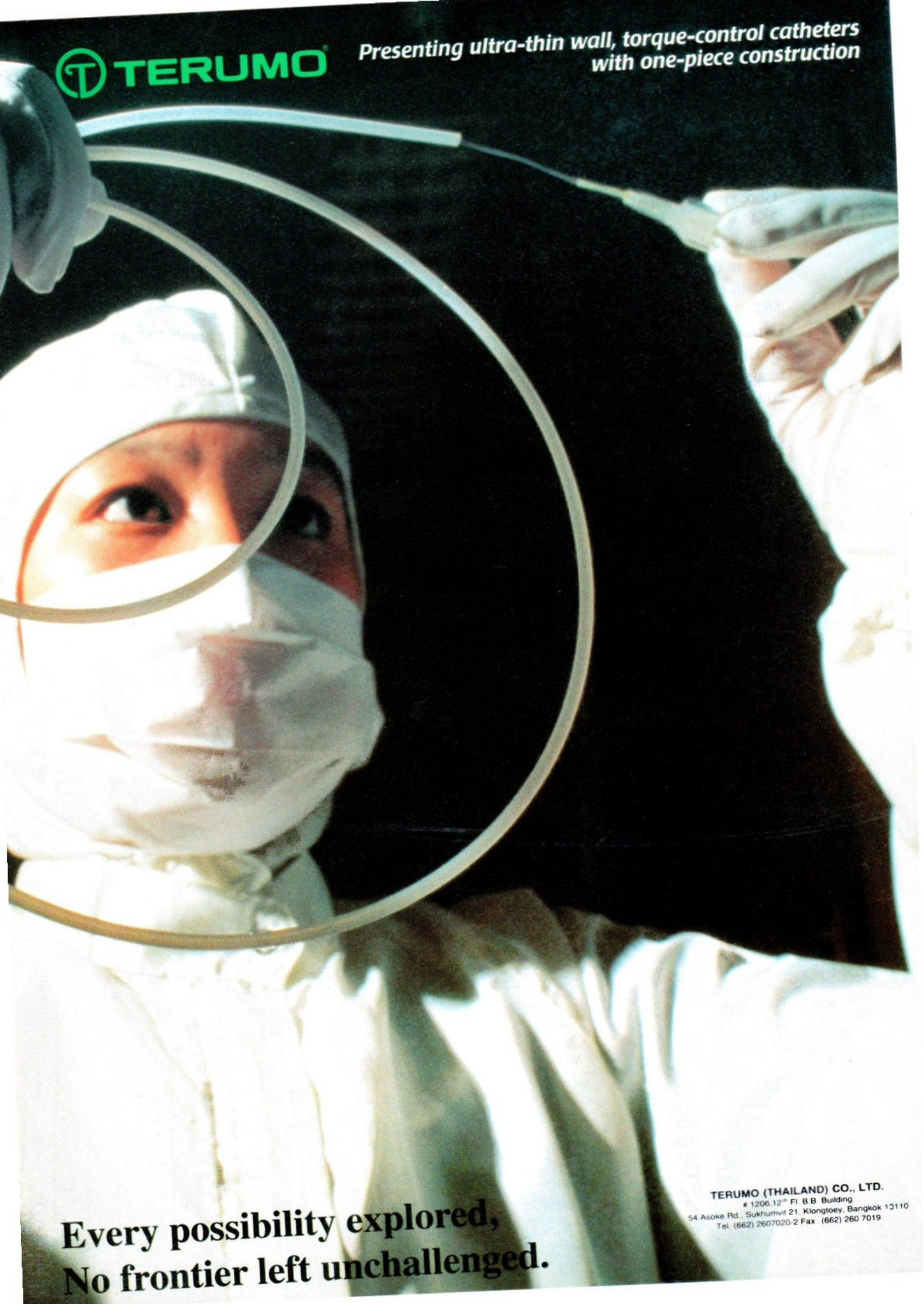
TERUMO
Presenting ultra-thin wall, torque-control catheters with one-piece construction
TERUMO (THAILAND) CO., LTD.
1206,12th Fl. B.B. Building
54 Asoke Rd., Sukhumvit 21, Klongtoey, Bangkok 10110
Tel. (662) 2607020-2 Fax (662) 260 7019
Every possibility explored,
No frontier left unchallenged.

SUBCAPSULAR HAEMATOMA OF THE LIVER IN A CASE ODISSEMINATED INTRAVASCULAR COAGULATION SECONDARY TO A BLEEDING PLACENTA PREVIA

BJJ ABDULLAH[1] , H KAUR[1] , ARUMUGAM K[2]

ABSTRACT

The following case report is on a 43 year old lady who had presented with profuse antepartum haemorrhage due to a placenta praevia Type 4 anterior. Following hysterectomy she developed DIVC that was corrected with platelets and FFP. Subsquently on 7th. Post-op day she had complains of abdominal distension and right hypochondrium fullness. An ultrasound and CT scan was done which showed a large subcapsular haematoma of the liver. This was then aspirated.

Formation of a subcapsular haematoma following DIVC is a rare event. No case of subcapsular haematoma has been reported following DIVC from a bleeding placenta praevia.This case illustrates the pathophysiology of DIVC as well as the imaging modalities in the diagnosis of a subcapsular haematoma.

Spontaneous subcapsular haematoma of the liver is a rare event. In most of the reported cases it was most often associated with toxaemias of pregnancy (2,4,5,6). No cases of spontaneous subcapsular haematomas have been reported following haemorrhage due to placenta praevia. The following report is of a case of Type 4 anterior placenta praevia who suffered excessive blood loss from ante and postpartum haemorrhage which eventually led to disseminated intravascular coagulation.

DIVC = Disseminated Intravascular Coagulation
FFP = Fresh Frozen Plasma

INTRODUCTION

Spontaneous subcapsular haematoma of the liver is a rare complication of pregnancy. The underlying factor is hepatic necrosis, the most likely cause being vascular disease (particularly toxaemias) and Disseminated Intravascular Coagulation (DIC). The incidence of liver haematoma in pregnancy is not known. In most of the reported cases during pregnancy, it was most often associated with toxaemias of pregnancy, other causes being fatty metamorphosis, hepatoma, diabetes and hypertension. Spontaneous subcapsular haematomas following hemorrhage

[1] Departments of Radiology
[2] Obstretics and Gynaecology

Address correspondence to: BJJ Abdullah, Department of Radiology, Universtiy of Malaya Medical Center, University of Malaya, 50603 Kuala Lumpur, MALAYSIA.

secondary to a placenta previa has not been reported before. The following report is of a case of Type 4 anterior placenta previa who suffered excessive blood loss from ante and postpartum haemorrhage which eventually led to disseminated intravascular coagulation, and developed a subcapsular haematoma of the liver.

CASE HISTORY

A 43 year old Gravida 8 Para 7 lady with a period of amenorrhoea of 26 weeks was admitted with sudden profuse per vaginal bleeding. She was having episodes of slight per vaginal bleeding for the past one month, though fetal movements were normal. There was no rupture of membranes nor was there fever. Her previous pregnancies were uneventful. On examination the patient was pale was otherwise stable with normal blood pressure and pulse. There was no evidence of pre-eclampsia of pregnancy.

Abdominal examination showed a uterus of 26 weeks. An ultrasound abdomen was done at admission and showed a single normal foetus with a Type 4 anterior placenta previa. Patient had an emergency Lower Section Caesarian Section (LSCS) on the 26th day of admission for persistent and profuse antepartum haemorrhage. However, immediately after the LSCS, she had massive postpartum haemorrhage and a haematological examination done showed prothrombin time to be raised i.e. 2.06, a low platelet count i.e. 87,000 E9/L and low fibrinogen levels i.e. 0.9G/L, consistent with that of DIVC. A total abdominal hysterectomy was done and the DIVC was corrected with platelets and fresh frozen plasma. On the 7th post-operative day, patient started to complain of abdominal distension and fullness over right hypochondrium. Chest radiograph revealed plate atelectasis in the right lung base. Ultrasound of abdomen showed a mixed echogenic mass inferior to the right lobe of the liver and anterior to the right kidney (Fig.1). This measured 14 x 10.5 x 8 cm. and was compatible with a large subcapsular haematoma of the liver.

A computed tomogram (CT scan) of the abdomen showed a large hypodense, well-defined, peripheral, subcapsular collection situated at the inferior aspect of the right lobe of liver. No enhancement of this collection was seen following intravenous contrast media. The CT value of this mass was 30 Hounsfield units (HU) which was consistent with that of blood (Fig.2). The haematoma was causing deformity of the liver. A diagnosis of a subcapsular haematoma was made.

Aspiration of this collection was done using a 16G branula under ultrasound guidence. This was done to relieve the patient of pain and discomfort. A total of 250cc of stale blood was aspirated. Following the aspiration, she was discharged well, and remained well on follow up 1 month later.

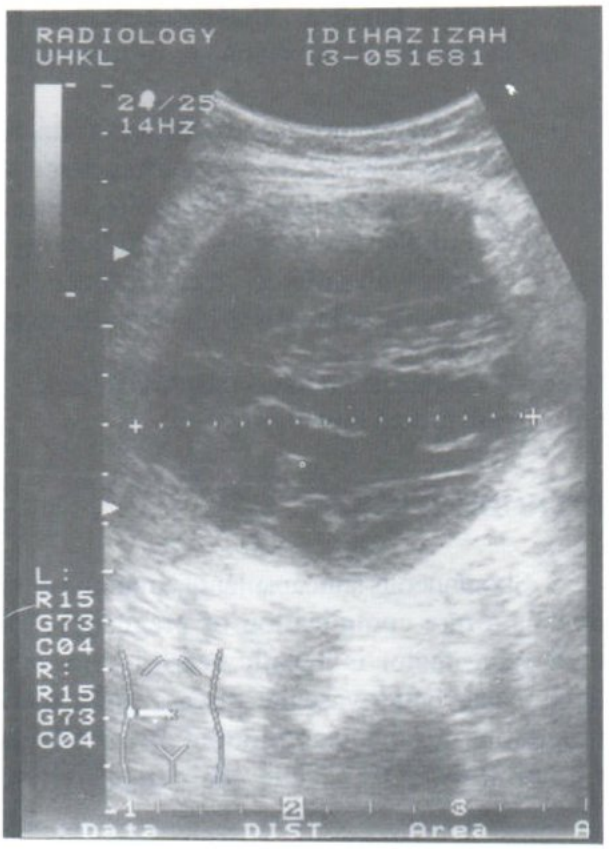

Fig.1. Ultrasound liver shows a large mass of mixed echogenicity inferior to the right lobe of liver.

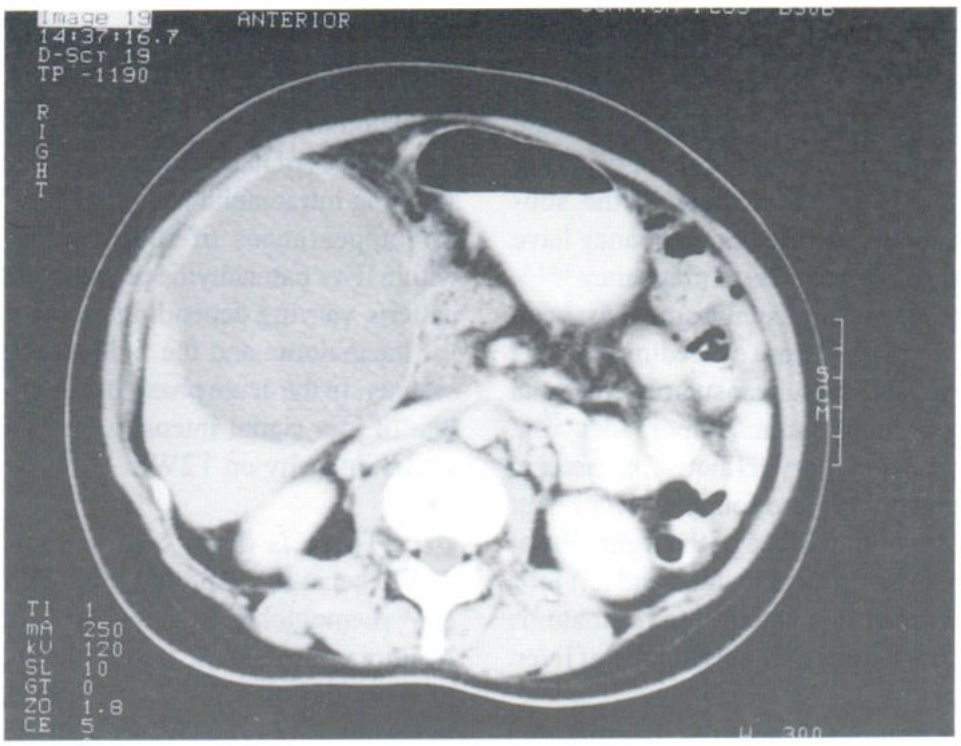

Fig 2. CT abdomen (axial) shows a non enhancing homogenous collection. The liver appears deformed.

DISCUSSION

Disseminated Intravascular Coagulation is defined as defective haemostasis due to the activation of the coagulation system by recognised triggers leading to the consumption of clotting factors and platelets[1]. Common causes of consumptive coagulopathy during pregnancy are intrauterine fetal demise, sepsis, amniotic fluid embolism, induced abortion, pre-eclampsia or eclampsia, excessive bleeding and acute fatty liver.

The key pathophysiological derangement in most obstetric cases is hypofibrinogenemia as in this case. Activation of the coagulation system by recognized triggers leads to the consumption of clotting factors and platelets. Coagulation inhibitors are swamped and large amounts of fibrin are formed and deposited in the small vessels of multiple organs, including the kidney, lung and brain. Ischaemic tissue damage and micro-angiopathic haemolysis may result. In the liver, tissue damage usually occurs at the periphery of the hepatic lobule especially involving the right lobe[3]. This accounts for the subcapsular haematoma that occurs.

Simultaneously, the fibrinolytic mechanism is activated to lyse the fibrin deposits. Thrombocytopenia, the depletion of coagulation factors, and the anticoagulant effect of fibrin degradation products all contribute to the continued bleeding that occurs in DIVC. Consumptive coagulopathy is usually manifested clinically by visible signs of disruption of normally intact haemostasis. These signs may include bleeding from venipuncture of intravenous access sites, gums, nose, vagina or rectum.

Haematuria, ecchymoses or petechiae and bleeding from surgical wounds or laceration may be evident. Subcapsular haematoma of the liver

and its rupture into the peritoneal cavity have been reported before[3]. However the incidence of subcapsular haematoma is not known. This case is unique as, a subcapsular haematoma occuring following DIVC is rare and most of the subcapsular haematomas reported in pregnancy have been associated with toxaemias of pregnancy [3,4,5,6]. No case of subcapsular haematoma has been reported following DIVC from a bleeding placenta previa. Other causes of a subcapsular haematoma are penetrating or blunt trauma, tumor, aneurysm or abscess and post surgery. Ninety-five percent of hepatic haematomas were found to occur over the anterior or superior surface of the right lobe of liver[3], other areas being caudate lobe and left lobe of liver. However in this patient the haematoma was at the inferior aspect of the right lobe of liver.

On ultrasound subcapsular haematoma appears sonographically solid with heterogenous echogenicity. Over time, cystic evolution of a subcapsular haematoma occurs. The haematoma retracts in size and becomes more cystic in appearance, often with multiple septations[7]. US is cheap, fast and has no radiation and its portability makes it ideal in the patient in Intensive Care Unit as well as for follow-up.

On axial CT of the abdomen subcapsular haematomas usually appear as crescent-shaped or lenticular well-marginated collections located just beneath the hepatic capsule. The density of the collection depends on the age of the haematoma, being of higher attenuation than non-contrast-enhanced liver early when clotted blood is present and decreasing in attenuation over time to low attenuation.

Most haematomas appear hypodense when compared with contrast-enhanced liver parenchyma, although freshly clotted blood usually remains hyperdense with enhanced liver parenchyma. It is also possible to quantify the amount of blood present in the pelvis as well as the amount of blood surrounding the liver[8].

There has been no reported experience with magnetic resonence imaging (MRI) in subcapsular haematoma.. Most knowledge concerning the MR appearances of haematomas has been from reports studying intracranial haemorrhage. Therefore the MR appearances of subcapsular haematomas within liver parenchyma probably follow the same pattern, varying depending on the time course of the haematoma and the field strength of the MR scanner. In the acute phase haemorrhage is usually that of low signal intensity on TIWI and higher signal intensity on T2WI.

There is often central hypointensity on T2WI because of preferential T2 shortening of deoxyhemoglobin. In the subacute phase, typically beginning around 72 hours, the methemoglobin present shortens the T1 of blood, resulting in hyperintensity on TIWI as well. This is initially seen at the periphery of haematomas and increases centrally over time. In the chronic haematoma a peripheral low signal rim may be seen as a result of formation of hemosiderin.

Other causes of post-operative right hypochondrium pathology that must be considered include liver abscess, Budd - Chiari syndrome, biloma, aneurysm and cholecystitis. However the US, CT scan and MRI features would be useful to differentiate between them.

The treatment of subcapsular haematomas of the liver is somewhat controversial. Left alone they may resolve spontaneously, expand and burst with delayed intraperitoneal bleeding, cause a hepatic abscess or decompress into the biliary tree and cause hematobilia[1]. With the imaging facilities available i.e. ultrasound, computed tomography and magnetic resonance imaging, nonoperative management of subcapsular or intraparenchymal haematomas has become popular i.e aspiration of the haematoma is preferably done under CT or US guidance. The CT scan allows one to accurately assess the severity of the liver subcapsular haematoma.

In summary, this case illustrates a rare complication of DIVC induced by haemorrhage from a placenta previa. Clinical findings and laboratory investigations strongly raise the suspicion of DIVC . The diagnosis of a subcapsular haematoma was then established by ultrasound and CT scan following which treatment was initiated by aspiration of the haematoma under ultrasound guidance.

REFERENCES

1. Gibson B. Disseminated Intravascular Coagulation In Philipp E, Setchell M & Ginsberg J (eds) Scientific Foundations Of Obstetrics And Gynaecology Butterworth-Heinemann, Oxford, 1991, 4th Edtion, pp-556
2. Richey M.E., M.D., Gilstrap L.C., III, M.D., and Ramin S.M., M.D. Management Of Disseminated Intravascular Coagulation. Clinical Obstetrics and Gynecology 1995;-38:514 -519.
3. Browne C.H., Hanson G.C. ,De Jode L .R. and Roberts P.A.. Rupture of Subcapsular Haematoma Of The Liver In A Case Of Eclampsia. Br. J. Surg. 1975; 62 : 237-238
4. Hibbard L.T., M.D. Spontaneous Rupture Of The Liver In Pregnancy : A Report Of Eight Cases. Am. J. Obstet. Gynecol. 1976;126: 334-337.
5. Stevenson J.T., M.D., Graham D.J., M.D. Hepatic Hemorrhage And The HELLP Syndrome : A Surgeon's Perspective. The American Surgeon 1995;61: 756-759.
6. Manas K.J., M.D.,Welsh J.D., M.D., Rankin R.A., M.D. and Miller D.D., M.D. Hepatic Haemorrhage Without Rupture In Preeclampsia. The New England Journal Of Medicine 1985;312: 424- 426.
7. Abbitt L. P. Subcapsular Hematoma. In Ultrasound: A Pattern Approach. McGraw-Hill Inc.,1995, pp 41.
8. Baron RL, Freeny PC & Moss AA. The Liver. In Moss, Gamsu, Genant (eds) C.T. of the body with M.R.I. 2nd edition. Philadelphia, W.B. Saunders Company, 1992, pp 813-814.

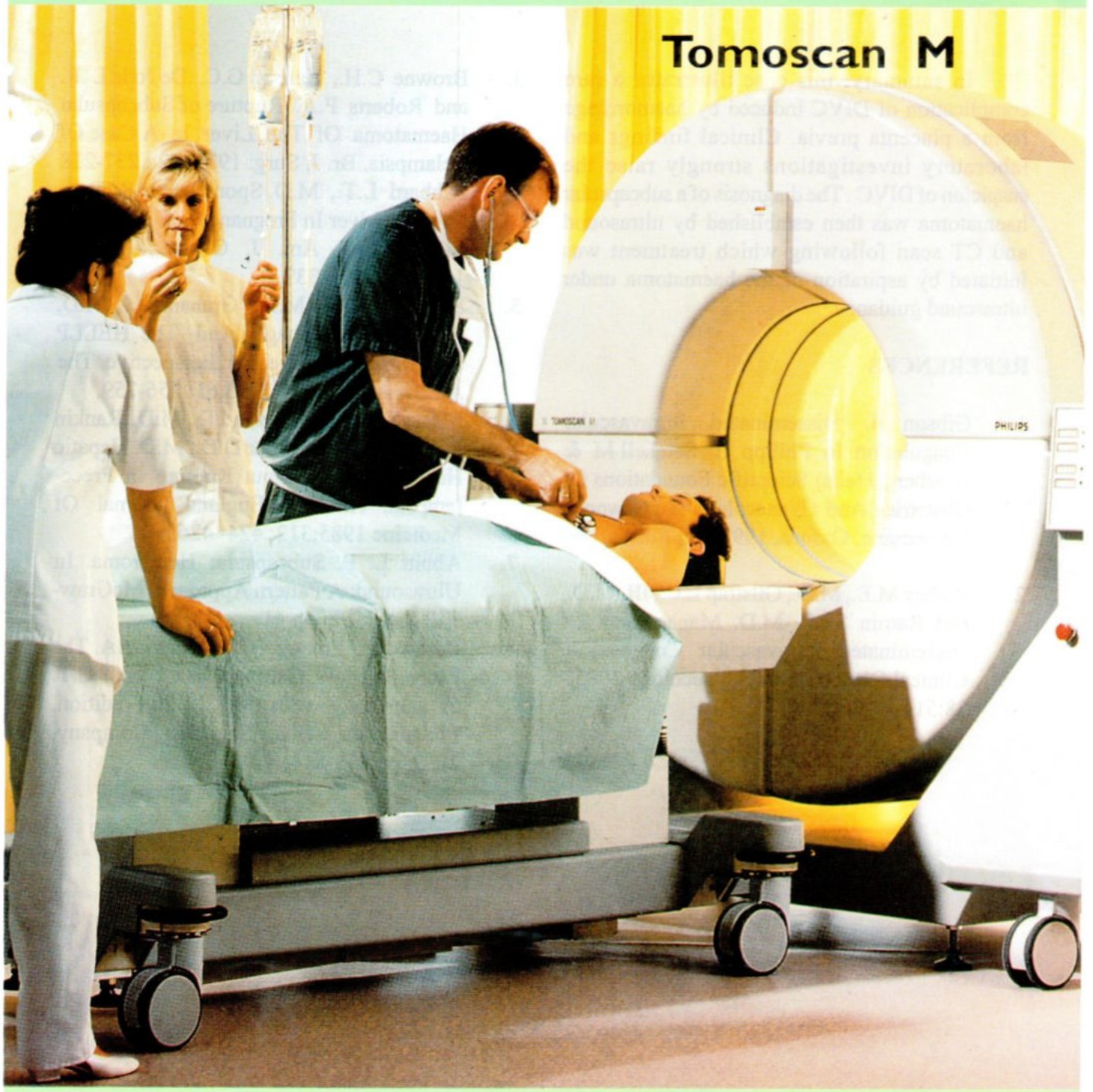

FOR MORE INFORMATION PLEASE CONTACT
PHILIPS MEDICAL SYSTEMS
• TEL. 745-4090 Ext. 3332
• FAX. 398-0792

Imported by
Philips Electronics (Thailand) Ltd.
209/2 Sanpavuth Road, Prakanong, Bangkok 10260

Let's make things better.

PHILIPS

PHILIPS

MAMMOGRAPHIC AND SONOGRAPHIC FEATURES OF MONDOR'S DISEASE

ANGSANA NIMMONRAT,M.D, MALAI MUTTARAK,M.D.

ABSTRACT

Mondor's disease, or superficial thrombophlebitis of the breast, is an uncommon condition. It has been associated with benign causes including direct trauma, operative trauma, extensive physical activity ,and rarely with breast carcinoma. The disease is usually self-limiting. Mammographic and sonographic findings of two cases of Mondor's disease are presented. Familiarity with this condition will help to avoid unnecessary biopsy.

Key words; Mondor's disease,breast,mammography,sonography.

INTRODUCTION

Mondor's disease is a rare, benign, thrombophlebitis of the subcutaneous vein on the anterolateral thoracoabdominal wall, usually in or near the breast.[1] The disease has been associated with direct trauma, breast surgery, extensive physical activity,[2,3] and rarely with breast carcinoma.[4-6] The cord of the thrombosed superficial vein is usually both visible and palpable. When unrecognized, it may result in an unnecessary recommendation for biopsy. Familiarity with its clinical and radiographic findings is essential and helps to avoid unnecessary biopsy.

We present two cases of Mondor's disease.

CASE REPORT;

Case 1:

A 36 year-old woman noticed a non-tender mass in her left breast for 4 days. She denied any medication or trauma. Physical examination revealed a rope-like mass in the upper outer quadrant of the left breast with no axillary mass. Mammograms demonstrated a 5-cm, rope-like lesion in the upper outer quadrant of the left breast (fig.1). Ultrasonography revealed a superficial hypoehoic tubular structure (fig 2). An anti-inflammatory drug was given, and the mass completely resolved in 2 weeks.

Case 2:

A 34 year-old-woman recognized a non tender mass in her right breast 1 week before coming to the hospital. She had taken hormonal supplement for 6 months after her transabdominal hysterectomy and bilateral salpingo-oophorectomy. Physical examination revealed a cord-like mass in the upper outer quadrant of the right breast with minimal skin retraction. No axillary mass was palpable. Mammograms revealed a 4-cm. longitudinal, superficial, tubular shaped lesion in the upper outer quadrant of the right breast. Ultrasound showed a hypoechoic cord-like lesion. The mass completely disappeared in 2 weeks without any treatment.

Department of Radiology,Chiang Mai University Chiang Mai 50200,Thailand

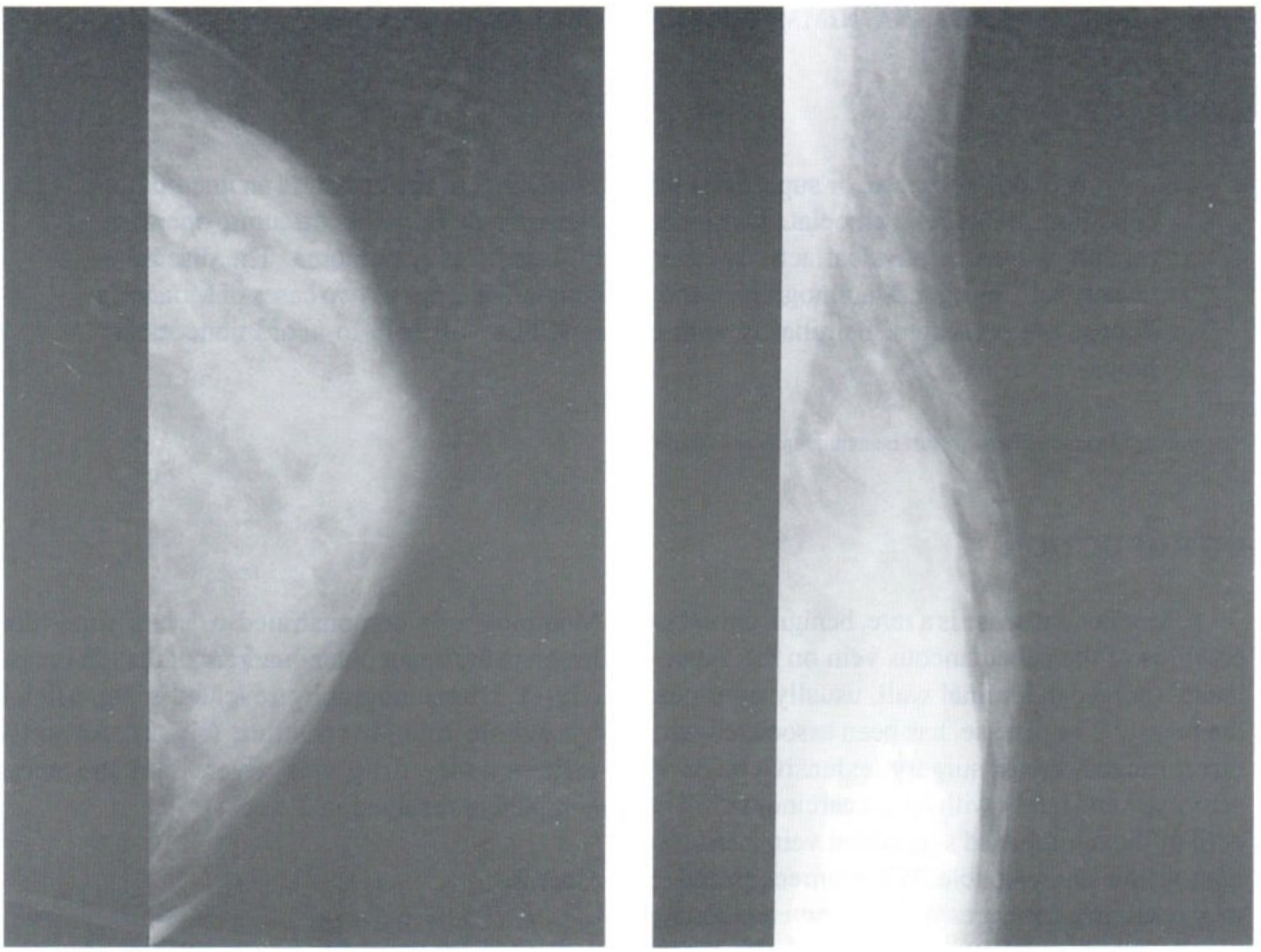

Fig 1. Craniocaudal(A) and tangential(B)mammograms show bead-like density in the upper outer quadrant of the breast.

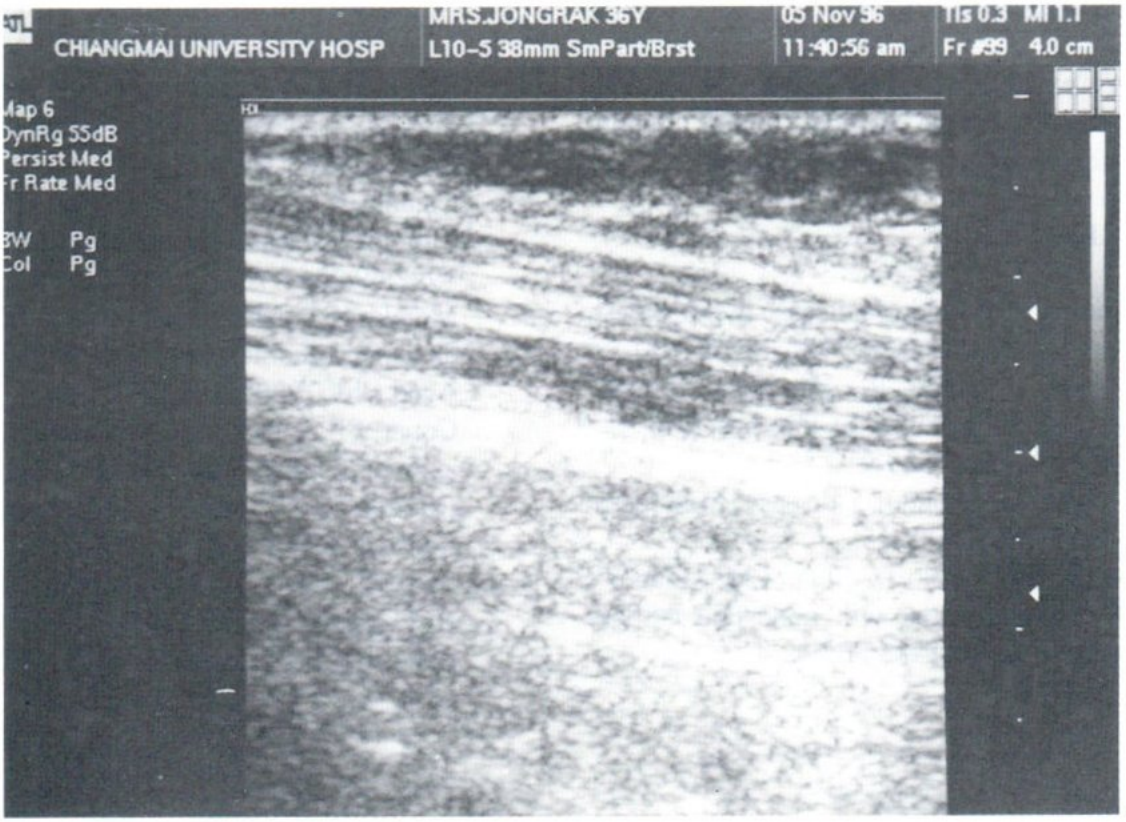

Fig. 2. Sonogram shows a hypoechoic tubular structure.

DISCUSSION

Mondor's disease was first described in 1939 by a French surgeon, Henri Mondor as subcutaneous angiitis of the breast.[7] Since then, the disease has carried his name. Less than 300 cases of Mondor's disease have been reported in the world literature[1-7] and there are few descriptions of the mammographic and sonographic findings.[1,6,8] It occurs three times more common in women than in men.[6,9] The etiology of the disease is unknown but has been associated with benign causes including local trauma, operative trauma,extensive physical activity[2,3] and rarely with breast carcinoma.[4-6] The diagnosis is usually made clinically by the presence of a painful cord-like structure beneath the skin of the breast. Occasionally, the radiologist has the opportunity to do mammography for the palpable abnormality. The tangential view is a good projection to demonstrate the thrombosed portion of the superficial vein and help to differentiate it from dense breast parenchyma or isolated ductal dilatation.[1,8] The thrombosd vein is seen on mammogram as the thickened rope-like density located superficially in the breast. Sonography confirms a superficial,hypoechoic tubular structure. Our two cases had no history of trauma,surgery or breast carcinoma. The thrombosed vein spontaneously resolved within a few weeks. Mammographic and sonographic follow-up showed resolution of the abnor-mality. As breast imaging is more widely used for symptomatic women,familiarity with the clinical and radiologic findings of Mondor's disease will help to obviate biopsy.

ACKNOWLEDGEMENT:

We express our appreciation to Dr.Paul Longstreth (McKenzie Medical Center, Oragon, U.S.A.)for reviewing the manuscript.

REFERENCES

1. Camiel Mr.Mondor's disease in the breast. Am J Obstet Gynecol 1985;152:879-81.
2. Honig C, Rado R. Mondor's disease: Superficial phlebitis of the chest wall.Ann Surg 1961;153:589-91.
3. Hogan GF. Mondor's disease. Arch Intern Med 1964;113:881-5.
4. Miller Dr,Cesario TC,Slater LM. Mondor's disease associated with metastatic axillary nodes. Cancer 1985;56:903-4.
5. Chiedozi LC. Aghahowa JA. Mondor's disease associated with breast cancer. Surgery 1988;103:438-9.
6. Catania S, Zurrida S, Veronesi P, et al. Mondor's disease and breast cancer.Cancer 1992:69:2267-70.
7. Mondor H.Tronculite sous-cutanee subaigue de la paroi thoracique antero-laterale. Mem Acad Chir 1939;65:1217-8.
8. Conat EF, Wikes AN , Mendelson EB, et al. Superficial thrombophlebitis of the breast (Mondor' s disease) : Mammographic findings.AJR 1993;160:1201-3.
9. Farrow JH. Thrombophlebitis of the superficial veins of the breast and anterior chest wall.Surg Gynecol Obstet 1955;101:-63-8.

COMPUTED TOMOGRAPHY OF SMALL BOWEL OBSTRUCTION

Pannee VISRUTARATNA, M.D., Nongyao PITAKKITRONAKORN, M.D.

ABSTRACT

Abdominal computed tomographs done between May and August 1996 of 5 patients with signs and symptoms of small bowel obstruction are reviewed. Four of these patients proved to have small bowel obstruction. The causes were adhesions (2 patients), peritoneal carcinomatosis (1 patient), and obturator hernia (1 patient). Thickening of the small bowel wall, submucosal edema of the small bowel, and ascites were seen in one of these four patients, who on surgery proved to have gangrene of the terminal ileum. On surgery the fifth patient was found to have radiation enteritis but no bowel obstruction.

INTRODUCTION

Small bowel obstruction is commonly encountered by surgeons and radiologists. This diagnosis is made on the basis of the patient's signs and symptoms. Plain abdominal radiography is usually used to confirm this diagnosis. Sometimes barium studies may be done to show the site and cause of obstruction. Recently computed tomography (CT) has been shown to be useful in revealing the site and cause of obstruction and possible bowel ischemia.[1-7]

MATERIALS AND METHODS

Abdominal CT scans done between May and August 1996 of 5 patients with signs and symptoms of small bowel obstruction were reviewed. There were 4 females and 1 male with ages ranging from 26 to 74 years with a mean of 51.4 years. The CT scans were done immediately after a 100-ml intravenous bolus injection of contrast medium using 10-mm slice thickness and 12-mm spacing for the entire abdomen. In two of these patients 2% iodinated water-soluble contrast medium was also administered orally 1 hour before scanning.

RESULTS

The clinical histories, CT findings, and treatments are in Table 1. The causes of small bowel obstruction in the first two patients (cases 1 and 2) were adhesions. CT scans showed the sites of obstruction in both cases. There were no masses at the obstruction sites (Fig. 1). In case 2, CT also showed signs of strangulation of the small bowel (Fig. 2). In case 3, CT scans showed obstruction of the small bowel by one of the masses of the peritoneal carcinomatosis (Fig. 3).

The CT scans in case 4 showed obstruction of the ileum and the small bowel loop in the right obturator canal (Fig. 4) consistent with a right obturator hernia causing small bowel obstruction, but there was no proof of this because this elderly patient's relative requested no surgery be done.

In case 5, a false diagnosis of small bowel obstruction was made (Fig. 5). The CT findings

Department of Radiology, Faculty of Medicine, Chiang Mai University, Chiang Mai 50200, THAILAND

were dilatation of the jejunum and ileum, and thickening of the wall of the terminal ileum and the ascending colon. On surgery, the patient was found to have radiation enteritis, but no bowel obstruction.

TABLE 1.

Patient No.	Clinical History	CT Findings	Treatment
1 42 y/F	Known CA rectum stage III, AP resection and colostomy 6 months prior. Chemotherapy and radiation therapy	Dilatation of jejunum and ileum. Distal ileum not dilated. Submucosal edema of segment of ileum.	Resection of distal ileum, end-to-end anastomosis, lysis of adhesions
2 52 y/F	Trans-abdominal hysterectomy, bilateral salpingo-oophorectomy and omentectomy for myoma uteri and endometriosis 7 years prior.	Dilatation of small bowel. Decrease in air in large bowel. Thickened wall of distal ileum, submucosal edema and ascites	Resection of the gangrenous segment of distal ileum, right half colectomy, lysis of adhesions
3 26 y/M	Right half colectomy for CA colon 2 years prior. Jejuno-sigmoidostomy for small bowel obstruction from peritoneal carcinomatosis in another hospital 20 days prior.	Dilatation of jejunum and ileum. Obstruction of ileum by masses in mesentery and pelvic cavity. Masses in greater omentum and recto-vesical pouch.	Symptomatic
4 74 y/F	No previous surgery	Obstruction of distal ileum by right obturator hernia.	Surgery refused
5 63 y/F	CA Cervix stage IIIB, in radiation therapy	Dilatation of jejunum and ileum. Thickening of wall of terminal ileum and ascending colon.	Intraoperative bowel decompression

DISCUSSION

Radiologic images supplement the patient's signs and symptoms to establish or exclude a diagnosis of small bowel obstruction, determine the level and site(s), establish a cause, and predict whether strangulation is present. The causes of small bowel obstruction vary; in general, the most common being adhesions, hernias, and neoplasms.[8]

Plain abdominal roentgenographic findings serve as the basis for a diagnosis of small bowel obstruction only 50-60% of the time.[9,10] They also can not be distinguished strangulating from non-strangulating obstruction easily. In the cases with strangulation, plain abdominal roentgenographic findings were positive in only 30% of the time.[11]

When the clinical picture or plain film examination does not lead to a diagnosis, further studies are necessary. Either small bowel series or barium enemas have been used in these situations. Our experience is that because most of

our patients do not seek medical help promptly, the small bowel series may require hours and peristaltic activity has been diminished. Furthermore the barium is diluted in the retained intestinal fluid. The point and cause of small bowel obstruction are difficult to be determined. Occasionally barium enemas are helpful in patients with distal small bowel obstruction when the barium refluxes into the terminal ileum.

The sensitivity of CT in diagnosing small bowel obstruction is 94-100%.[1,5,6] In one study the cause of obstruction was predicted correctly in 47 of 64 cases (73 %).[1]

A great variety of obstructive processes can be demonstrated by CT. The diagnosis of adhesions is made after all other causes of obstruction have been eliminated.[1] Most adhesions cannot be seen.

Obturator hernia is rare as a cause of intestinal obstruction. It is difficult to be diagnosed and has a high mortality rate.[12] The characteristic clinical profile is an elderly, emaciated, ill woman with intestinal obstruction but no previous abdominal surgery. The incidence of correct preoperative diagnosis is 20-30%. The contents of an obturator hernial sac vary. Small bowel is most commonly encountered, the ileum being more frequent than the jejunum. There have been a few reported cases which have shown the usefulness of CT in diagnosing an obturator hernia causing small bowel obstruction.[13,14]

Intestinal obstruction in patients with previously treated cancer is common. It has occurred in up to 28% of patients with a history of colorectal cancer and 42% of patients with ovarian cancers.[15] The causes of obstruction include adhesions, peritoneal carcinomatosis, and radiation enteritis. A diagnosis of peritoneal carcinomatosis is based on demonstration of a mass or bowel wall thickening at the site of obstruction.[16]

Regarding radiation enteritis, the ileum is the most common part of the small intestine injured by radiation therapy because the terminal ileum is less mobile than the remainder of the small intestine. The CT findings in radiation enteritis include bowel wall thickening, submucosal edema, and increased density of the mesentery from mesenteric fibrosis or edema.[17]

In strangulating obstructions, the CT findings are (1) evidence of small bowel obstruction; (2) circumferential thickening of the bowel wall, submucosal edema, air in the bowel wall, high attenuation of the bowel wall in unenhanced CT scans, or delayed enhancement of the bowel wall; and (3) fluid in the mesentery.[16,18,19] The sensitivity of CT in diagnosing strangulation in patients with bowel obstruction has been reported as 63%.[20] In a recent study,[7] the sensitivity was 100%, but the specificity is 61% because thickening of the bowel wall, submucosal edema, and fluid in the mesentery can be seen in other situations, such as inflammatory bowel disease, peritonitis, and radiation enteritis.

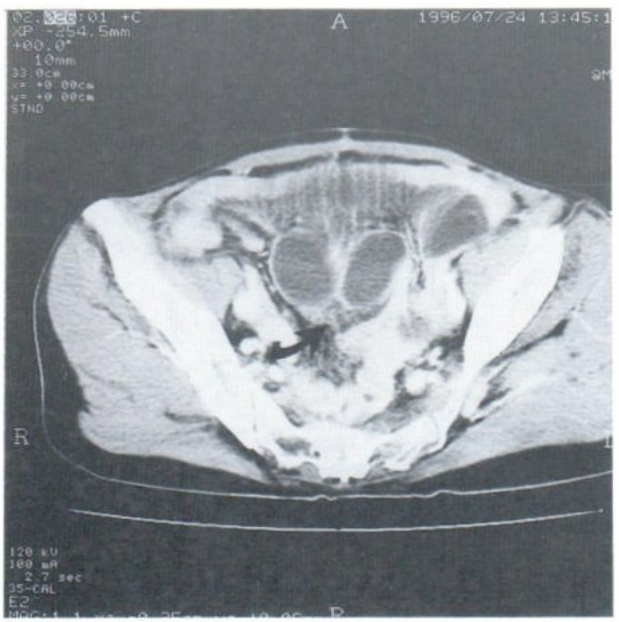

Fig 1. 42-year-old woman with ileal obstruction from adhesions. Note obstruction site adjacent to strands and inflammatory change in mesentery (arrow).

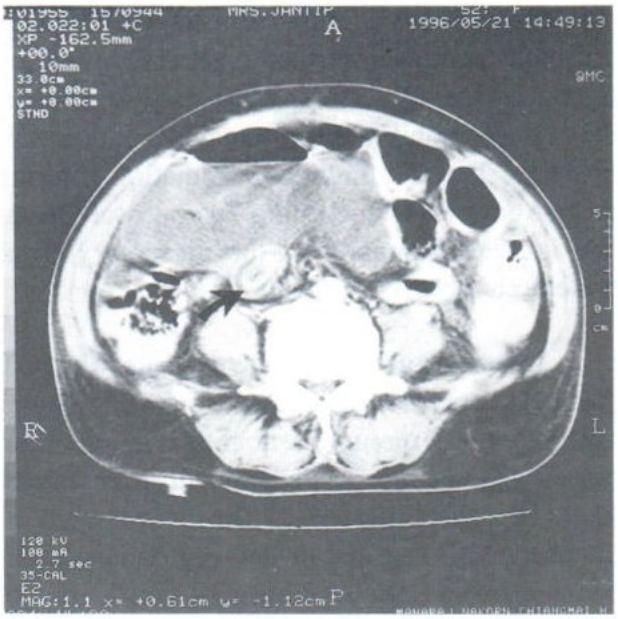

Fig 2. 52-year-old woman with strangulated ileal obstruction from adhesions. Note dilatation of small bowel loops, and submucosal edema (arrow).

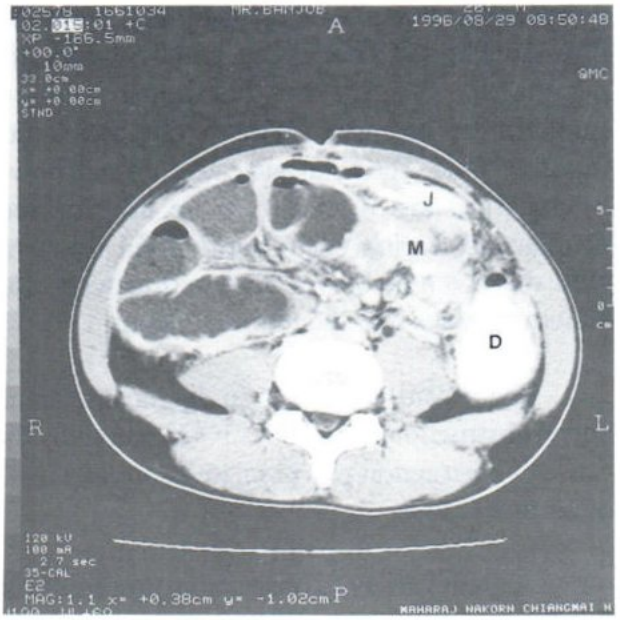

Fig 3. 26-year-old man with small bowel obstruction from peritoneal carcinomatosis. Note dilatation of small bowel loops, soft tissue mass in the mesentery (M), and abnormal enhancement of the small bowel wall. Also note contrast medium in jejunum (J) and sigmoid colon (D) from bypass surgery.

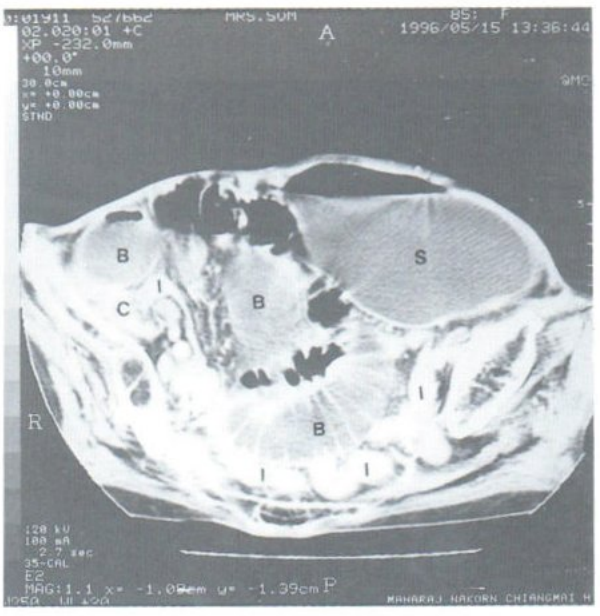

Fig 4. 74-year-old woman with small bowel obstruction from a right obturator hernia.

4A: Note dilatation of stomach (S) and small bowel loops (B). The terminal ileum (I) and cecum (C) are not dilated.

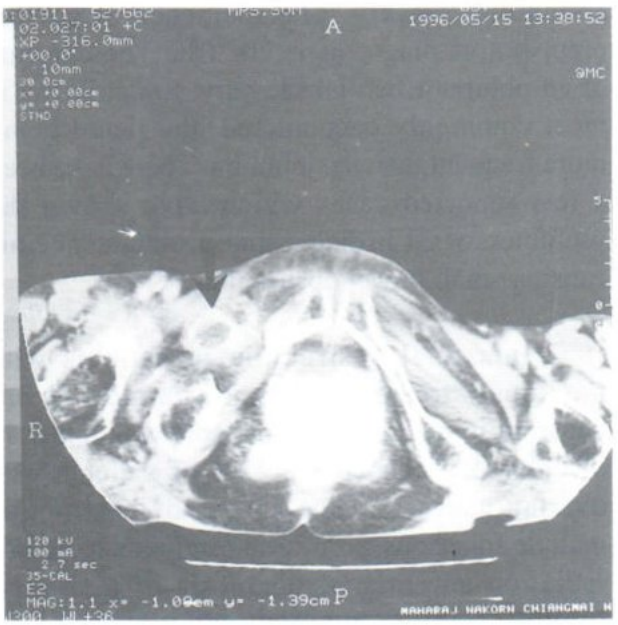

4B: Note a small bowel loop in right obturator canal (arrow).

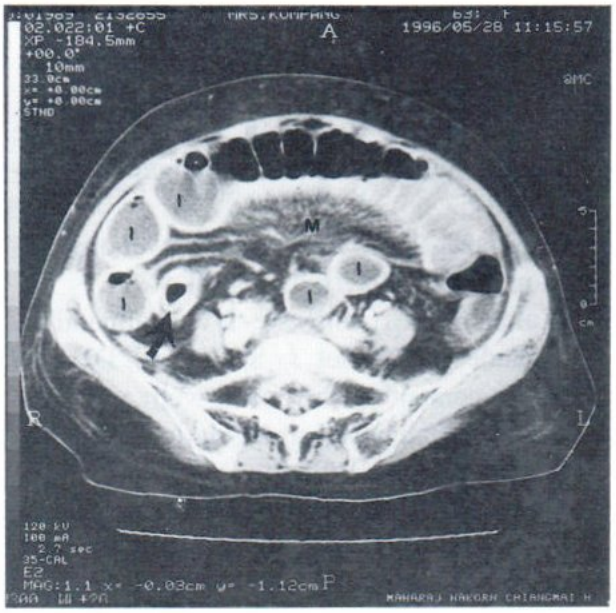

Fig. 5. 63-year-old woman with acute radiation enteritis. Note dilatation of small bowel loops, increased density of mesenteric fat (M), thickening of ileal wall (l), and submucosal edema of ileum (arrow).

CONCLUSION

Since CT is expensive and a plain abdominal radiograph is sufficient for diagnosis in 50-60% of cases, the plain abdominal radiograph remains the primary radiologic method to diagnose intestinal obstruction. Because of the high sensitivity of CT in diagnosing small bowel obstruction, its rapidity, and its ability to diagnose bowel strangulation, CT is recommended in (1) patients with a possibility of small bowel obstruction with normal or nonspecific plain abdominal radiographs,[16] (2) patients with histories of abdominal malignancy and clinical symptoms of bowel obstruction;[1] (3) patients where obstruction is suspected and the patients have inflammatory disease, sepsis, a palpable abdominal mass, or a possibility of strangulation.[18]

Barium studies are recommended in patients with histories of recurring obstruction or low grade mechanical obstruction to define the obstructed segment precisely

REFERENCES:

1. Megibow AJ, Balthazar EJ, Cho KC, Medwid SW, Birnbaum BA, Noz ME. Bowel obstruction : evaluation with CT. Radiology 1991;180:313-318.
2. Maglinte DDT, Gage SN, Harmon BH, et al. Obstruction of the small intestine: accuracy and role of CT in diagnosis. Radiology 1993;188:61-64.
3. Ha HK, Park CH, Kim SK, et al. CT analysis of intestinal obstruction due to adhesions: early detection of strangulation. J Comput Assist Tomogr 1993;17(3):386-389.
4. Gazelle GS, Goldberg MA, Wittenberg J, Halpern EF, Pinkney L, Mueller PR. Efficacy of CT in distinguishing small-bowel obstruction from other causes of small-bowel dilatation. AJR 1994;162:43-47.
5. Frager D, Medwid SW, Baer JW, Mollinelli B, Friedman M. CT of small-bowel obstruction : value in establishing the diagnosis and determining the degree and cause. AJR 1994; 162:37-41.
6. Frager DH, Baer JW, Rothpearl A, Bossart PA. Distinction between postoperative ileus and mechanical small-bowel obstruction: value of CT compared with clinical and other radiographic findings. AJR 1995;-164:891-894.
7. Frager D, Baer JW, Medwid SW, Rothpearl A, Bossart P. Detection of intestinal ischemia in patients with acute small-bowel obstruction due to adhesions or hernia: efficacy of CT. AJR 1996;166:67-71.
8. Mucha P. Small intestinal obstruction. Surg Clin North Am 1987;67(3):597-620.
9. Gough IR. Strangulating adhesive small bowel obstruction with normal radiographs. Br J Surg 1978;65:431-434.
10. Nelson SW, Christoforidis AJ. The use of barium sulfate suspensions in the study of suspected mechanical obstruction of the small intestine. AJR 1967;101(2):367-378.

11. Czechowski J. Conventional radiography and ultrasonography in the diagnosis of small bowel obstruction and strangulation. Acta Radiol 1996;37:186-189.
12. Lo CY, Lorentz TG, Lau PWK. Obturator hernia presenting as small bowel obstruction. Am J Surg 1994;167:396-398.
13. O'Connell G, Cole A. Obturator hernia: diagnosis through medical imaging. Australas Radiol 1995;39:306-308.
14. Roston AD. Rahmin M, Eng A, Dannenberg AJ. Strangulated obturator hernia: a rare cause of small bowel obstruction. AJG 1994;89(2):277-278.
15. Tang E, Davis J, Silberman H. Bowel obstruction in cancer patients. Arch Surg 1995;130: 832-837.
16. Megibow AJ. Bowel obstruction evaluation with CT. Radiol Clin North Am 1994;32(5)-:861-870.
17. DuBrow RA. Radiation changes in the hollow viscera. Semin Roentgenol 1994;-29:38-52.
18. Balthazar EJ. CT of small-bowel obstruction. AJR 1994;162:255-261.
19. Zalcman M, Gansbeke DV, Lalmand B, Braude P, Closset J, Struyven J. Delayed enhancement of the bowel wall: a new CT sign of small bowel strangulation. J Comput Assist Tomogr 1996;20(3):379-381.
20. Balthazar EJ, Birnbaum BA, Megibow AJ, Gordon RB, Whelan CA, Hulnick DH. Closed-loop and strangulating intestinal obstruction: CT signs. Radiology 1992;-185:769-775.

TRANSMISSION OF NOSOCOMIAL INFECTIONS VIA THE ULTRASOUND PROBE AND GEL- in vivo and in vitro study.

B.J.J. ABDULLAH , M.Y. MOHD YUSOF.

ABSTRACT

Transmission of diseases may occur via the ultrasound probes as they are used to scan a large number of patients every day. This may especially be a problem with those patients who are immunocompromised and those with breaks in the skin. This study was to try and ascertain if the ultrasound probe and coupling agent can act as a vector in the transmission of nosocomial infection for patients with no break in the skin and to determine a cheap ,efficient and cost-effective way of preventing transmission. The ultrasound probes were cleaned before every session and between patients with paper towel. At the end of the session the ultrasound probes from two ultrasound machines i.e. three probes were swabbed and then transferred to the Medical Microbiology Department where they were plated and cultured. The probes were inoculated with an ultrasound gel (Aquasonic, NJ) contaminated with Staphylococcus aureus and then cleaned with a dry paper towel, wet paper towel and chlorhexidine solution. The probes were swabbed and cultured. In addition plates of agar were inoculated with a confluent growth of Staphlococcus aureus and then half the plate was covered by the ultrasound gel to see if there was any inhibition of the growth. A total of 12 specimens out of 51 showed growth of Staphylococcus epidermidis.. Cleaning the probe with alcohol did not reveal any growth of Staphylococcus aureus as was the case with the chlorhexidine. The dry paper towel was not very good with 6 of the 7 swabs showing moderate growth and only 1 with minimal growth. The wet paper towel fared better 4 of the 8 swabs showing no growth and 3 showing minimal growth. The ultrasound gel did not inhibit the growth of the Staphylococcus aureus. Unlike other studies there seems to be high rate of transmission with the ultrasound probe and gel and chlorhexidine and alcohol were found to be effective cleaning agents.

INTRODUCTION

Ultrasound scanning is playing an increasingly important role in the management of patients. This is due to its low cost, lack of ionising radiation, portability and general easy access to the modality. This increase in use and its portability especially in the intensive care units and the very sick/immunocompromised patients may however lead to an increase in the possibility of cross transmission. The patient with discharging pus either primarily or post-operatively may be another source of cross infection. This may occur both via the medical personnel handling several

Departments of Radiology and Medical Microbiology, Faculty of Medicine, University of Malaya, Kuala Lumpur.
Tel. No. 03-7502069 Fax No. 603-7581973

Address Correspondence to: Basri Johan Jeat Abdullah, Department of Radiology,
University of Malaya Medical Center, 50603, Kulala Lumpur, MALAYSIA

patients without proper precautions. Transmission of diseases may also occur via the ultrasound probes as they are used to scan a large number of patients every day. Even though there have not been any documented cases of transmission of nosocomial infection via the probe or gel the possibility exists as other medical equipment e.g. stethoscopes, bronchoscopes as well as endoscopes have been implicated.[1,2] This may especially be problem with those patients who are immunocompromised and those with breaks in the skin. The problem of cross infection is further compounded by the rise in antibiotic resistant strains of bacteria e.g. methicillin resistant S. aureus.

OBJECTIVE

The aim of the study was to ascertain the potential risk of the ultrasound probe and coupling agent acting as a vector in the transmission of nosocomial infection for patients with no break in the skin. A cheap, efficient and cost-effective way of reducing transmission of nosocomial infection was also explored. The sterility of the ultrasound gel was investigated and also to determine if it had any bacteriostatic or bactericidal properties.

METHOD

All patients (in- and out-patients) having ultrasound examinations at the Dept. Of Radiology, University Hospital, Kuala Lumpur were included in the study. The patients were scanned on two ultrasound machines i.e. Aloka 620 and 650. The ultrasound probes were thoroughly cleaned before the every session and between patients with paper towel. The patients included both in- and out-patients. There were patients who were post-operative and no effort was made to exclude any patients. Both adults and children were scanned. At the end of either the morning or afternoon session the ultrasound probes from two ultrasound machines i.e. three probes, were swabbed using a sterile wet cotton swab and then transferred to the Medical Microbiology Department where they were inoculated onto blood agar plates and incubated aerobically at 35^{0}C for 48 hours. The bacterial colonies were then identified and enumerated.

For the second part of the study the probes were intentionally inoculated with an ultrasound gel (Aquasonic, NJ) infected with Staphylococcus aureus and Escherichia coli seperately. The infected gel was prepared by inoculating half a bottle of ultrasound gel with 10 mls. of broth culture of either Staphylococcus aureus or Escherchia coli and mixed. The broth culture contained approximately 1 power 8 colony forming units(CFU)/ml. The probes were then used to scan a sterile agar plate for several minutes in order to simulate the normal ultrasound examination .The probes were then cleaned with either a dry paper towel, wet paper towel, alcohol and chlorhexidine solution until all traces of the ultrasound gel had been removed. The surface of the probes was then swabbed with a wet cotton swab and inoculated onto blood agar plates and incubated at 35^{0}C aerobically for 48 hours.

In addition 10 Muller Hentan plates were infected with a confluent growth of Staphylococcus aureus and then half of the each plate was covered by the ultrasound gel. The plates were subsequently examined to see if there was any inhibition of the growth by the gel.

Ultrasound gel from the unused bottles was also cultured to determine if these showed any evidence of infection.

RESULTS

A total of 51 swabs were collected from the ultrasound probes at the end of the sessions. Of these, 12 showed growth of Staphylococcus epidimidis (23.5%). None of the specimens showed growth of Staphylococcus aureus or Eschericia coli. Cleaning the probe with chlorhexidine and alcohol did not show any growth of either S. aureus or E. coli (Table I). However cleaning the probe with the dry towel (8

swabs) showed minimal growth of E. coli but was poor for the gel infected with S. aureus. On the other hand cleaning the probe with the wet paper towel was poor for E. coli but good for the S. aureus.

The ultrasound gel did not inhibit the growth of the confluent growth of S. aureus. In addition there was no evidence of any growth from the swabs taken from the unused bottles of ultrasound gel.

Table Ia. Gel infected with E. coli

Type of cleaning agent	Number of swabs	Results
Wet towel	7	1 No growth 2 Less than 10 colonies 4 40-50 colonies
Dry towel	8	7 No growth 1 Less than 10 colonies
Alcohol	8	No growth
Chlorhexidine	7	No growth

Table Ib. Gel infected with S. aureus

Type of cleaning agent	Number of swabs	Results
Wet towel	8	4 No growth 4 Less than 10 colonies
Dry towel	7	2 Less than 10 colonies 5 Greater than 30 colonies
Alcohol	9	No growth
Chlorhexidine	8	No growth

DISCUSSION

Nosocomial infections are on the rise and the problem has been further compounded by the presence of antibiotic resistant strains e.g. methicillin resistant S. aureus and gram negative bacilli resistant to multiple antibiotics. There have reports of numerous medical equipment being involved as transmitters of infection.[1,2] Though there have been no documented cases of the ultrasound probe and gel being a cause of transmission of nosocomial infection but in a study by Spencer & Spencer[3] they showed that ultrasound scanning in patients with post-operative wounds, 33% showed growth of skin flora including S. aureus.

Even though most of the pathogens cultured from the probe and gel are not serious pathogens in the normal patient, in those who are

immunocompromised, debilitated or with open wounds,[4] this may result in serious consequences. S. epidimidis is a under-reported cause of systemic infections involving the prosthetic valves and the urinary tract.[5] These infections may be life-threathening.

In our study there was a high rate of growth of S. epidimidis (23.5%) with the ultrasound probe and gel but no growth of S. aureus. However Muradali et al[6] showed only 1 out of the 27 swabs taken showed growth of S. epidimidis even though they used the same method of cleaning i.e. dry unsterile paper towel. The differences could probably be accounted for by the vigour of cleaning. In our study the other users of the ultrasound machines were not aware of the study being done and therefore maybe a better reflection of the actual rate of transmission. In addition the swabs in our study were done between session where between 15 to 20 patients would have been scanned rather than between each patient. There were no cases of S. aureus detected during their study. A study done by Spencer and Spencer[3] found there was a 33% incidence of bacterial growth (including S. aureus)of the gel prior to cleaning the probe with alcohol. They did not specifically look at the value of cleaning with dry paper towels. Their patient scanned had post-operative wounds.

Spencer and Spencer[3] also found that ultrasound gel infected with organisms showed viability for 72 hours. This is important because similar to our study the gel has no bactericidal or bacteriostatic properties and therefore gel left on the probes overnight may still alllow transmission of infection.

Even though the most common method that is in use for cleaning the probe is a dry paper towel, the effectiveness is suspect. Studies have found it to be effective[3, 6,7] though our study showed that its effectivenss was limited. Chlorhexidine and alcohol are excellent at cleaning of the infected probes though this advantage may be offset by the increased risk of damage to the probe. There have been some vendors who are looking at over-coming this problem. The wet paper towel was good for the S. aureus but not very effective against the E. coli and the reverse for the dry paper towel. The other methods like using plastic bags, surgical gloves or otheer antiseptic solutions ahve been advocated but not assessed.

In conclusion the ultrasound probe and gel may act as transmitters of infection and that care should be taken when scanning patient s with open wounds or those who are immunocompromised or in the intensive care units. Cleaning the probe with alcohol or chlorhexidine is very effective at eliminating cross-infection though the effects on the probe may be a problem. Better methods of reducing cross-infection may need to be explored. The ultrasound gel has no bacteriostatic or bacteriostatic properties and is inherently sterile.

REFERENCES

1. Steinberg PJ, deHoop D. The stethoscope as a vehicle of pathogenic microorganisms in the hospital. Neth Tijdschr
2. Spach DH, Silverstein FE, Stamm WE. Transmissiion of infection by gastrointestinal endoscopy and bronchoscopy. Ann. Intern Med 1993;118:117-128.
3. Spencer P & Spencer C. Ultrasound scanning of post-operative wounds- the rsiks of cross-infection. Clinical Radiology 1988;39:245-246.
4. Bucknall TE. Factors influencing wound complication. Annals of Royal College of Surgeons 1983;65:71-77
5. Mandell GL, Douglas RG & Bennett JE (eds) Principles and Practice of infectious diseases, Ed 2. Wiley Medical 1985
6. Muradali D, Gold WL, Philips A & Wilson S. Can Ultrasound Probes and Coupling Gel Be A Source of Nosocomial Infection in Patients Undergoing Sonography? An In Vivo and In Vitro Study. AJR 1995;164:1521-1524
7. Talbot GH & Skros. 70% alcohol disinfection of transducer heads: experimental trials. Infection Control 1977;6:237-239.

ANTENATAL MR IMAGING OF CERVICAL TERATOMAS

M. PUVANESWARY, P. NG

ABSTRACT

The majority of cervical teratomas in the newborn are histologically benign and diagnosed on antenatal ultrasound. The extent of such tumours and their relationship to vital structures such as major blood vessels and the trachea are better delineated with magnetic resonance imaging (MRI). A case of cervical teratoma imaged antenatally with MRI for assessment of airway patency and surgical planning is reported.

Key Words: teratoma; magnetic resonance imaging; computed tomography; pregnancy

CASE REPORT

A 27 year old woman, G5P2, was admitted with rapidly increasing polyhydramnios at 34 weeks gestation. Antenatal ultrasound revealed a 35 week foetus with a large solid neck mass and associated polyhydramnios. Antenatal MRI was performed to assess tracheal patency and for surgical work-up with excision being planned for the day after birth.

Coronal T1 and T2-weighted sequences of the pelvis and axial T1 and T2-weighted acquisitions of the foetal mass were performed. MRI demonstrated a single cephalic foetus and polyhydramnios. A well marginated, slightly lobulated solid mass was arising from the left antero-lateral aspect of the foetal neck. The tumour crossed the midline and extended from the floor of the mouth to the level of the thoracic inlet. The tumour appeared separate from the tongue and compressed the laryngopharynx and trachea with the latter being displaced to the right. The spinal column was uninvolved. The tumour was fairly homogeneous in signal intensity, being isointense to muscle on T1 and hyperintense on T2-weighted images. Several curvilinear foci of signal void were present within the mass and were subsequently shown on computed tomography (CT) to be due to calcification (Figs. 1&2). A diagnosis of cervical teratoma was made.

After delivery of a 3380 gram female, initial attempts at intubation were unsuccessful. A large tumour was arising from the left antero-lateral aspect of the neck and extended under the jaw into the face, over the chest wall, and across to the right side of the neck. Bronchoscopy revealed that the trachea was rotated and markedly displaced to the right. There was a degree of tracheomalacia involving the upper third of the trachea where the tumour was causing compression.

CT scan performed pre-operatively confirmed a multiloculated mass arising from the left side of the neck extending superiorly to the skull base and inferiorly to the thoracic inlet. The tumour was heterogeneous in attenuation with multiple flecks of calcification. The mass displaced the laryngopharynx and upper trachea

Department of Medical Imagimg, John Hunter Hospital, Newcastle, Australia

Corresponding Author: Dr. M. Puvaneswary, Department of Medical Imaging, John Hunter Hospital, Locked Bag No.1, Newcastle Mail Centre, Newcastle, NSW 2310, Australia.

Phone: (049) 213-457 Fax: (049) 213-415 E-mail: png@hunterlink.net.au

to the right (Figs. 3a&3b).

At surgery the tumour was well encapsulated and extended to the right of midline from the left side of the neck as well as posterior to the thyroid gland, displacing it anteriorly. The mass did not appear to be infiltrating the gland and measured 100x70x60 cm. The tumour extended superiorly to the base of the skull and was retracted at operation without difficulty but was densely adherent to the left thyroid lamina.

Macroscopically, the tumour was composed of solid and cystic components. It was firm with areas of palpable calcification.

Histologically, bone, cartilage, mucin-containing epithelium, neural tissue with varying degrees of maturity and immature neuroectodermal tissue were present.

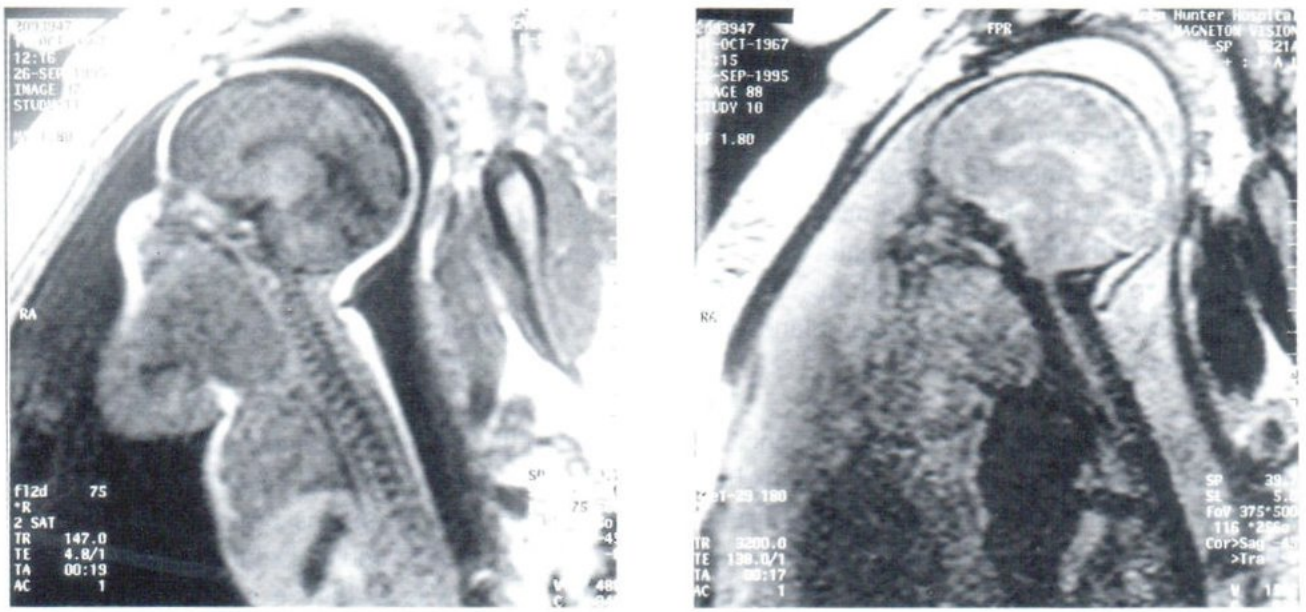

1(a) 1(b)

Fig. 1. T1-weighted (a) and T2-weighted (b) sagittal images demonstrate an inhomogeneous, well-circumscribed mass producing mass effect on the adjacent laryngopharynx and trachea.

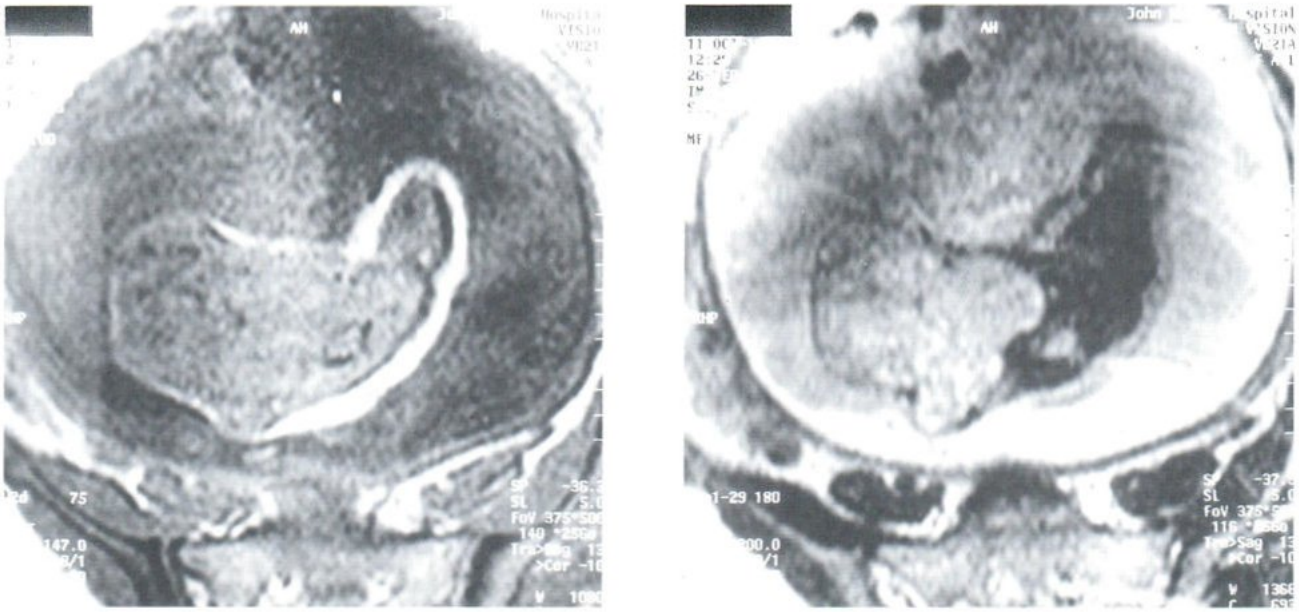

2(a) 2(b)

Fig. 2. T1-weighted (a) and T2-weighted (b) axial images demonstrate a large lobulated mass arising from the left anterolateral aspect of the foetal neck. Curvilinear signal void represents calcification.

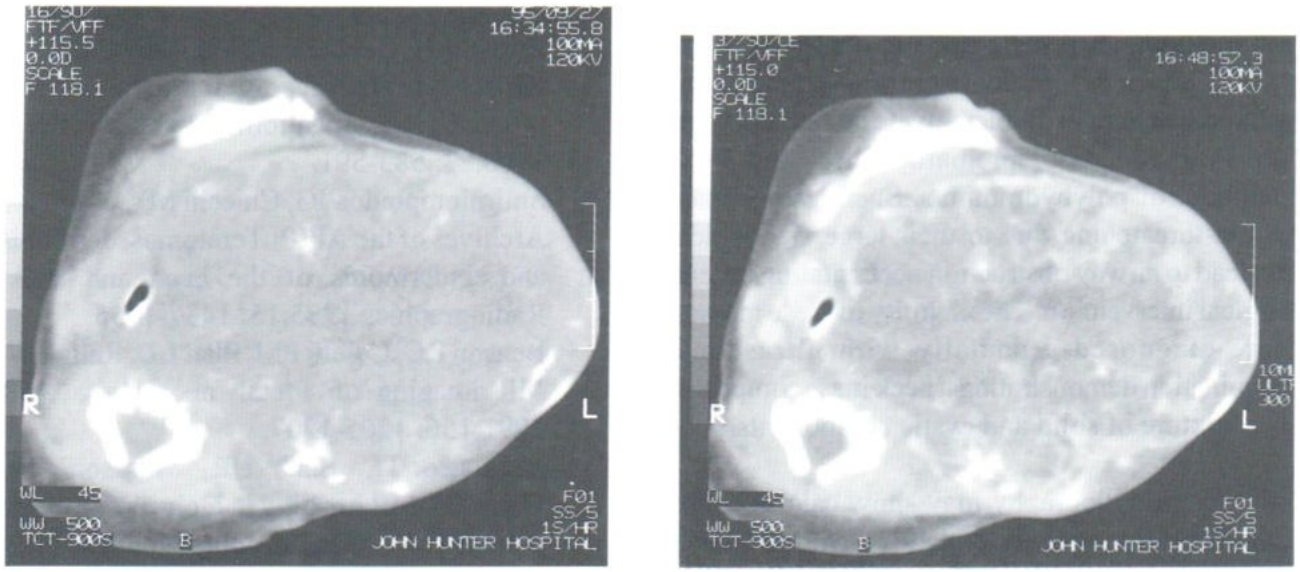

3(a) 3(b)

Fig. 3: Pre-contrast (a) and post-contrast (b) CT scans demonstrate a multiloculated, enhancing, heterogeneous mass extending from the mandible to the spine and displacing the hypopharynx.

DISCUSSION

Cervical teratomas are neoplasms arising from ectopic embryologic germ cells. They are composed of tissue from two or more embryonic layers. In adults they are typically small masses with a high incidence of malignancy. In contrast, the majority of cervical teratomas in the newborn are histologically benign and are usually large, bulky masses with variable location. Laterally positioned tumours frequently cross the midline and can extend caudally into the superior mediastinum and cranially into a submandibular location with involvement of the floor of the mouth. Giant tumours can encompass the entire neck and may be larger than the foetal head.

Conditions reported in association with cervical teratomas include imperforate anus, chondrodystrophia fetalis and hypoplastic left ventricle associated with a small mitral valve orifice and pulmonary hypoplasia.[1]

In 1988, Jordan et al[1] reviewed the literature and including 5 of their patients reported a total of 217 cases of cervical teratomas. Tumours greater than 8cm in diameter were associated with a 59% incidence of premature birth and 49% incidence of polyhydramnios. Such lesions may be life-threatening due to their large size which can lead to airway obstruction necessitating urgent surgical intervention. The majority of these masses were diagnosed prenatally with ultrasound examination demonstrating a neck mass composed of a mixture of solid and cystic components.

Plain radiography may show calcification. Computed tomography typically demonstrates a multiloculated, heterogeneous mass with calcification and/or scattered lipid foci. Differential diagnoses for a large neck mass either in a foetus or infant include cystic hygroma, congenital goitre, lymphangioma, dermoid cyst and neuroblastoma. Teratoma is suspected on MRI when a multiloculated lesion with focal areas of high signal intensity is seen on a T1-weighted study.[2]

Although these foetal anomalies are usually detected sonographically during pregnancy, MR imaging is advantageous because of its large field of view and multi-parameter variability of tissue contrast. MRI is superior in depicting tumour extent and airway compromise. Disadvantages of MRI include expense and a relatively long acquisition time resulting in movement artifact.

Although oligohydramnios and maternal sedation reduces movement, neither will entirely eliminate it.[3-5] Foetal movement is less of a problem in later pregnancy especially if the foetus is markedly abnormal.

REFERENCES

1. Jordan RB, Gauderer MWL. Cervical Teratomas: An analysis - literature review and proposed classification. J Paediatr Surg. 1988;23: 583-591.
2. Smirniotopoulos JG, Chiechi MV. From the Archives of the AFIP: Teratomas, dermoids and epidermoids of the head and neck. Radiographics 1995;15: 1437-1455.
3. Benson RC, Coletti PM, Platt LD, Ralls PW. MR imaging of foetal anomalies. AJR 1991;156: 1205-1207.
4. Angtuaco TL, Shah HR, Mattison DR, Guirk JG. MR imaging in high-risk obstetric patients: A valuable complement to US. Radiographics 1992;12: 91-109.
5. Williamson RA, Weiner CP, Yuh WTC, Abu-Yousef MM. Magnetic resonance imaging of anomalous foetuses. Obstet Gynecol. 1989;73: 952-956.

CHILDHOOD PRIMARY TUBERCULOSIS IN RAMATHIBODI HOSPITAL, RADIOGRAPHIC MANIFESTATIONS

Siriporn THANAMEE, Shashilekha BALACHANDRA, Patchrin PEKANAN.

ABSTRACT

The aim of this study was to review the radiologic features of primary tuberculosis in childhood and to determine whether there is any significant difference in the pattern of disease which occurs among different age groups. Chest radiographs of 84 children with pediatric primary tuberculosis who were treated at Ramathibodi hospital were reviewed. Pulmonary infiltration was found in 84.09% of the cases and was the most common abnormality identified on the initial chest radiograph. The infiltration was more common in the right lung. Lymphadenopathy was found in 72.73% that typically involved the hilar and paratracheal regions. Both the younger (0-5 years old) and the older (6-15 years old) children had high prevalence of parenchymal abnormalities and lymphadenopathy.

MATERIALS AND METHODS

The hospital records and radiographs of pediatric tuberculosis patients in Ramathibodi hospital from June 1992 to May 1995 were reviewed.

Over 100 children under the age of 15 years were selected for initial analysis. Eighty four cases with adequate clinical and radiological information were included in our series (table 1) .

Table 1. Epidemiologic characteristics of study group (n = 84).

Characteristic		No. of patients	percent
Age (years)	0 - 5	36	42.86
	6 - 15	48	57.14
Sex	female	49	58.33
	male	35	41.67

The cases ranged in age from 1 month - 15 years old. Thirty six of eighty four children (42.86%) were younger than 6 years of age and 48 children (57.14%) were older than 6 years. There was a slight female predominance with 49 girls (58.33%) and 35 boys (41.67%).

The diagnosis of tuberculosis was accepted if mycobacterium tuberculosis was isolated from any body site or if the clinical findings were

Department of Radiology, Ramathibodi Hospital, Rama 6 Street, Bangkok 10400, Thailand

consistent with tuberculosis; and at least two of the three following criteria were also met[1]:-

1. Tuberculosis skin test with 5 TU purified protein derivative units resulted in an area of induration 10 mm. or greater in size.

2. Other disease entities were ruled out and the subsequent clinical course was consistent with tuberculosis.

3. An adult source patient with contagious disease caused by M. tuberculosis was discovered.

After reviewing the hospital records and radiographs of these proven tuberculosis children, these criteria were met in 84 cases. These cases had adequate clinical and radiologic documentation and were selected for further analysis. There were only 39 cases whose radiographs were available for review. The remainder 45 cases with missing radiographs were also included in our series. The radiologic reports of these latter cases were used for the analysis. There were 49 boys and 35 girls. The chest radiographs obtained at presentation were assessed for the presence and location of pulmonary infiltration, lymphadenopathy, atelectasis, calcification, scarring and pleural effusion. (Some of the cases in our series are illustrated in Figures 1 - 6). Pulmonary infiltration was classified as being in the upper, middle, lower zone or multifocal i.e. infiltrates involving more than one lung zone or bilateral involvement. Atelectasis was classified as either lobar or segmental in distribution.

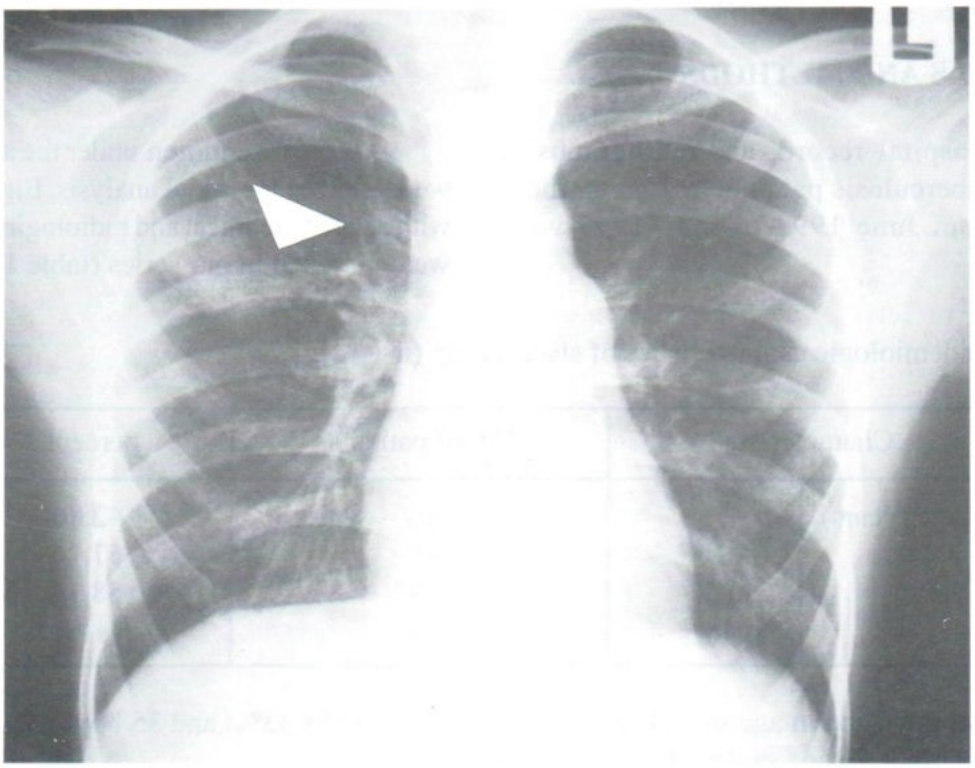

Fig.1. An 8 year old girl developed hemoptysis. She also had the history of tuberculous contact. PA chest film shows fibro-patchy infiltration in the RUL.

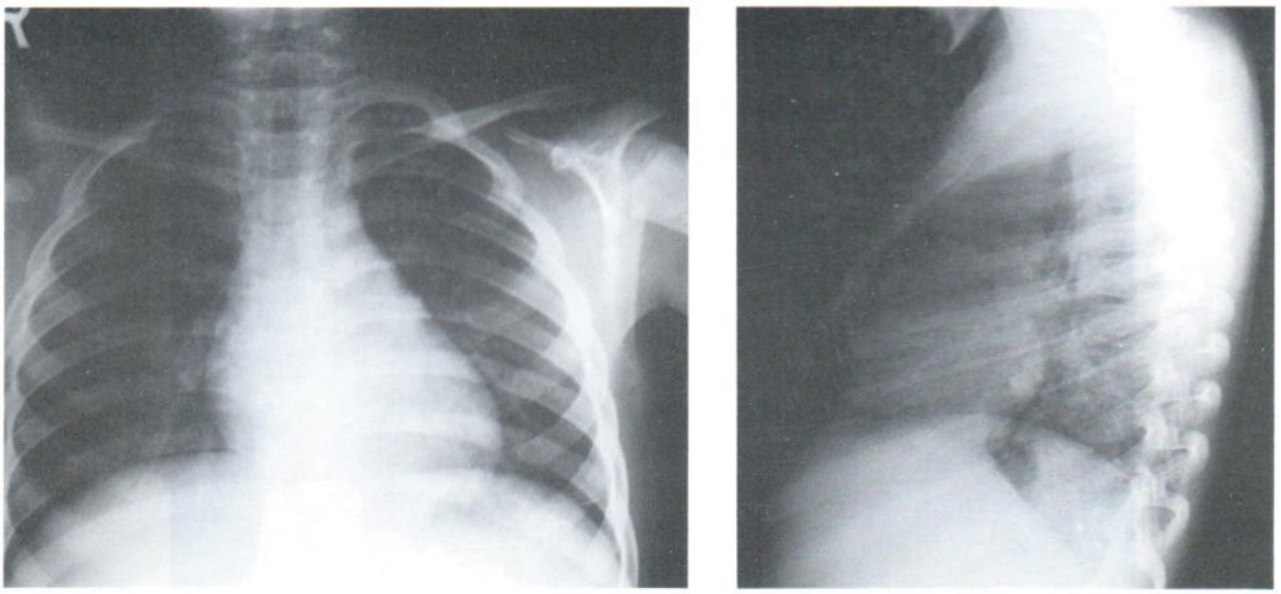

A. B.

Fig. 2A,B. A 5 year old boy with positive tuberculin test. PA and lateral chest radiographs show reticulo-nodular infiltration in RLL. with bilateral hilar adenopathy.

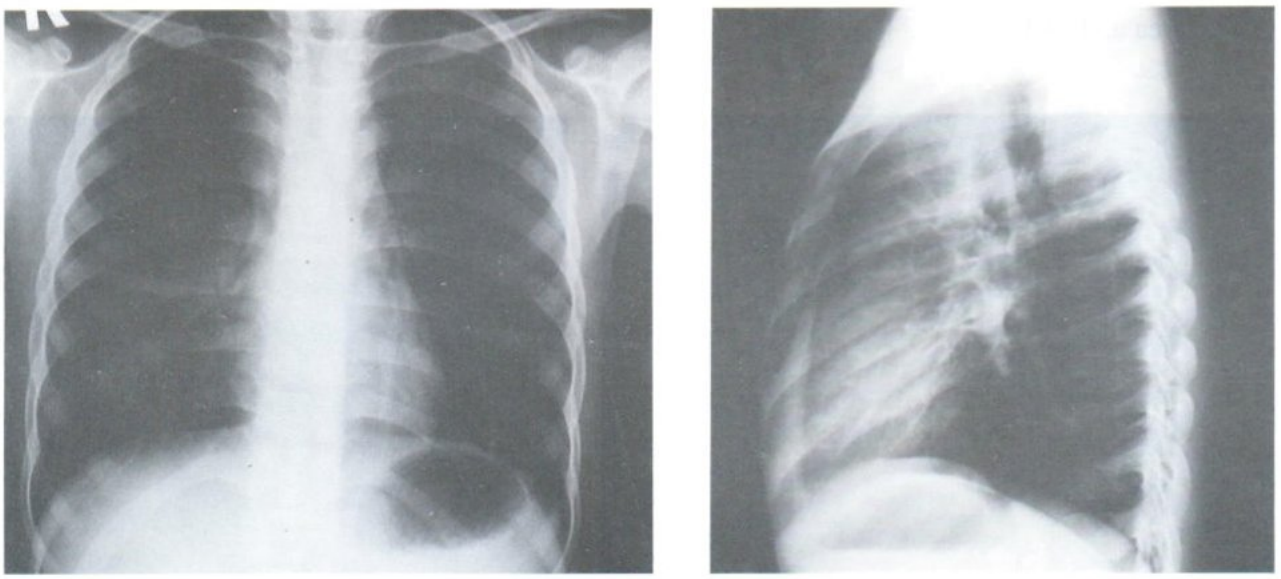

A. B.

Fig. 3A,B. An 8 year old girl presented with fever and cough for 1 month. PA and lateral chest radiographs show right para-tracheal and right hilar adenopaty.

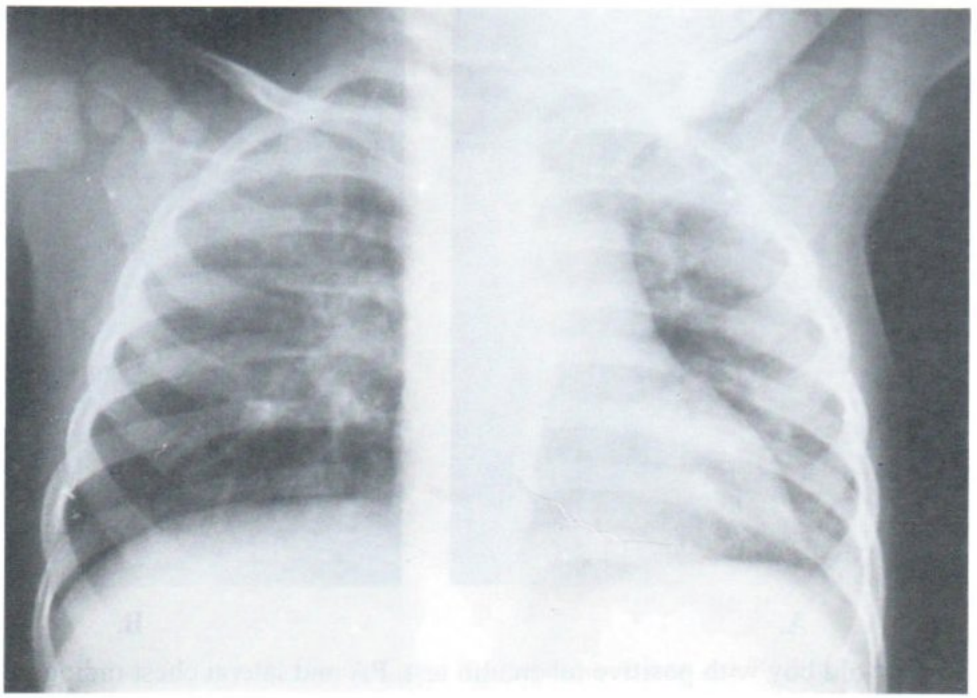

Fig.4. A 1 year old girl came in with the history of close tuberculous contact. AP chest radiograph shows interstitial infiltration in peri-bronchial areas of both lungs, more in the right peri-hilar area and LLL.

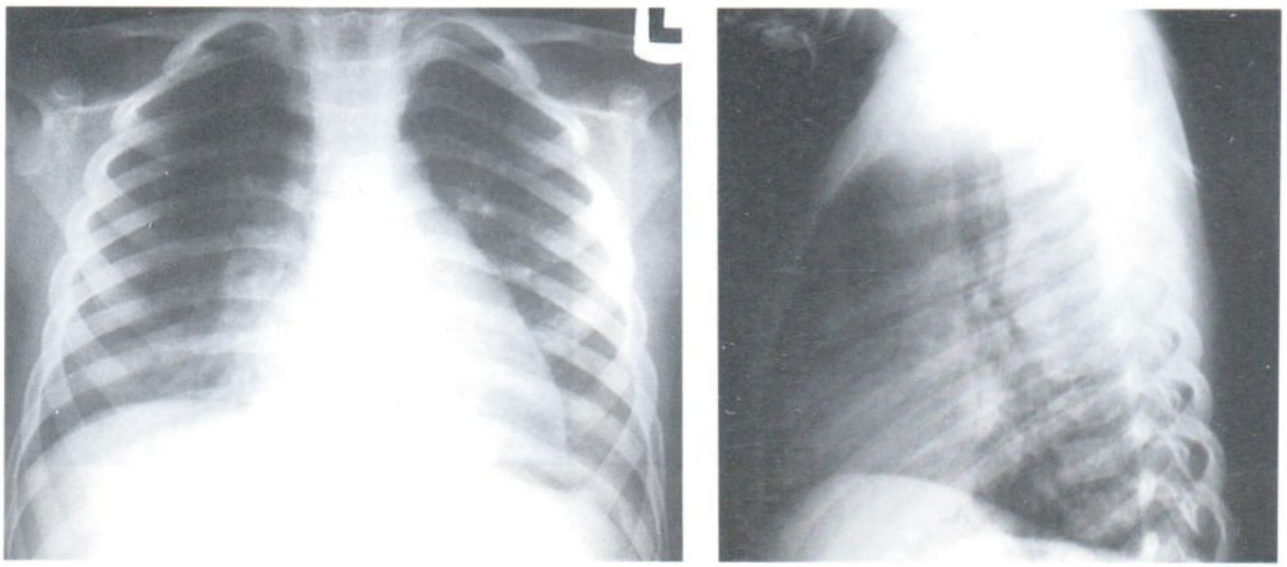

Fig.5A,B. A 2 year old boy with high fever and cough for 3 weeks. PA and lateral chest radiographs show patchy infiltration in right peri-hilar area, RML. and both lower lobes. Rt. hilar adenopathy is noted.

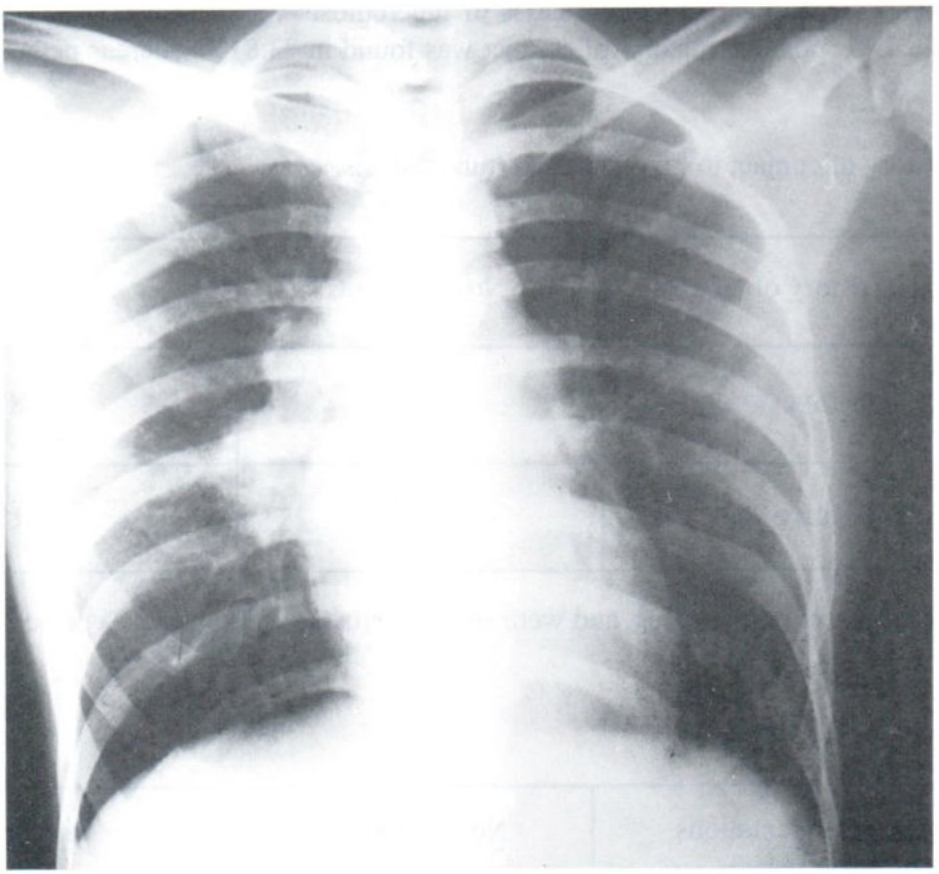

Fig.6. A 10 year old girl with clinical history suggestive of tuberculosis. PA chest radiograph shows right broncho-pulmonary, hilar and para-tracheal adenopathy.

There were 77 cases (91.67%) with the history of BCG immunization and positive BCG scars (Table 2). The rest was non-immunized with negative scars (7cases or 8.33%) .

Table 2. Cases were analyzed according to BCG scars.

BCG scars	No. of patients	percent
present	77	91.67
absent	7	8.33

The history of contact to known cases of tuberculosis was helpful in the initial diagnostic work up (Table 3). A positive history of contact was found in 73.81% whereas negative history was 26.19% .

Table 3. History of contact to known case of tuberculosis.

History of contact	No.of patients	percent
positive	62	73.81
negative	22	26.19

The clinical presentation varies, and were shown in (table 4.) Some cases presented with many problems.

Table 4. Clinical presentations.

Clinical presentations	No.of patients	percent
Lymphadenopathy	28	33.33
Fever	25	29.76
Cough	23	27.38
No symptoms	17	20.23
Weight loss	10	11.90
Hemoptysis	3	3.57

There were 20.23% of children who were asymptomatic at presentation and 79.77% had symptoms. The most frequent occurring symptoms were lymphadenopathy (33.33%), fever (29.76%) and cough (27.38%). Some patients presented with many symptoms. Patients with documented childhood tuberculosis had positive chest radiographic findings in only 44 cases (52.38%), and the remainder (47.62%) had negative findings (Table 5).

Table 5. Radiographic findings.

Radiographic findings	No.of patients	percent
positive	44	52.38%
negative	40	47.62%

The most common abnormality identified on the initial chest radiograph was pulmonary infiltration (84.09%) which was prominent in the right lung but there was no predilection for specific lobe or zone involvement (Table 6). There were no cases of cavitary lesion, miliary pattern or bronchiectasis in our series. There was one case of obstructive emphysema which also had a CT scan done. (Figure 7). None of the cases in our series had HIV infection.

Table 6. Radiographic findings at presentation (n = 44).

Findings	No.of patients	percent
Pulmonary infiltration	37	84.09
Rt. lung	27	
upper zone	11	
middle zone	9	
lower zone	10	
Lt. lung	21	
middle zone	7	
lower zone	8	
Multifocal	11	
Lymphadenopathy	32	72.73
Calcification	10	22.73
Pleural effusion	4	9.09
Atelectasis	2	4.55
- segmental	0	
- lobar	2	
Obstructive emphysema	1	2.27
Scarring	1	2.27

Lymphadenopathy was another common radiographic finding and was found in 72.73% in this study .

Other findings were calcification (22.73%), pleural effusion (9.09%), atelectasis (4.55%) and scarring (2.27%).

The common radiographic findings of pulmonary infiltration and lymphadenopathy were analysed and compared between two age groups (Table 7).

Table 7. Pulmonary infiltrates and lymphadenopathy .

Age (yrs.)	No.of patients.	Infiltration	Lymphadenopathy
0 - 5	36	14	14
6 - 15	48	23	18

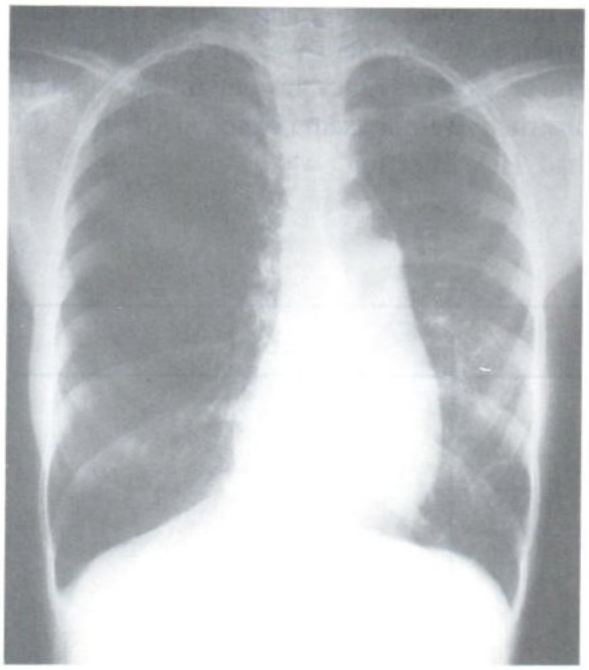

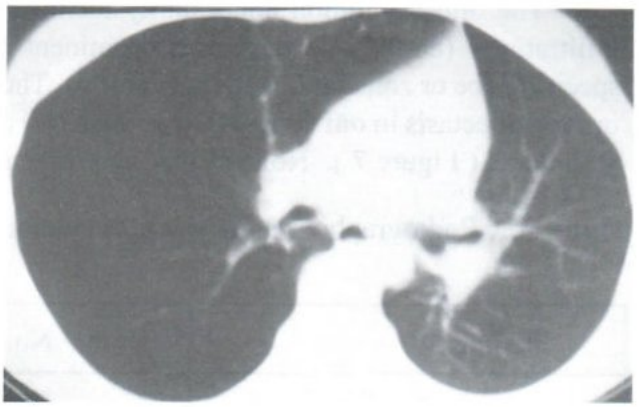

Fig.7B. CT scan confirms obstructive emphysema of the right lung with contra-lateral herniation of right lung across the anterior mediastinum.

Fig.7A. A 13 year old girl presented with weight loss. PA chest radiograph shows obstructive emphysema of the right lung with contra-lateral herniation of right lung. Minimal fibrosis in both upper lobes is noted.

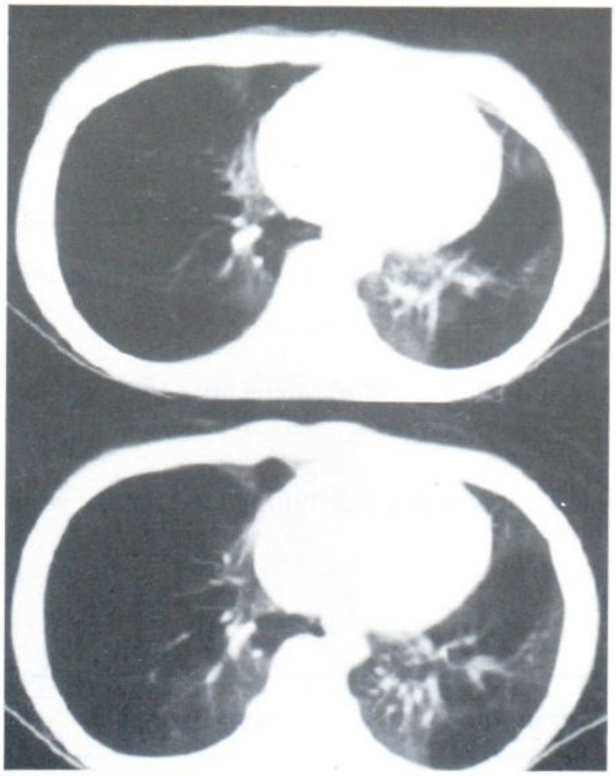

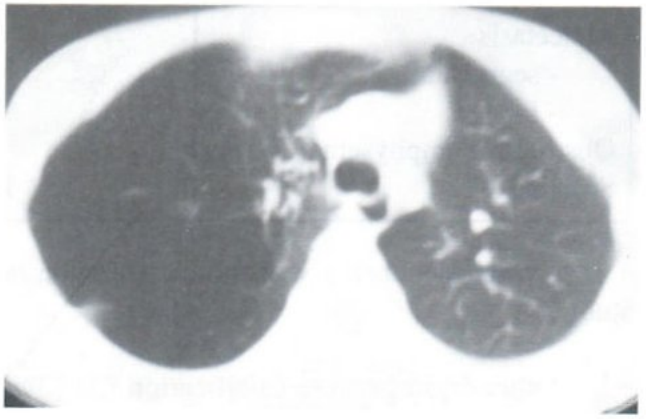

Fig.7D. Small calcified granulomas in the LUL and minimal pleural fibrosis in posterior segment of RUL are shown.

Fig.7C. CT scan of the lower chest shows pan-lobular emphysema of the lingular segment of LUL and postero-basal segment of LLL

There was no significant difference of the above findings in the two age groups (chi-square test , p = 0.50 and 0.95 for pulmonary infiltration and lymphadenopathy, respectively).

Comparison of the frequency of pulmonary infiltrates and lymphadenopathy found in our series and the other three series were also made as shown in (table 8).

Table 8. Comparison of the major findings with other series .

Series	Pulmonary infiltration (%)	Lymphadenopathy (%)
Leung AN. et al.(1)	69.11	92
Starke JR et al .(5)	52.73	73.64
Balachandra S.et al.(2)	36.17	14.93
Thanamee S. et al .	84.09	72.73

DISCUSSION

Koch isolated the etiologic agent Mycobacterium tuberculosis in 1882[3]. It is an obligate aerobic, non motile bacillus with acid fastness that is attributable to mycalic acid within the cell wall. Culture on enriched media is possible but slow, taking 2 to 8 weeks and sputum specimens are difficult to obtain in children. Diagnosis of tuberculosis in childhood is mostly indirect and is usually made on the basis of epidemiologic data, history of recent exposure to an infected adult, tuberculosis skin testing, the chest radiograph and physical examination[4].

Our series had a slight older children predominance. There was 57.14% of cases in the " favored age "of 5 - 15 years. This is different from previous studies[1,5]. The girls were affected more than boys in our series. There were 99.67% of cases with BCG vaccination. BCG vaccination, when effective apparently does not prevent infection but interferes with the hematogenous spread of tubercle bacilli, thus reducing the risk of severe pulmonary disease and its complications[6].

The history of contact is an important clue that supports the diagnosis. A positive history of contact in our series was found in 73.81% of the cases.

The diagnosis of primary tuberculosis in childhood is difficult to establish clinically due to lack of physical symptoms. At the time of diagnosis, 56-65% of children may be asymptomatic[5,1]. In our series 20.23% were asymptomatic. The majority of these children were discovered by contact investigation of an adult with contagious tuberculosis. This strongly emphasized the need for diligent and thorough household investigation of adults with tuberculosis.

The major symptoms were fever, cough, weight loss, lymphadenopathy and hemoptysis. The positive chest radiographic findings were found in only 52.38% of the cases, confirming that active tuberculosis occurring in the pediatric population often has a negative chest radiograph in the early stage. The radiologic findings in our series were pulmonary infiltration, lymphadenopathy, calcification, pleural effusion, atelectasis and scarring.

The prominent abnormal finding identified

on the initial chest radiograph was pulmonary infiltration that was similar to the previous study[2] but was different from the other studies[1,5] in that the radiologic hallmark of primary tuberculosis in childhood was lymphadenopathy. Findings reflect that each population must look at its own patients with tuberculosis and develop its own criteria for diagnosis. The published criteria used to diagnose tuberculosis from the United States or other countries may not be universal. In our series, pulmonary infiltration had a slight predilection for right lung involvement whereas no specific site or segment of pulmonary parenchymal involvement were noted in other series, documenting upper lobe[7], and lower lobe[8]. Lymphadenopathy is one of the characteristics of chilhood pulmonary tuberculosis in our series, but not a major feature. The nodal enlargement typically involved the hilar and paratracheal nodes, and the lateral chest radiograph was essential and of great diagnostic importance.

In our series, age group differences according to the radiographic pattern of pediatric primary tuberculosis were not as distinct as other studies[1,2]. Calcification was usually found in the intrathoracic lymphadenopathy which almost always represent tuberculosis. Pleural effusion in primary tuberculosis was usually unilateral and loculated. Atelectasis and scarring were the least frequent findings in our series.

We conclude that the common radiologic findings in pediatric patient with primary tuberculosis in our series were pulmonary infiltration and lymphadenopathy, which were found in 84.09 % and 72.73 %, respectively Another important point to emphasize is that negative chest roentgenograms will not exclude tuberculosis.

ACKNOWLEDGEMENT

We would like to express our appreciation to Professor Puangtong Kraiphibul , Head of the Department of Radiology, Dr. Somjai Dangprasert and Dr. Mantana Dhanachai for their advices and comments on this paper.

REFERENCES

1. Leung AN, Muler NL, Pineda PR. Pulmonary tuberculosis in childhood: radiographic manifestations. Radiology 1992; 182:87-91.
2. Balachandra S, Pornkul R. The radiological manifestations of childhood pulmonary tuberculosis. The Thai Journal of Radiology 1984; 21: 107-16.
3. Smith MHD, Marquis JR. Tuberculosis and other mycobacterial infection. In:Feigin RD, Cherry JD. Text book of Pediatric Infectious diseases. Philadelphia: Saunders, 1987:1342-87.
4. Starke JR. Modern approach to the diagnosis and treatment of tuberculosis in children. Pediatr. Clin. North. Am. 1988;-35:441-64.
5. Starke JR, Taylor-Watts KT. Tuberculosis in the pediatric population of Houston, Texas. Pediatrics 1989;84:28-35.
6. Suider OE, Rieder HL. Tuberculosis in children. Pediatr Infect Dis J. 1988;7:271-8.
7. Weber AL, Bird RT, Janown ML. Primary tuberculosis in children with particular emphasis on changes affecting the tracheo bronchial tree. AJR 1966;103:123-32.
8 Woodring JH, Mac Vandeviere H, Fried AM. Update: the radiological features of pulmonary tuberculosis. AJR 1986;146:497-506.

SPIRAL CT SCAN OF RIGHT ADRENAL MYELOLIPOMA: IMAGES DEMONSTRATION

Patchrin PEKANAN[1,2], Kamthorn JINDAVICHAK[2], Damrongrak PROEDPRING[3]

Myelolipoma occur most commonly in the adrenal gland. Extra-adrenal sites include the mediastinum, perirenal, and presacral areas, as well as the liver and stomach.[1,2] Most common in the 5th to 7th decades of life, they are unusual under 30 years of age. There is a roughly equal sex predilection. In about half of patients with adrenal myelolipoma the lesion is an incidental finding. With the use of high-resolution CT and ultrasound, adrenal myelolipmas are discovered with increasing incidence. The most common symptoms are abdominal or flank pain followed by hematuria, palpable mass, hypertension, dysuria, or an associated hormonal disorder such as Cushing's syndrome. Myelolipomas are grossly circumscribed. Microscopic section show that the lesion is sharply demarcated but lacks a capsule. The lesions are usually solitary and unilateral but this is not always the case. The gross appearance of the lesion on cross section depends on the amount of adipose tissue versus hematopoietic component. If the former predominates, the cut surface is frequently yellow, and the hematopoietic or myeloid constituent may be red or purple. Adrenal myelolipomas can be large, measuring up to 34 cm in dismeter, or the lesion may be discovered incidentally at autopsy and be quite small. Microscopically, myelolipomas consist of hematopoietic elements usually representing all three maturation sequences admixed with mature adipose tissue. Occasionally one can seen bony trabeculation.

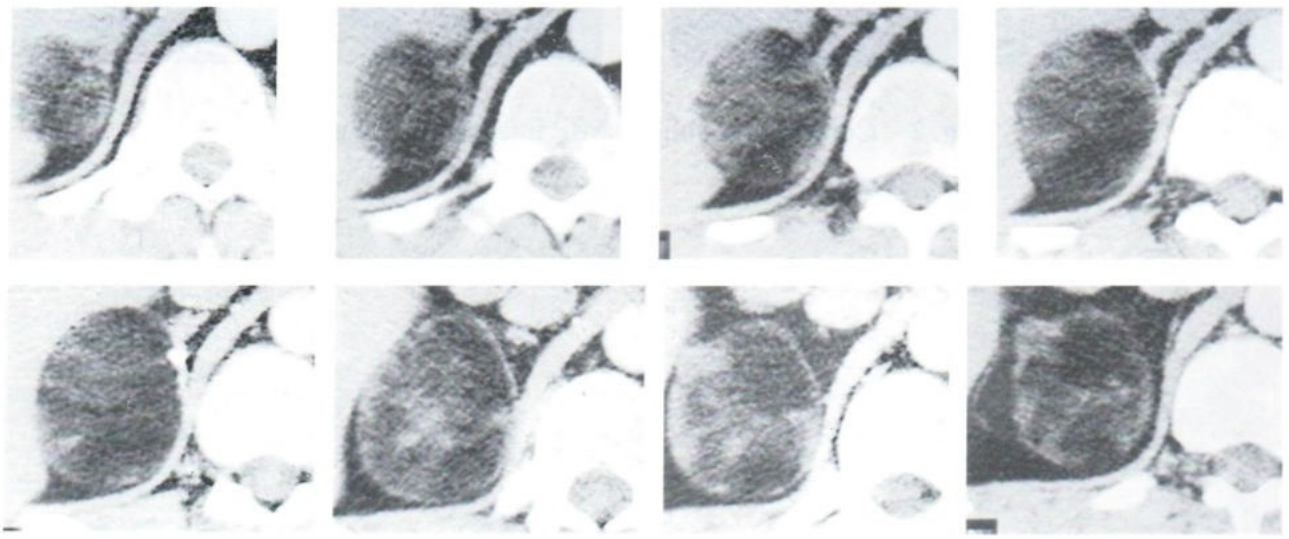

Fig. 1 Axial images of the right adrenal myelolipoma, the tumor contains mainly fatty tissue with less soft tissue density component as nodular and patches. The tumor has well defined sharp border, containing medial wall calcification.

[1] Department of Radiology, Ramathibodi Hospital, Rama 6 Street, Bangkok 10400, Thailand.
[2] Urosurgery section, Urupong Medical Center, BKK.
[3] Application specialist, Urupong Medical Center.

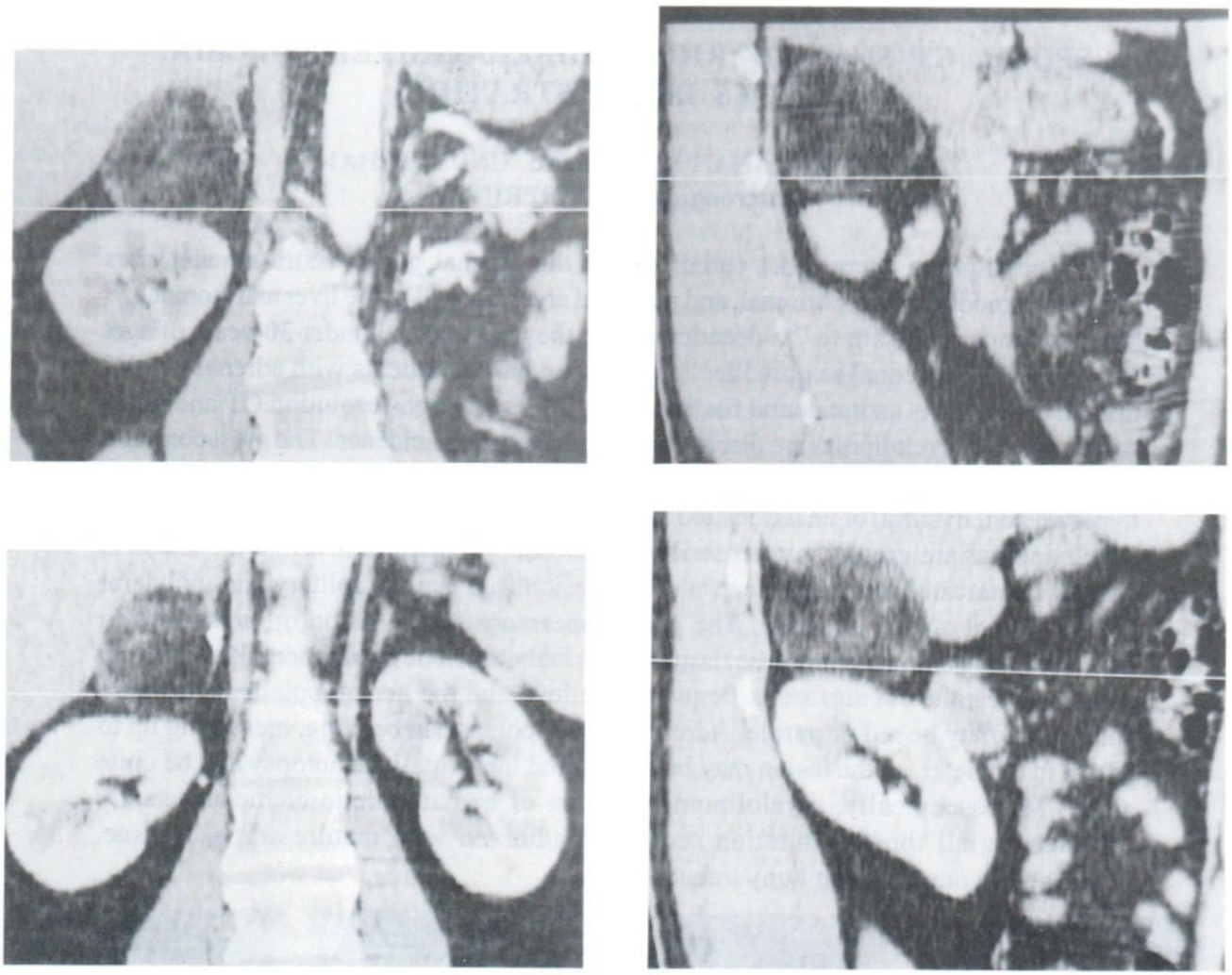

Fig. 2 Coronal and oblique MIP images of the tumor.

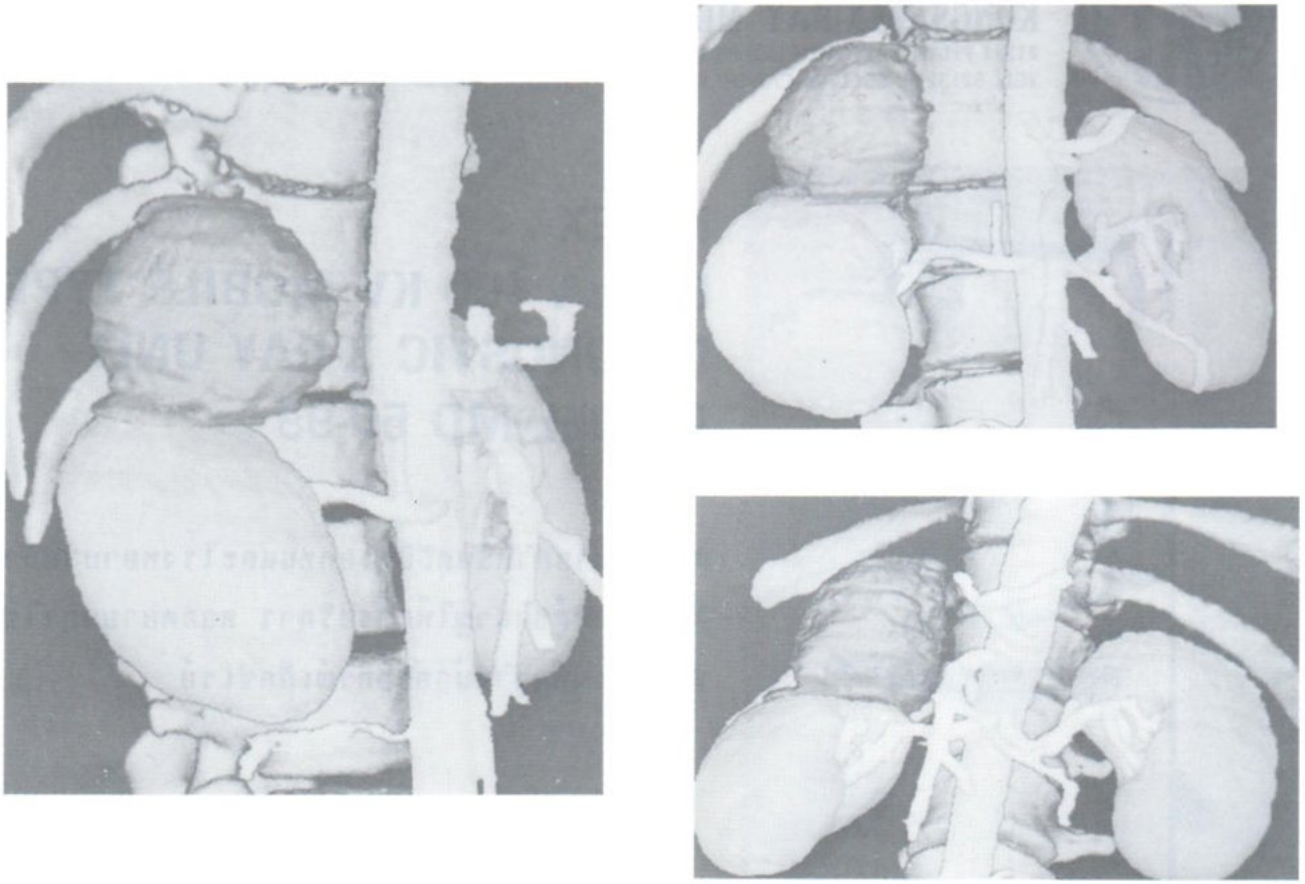

Fig. 3 3D reconstruction of the tumor and the ipsilateral kidney.

REFERENCE

1. Travis WD. Oertel JE, Lack EE. Miscellaneous tumors and tumefactive lesions of the adrenal gland. In Lack EE, editor: Pathology of the adrenal glands. New York, 1990. Churchill Livingstone.
2. Damjanov I, Linder J. Anderson's Pathology. 10th ed. St. Louis:Mosby, 1990:2036.

บริษัท คงศักดิ์เอ็กซเรย์การแพทย์อุตสาหกรรม จำกัด
KONGSAK X-RAY MEDICAL INDUSTRY COMPANY LIMITED
212/1 PHAHONYOTHIN SOI 55 BANGKHEN BANGKOK 10220
TEL. 5213214, 5511794 CABLE: KELEX FAX: 5523744

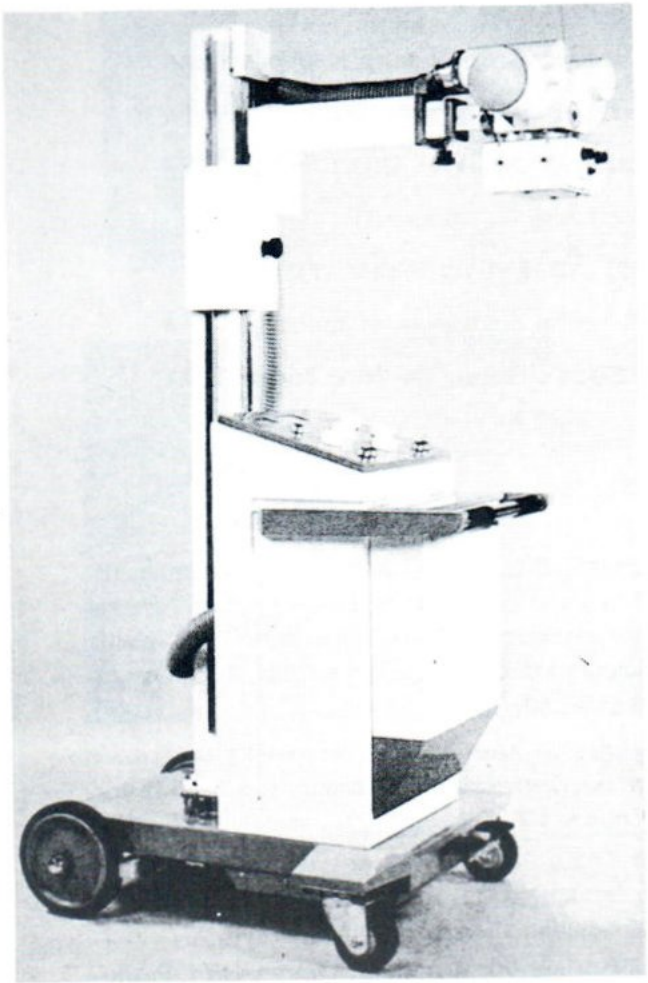

KELEX
50 mA 100 KV MOBILE TYPE DIAGNOSTIC X-RAY UNIT MODEL MD 50-99

- # เหมาะสำหรับคลินิคเอกชนและโรงพยาบาลทั่วไป
- # มีช่างผู้ชำนาญให้การบริการ ตลอดอายุการใช้งาน
- # พร้อมทั้งจำหน่ายอุปกรณ์เอ็กซเรย์

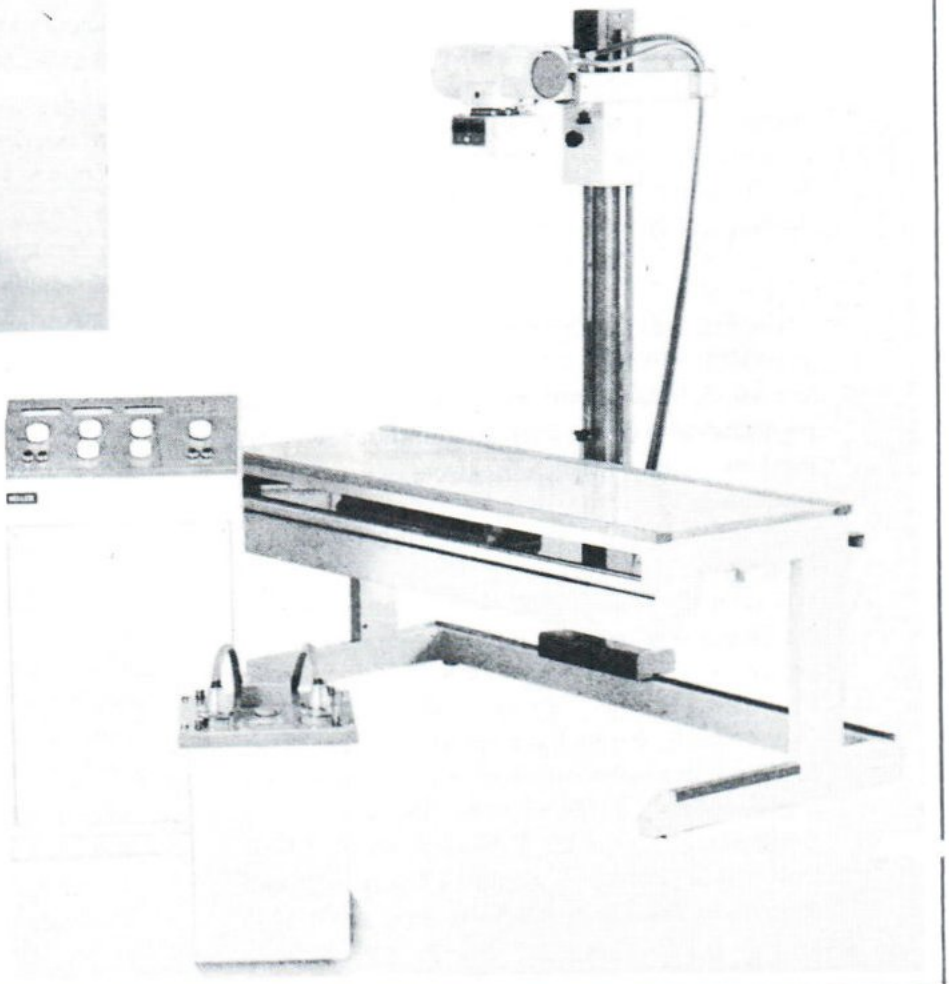

KELEX
MD 100-99 X-RAY SYSTEM
FULL WAVE 100 MA 100 KV

ACUTE ABDOMEN IN HENOCH-SCHOLEIN PURPURA

Khomdao BOONCHIT

ABSTRACT

Abdominal pain is a frequent symptom in the child with Henoch-Scholein purpura and raises the suspicion of intussusception or perforation. Careful clinical evaluation in the face of radiological appearance of intestinal obstruction in Henoch-Scholein purpura will avoid the morbidity associated with a missed intussusception or perforation.

We report a case of intussusception and perforation in Henoch-Scholein purpura.

INTRODUCTION

Henoch-Scholein purpura is a disorder caused by cutaneous and systemic small vessel vasculitis of unknown etiology characterized by a rash that is frequently purpuric, abdominal pain associated with gastrointestinal hemorrhage, arthralgia and sometimes nephritis. Abdominal pain most likely results from submucosal, subserosal hemorrhage and accumulation of edema fluid in the wall of the bowel due to vasculitis and thrombosis of small vessels. These changes may lead to gastrointestinal hemorrhage, some may be complicated by intussusception and perforation.[1] Incidence of intussusception in Henoch-Scholein purpura is 2-3%.[2,3]

CASE REPORT

A 4 year old girl was in her usual state of good health until three days prior to the presentation, she developed swelling of her wrists, ankles and feet with two days history of purpuric rash over both feet. On the morning of presentation, she had acute left upper quadrant pain, tenderness all over the abdomen but no mass was pulpable. Laboratory data revealed occult blood stool, normal hematocrit, white blood cell count, urinalysis and clotting studies. The admitted diagnosis was Henoch-Scholein purpura.

Plain radiographs on the admission day revealed gas fluid levels in dilated small bowel loops with thickened folds and decreased colonic gas, fecal content(Fig. 1) Three days later showed increased abdominal distention and small bowel obstruction (Fig. 2,3).

Eight day after admission she developed severe abdominal pain. Physical examination showed generalized quarding and rebound tenderness. The plain radiographs revealed discrete mottle radiolucencies over the abdomen, more pronoun-ced on the left side with evidence of free air in the right lower quadrant and beneath the liver. The preoperative diagnosis was intususception with bowel perforation and intraperitoneal abscess. The patient underwent exploratory laparotomy whereupon a perforation in the ileum 20 cm. from the ileocaecal valve. The terminal ileum distal to the perforation had submucosal hemorrhage and edema. 17 cm. terminal ileum resection and end to end anastomosis were accomplished.

Department of Radiology, Udornthani Hospital, Meung,Udornthani,41000,THAILAND

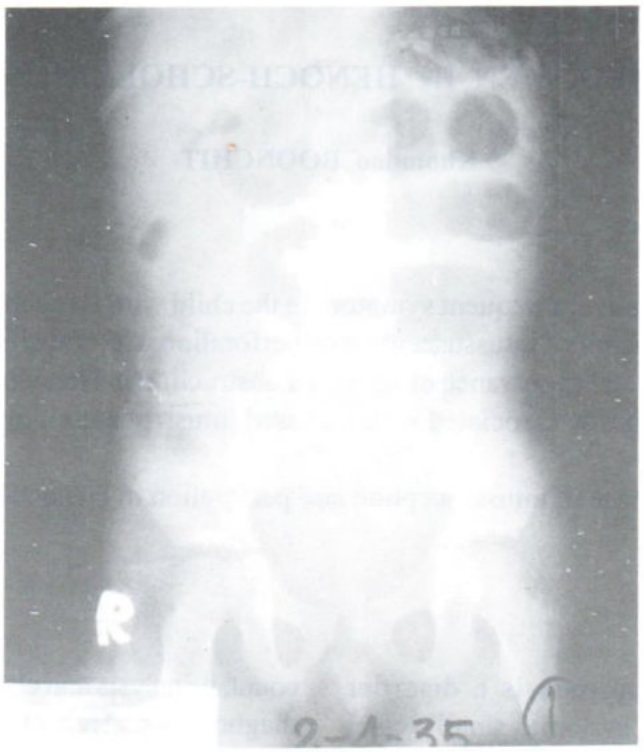

Fig. 1 Plain abdomen supine on the admission day showed dilated small bowel loops.

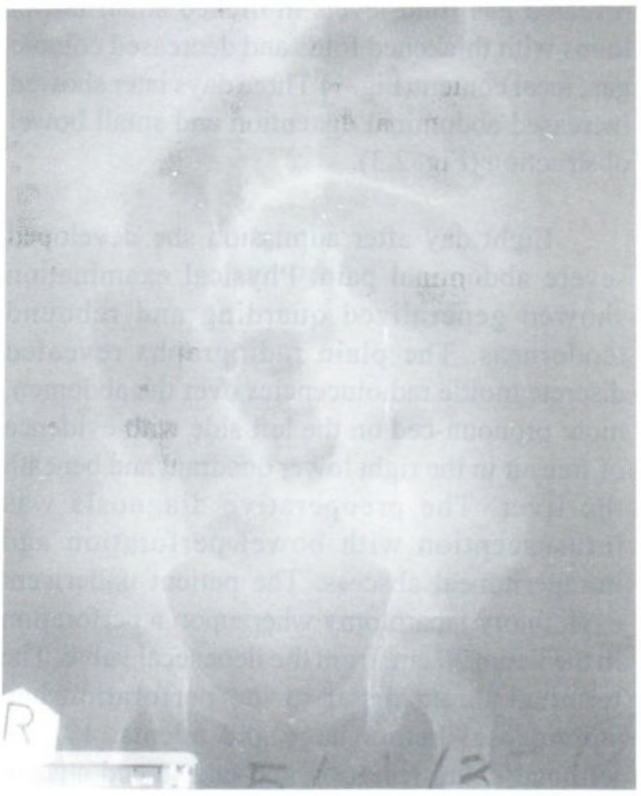

Fig. 2

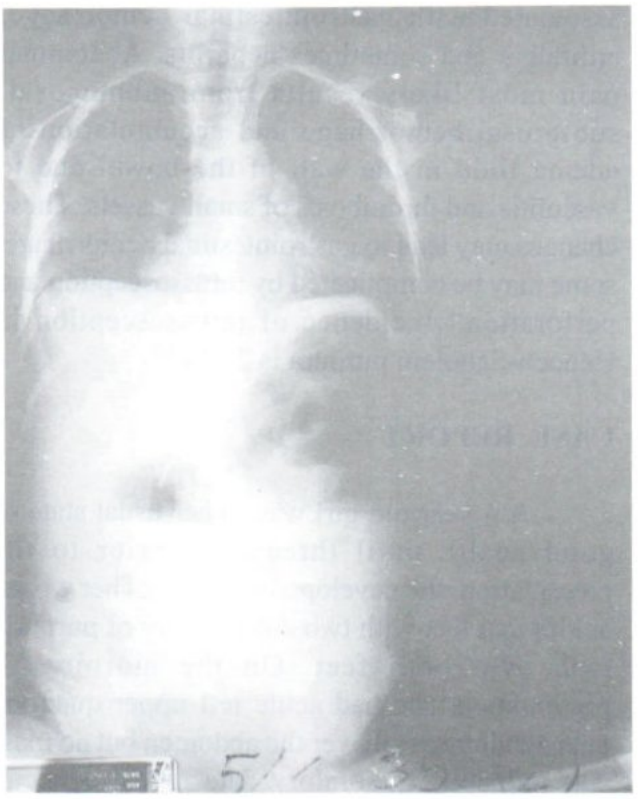

Fig. 3

Fig. 2, 3 Three days later, Plain Abdomen supine and upright showed evidence of small bowel obstruction.

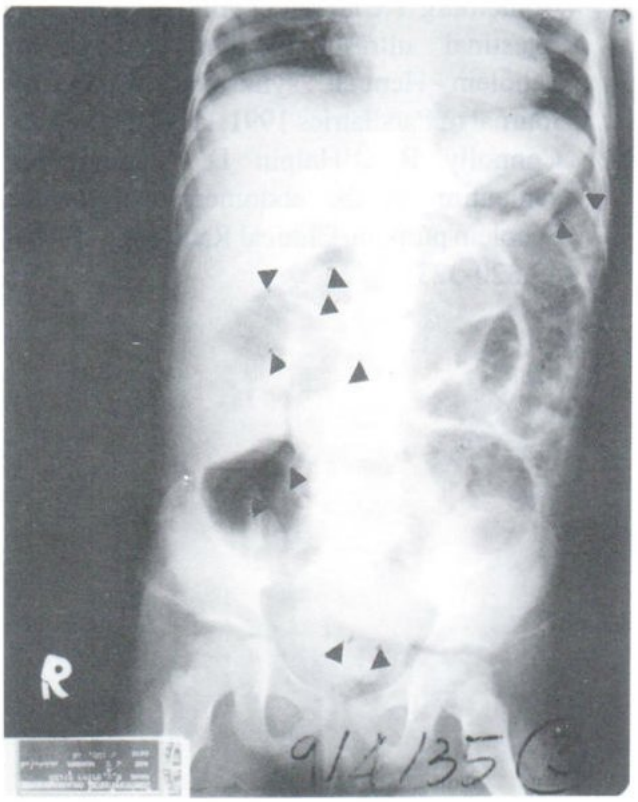

Fig. 4 Free air and abnormal air were observed.

DISCUSSION

Some authors have drawn attention to difficulty in the diagnosis of intussusception in Henoch-Scholein purpura.[4-6] Identification of patients with this complication may be obscured for a number of reasons:

1. Abdominal symptoms are frequent among patients with Henoch-Scholein purpura who do not have intussusception.
2. The presentation of intussusception variable and may be identical to that of intestinal vasculitis and edema or mural hematoma, not requiring surgery.[5,7,8]
3. Intussusception may occur at any stage of illness.[5,8]
4. After surgery intussusception may occur at a different site.[9]
5. The place of contrast studies is limited by its invasiveness and by the fact that most intussusceptions in Henoch-Scholein purpura are in the small bowel.[10] Especially in the presence of vascultis with severe intestinal involvement, there may be a high risk of perforation.

Some studies assess the role of Ultrasound in patients with abdominal symptoms due to Henoch-Scholein purpura.[6,9,11,12]

ACKNOWLEDGMENT

Thanks to Dr. Sudee Chomdej Department of Radiology Chulalongkorn Hospital for her valuable suggestions and reviewing of this manuscript.

REFERENCES

1. Katz S, Borst M, Seekri I, Grosfeld JL. Surgical evaluation of Henoch-Scholein purpura: experience with 110 children. Arch Surg 1991;126:849-854
2. Allen DM, Diamond LK, Howell DA. Anaphylactoid purpura in children. Am J Dis Child 1960;99:147-167
3. Lindenauer SM, Tank ES. Surgical aspects of Henoch - Scholein purpura. Surgery 1966;59: 982-987
4. Glasier CM, Seigel MJ, McAlister WH, Shackelford GD. Henoch-Scholein syndrome in children: Gastrointestinal manifestations. AJR 1981;136:1081-1085
5. Martinez - Frontanilla LA, Haase GM, Ermster JA, Bailey WC. Surgical complications in Henoch - Scholein purpura: J Pediatr Surg 1984;19:434-436
6. Martinez - Frontanilla LA, Silverman L, Meagher DP. Intussusception in Henoch-Scholein purpura: diagnosis with Ultrasound. J Pediatr Surg 1988;23:375-376
7. Harvey JG, Colditz PB. Henoch-Scholein purpura: a surgical review. Aust Pediatr J. 1984;20:13-16
8. Mir E. Complications in Henoch-Scholein purpura in children. Z. kinderchir. 1988;-43:391-393

9. Hu SC, Feency MS, McNicholas M, O'Halpin D,Fitzgerald RJ. Ultrasonography to diagnosis and exclude intussusception in Henoch-Scholein purpura. Arch Child 1991;66:1065-1067
10. Cull DL, Rosario V, Lally KP, Ratner I, Mahour GH. Surgical implications of Henoch-Scholein purpura. J Pediatr Surg. 1990;25:741-743
11. Bomelburg T,Claasen U,vomLengerke HJ. Intestinal ultrasonographic findings in Scholein - Henoch syndrome. European Journal of Paediatrics 1991;150(3):158-160.
12. Connolly B, O'Halpin D. Sonographic evaluation of the abdomen in Henoch-Scholein purpura. Clinical Radiology 1994;-49:320-323.

THREE DIMENTIONAL COMPUTERIZED PLANNING AND PERIODICAL IRRADIATION WITH THE CORRESPONDING OF PATIENT'S RESPIRATION PHASE FOR SOLITARY LUNG METASTASIS : A CASE REPORT.

Pattaranutaporn P, MD.[1], Chansilpa Y, MD.[1], Kakanaporn C, MSc. (Med. Phys.)[1], Onnomdee K, BSc.(Med. Tech.)[2], Mungkung N, BSc.(Med. Tech.)[2], Santisiri R, BSc.(Med.Tech.)[2].

ABSTRACT

A case report of metastatic lung from carcinoma of the rectum was treated with 3D-CT planning and periodical irradiation with the corresponding of patient respiration phase. This technique permits the precise delivery of high dose of radiation to the target while sparing the most of normal lung tissue. The radiation dose was 20 Gy single dose, encompassed the target at the 90 per cent isodose line. The tumor was totally disappeared 1 month after the completion of treatment. The patient could tolerate to the treatment procedure well without any complications inherent to the technique. This technique is an effective and safe treatment for localized lung metastasis. However, long term follow-up should be done to evaluate the late radiation effect of the single fration radiation therapy.

INTRODUCTION

The optimal treatment for patients with pulmonary metastases from colorectal carcinoma is still controversial. Currently, the only treatment capable of significantly prolonging survival in patients with isolated pulmonary metastases from colorectal cancer is complete resection. Surgery represents the first-choice treatment to manage the pulmonary metastases from colorectal cancer when the primary tumor has been controlled and there is no evidence of metastatic spreading to any other organs.The three and five years survival post metastatectomy were 71.6 and 23-43 per cent respectively and some reported in ten year survival.[1-4] A significant difference was noted in the survival rate according to both number and size of the metastatic lesions ($P<0.05$).[1-3,5]

Conventional radiation therapy for pulmonary metastases is limited by the tolerance of the lung tissue. With the improvement of radiation technique such as stereotactic radiotherapy, it is accepted to be an effective loco-regional treatment modality as surgery. Three dimensional treatment planning system and conformal radiotherapy facilitates treatment by providing a mechanism for conforming the high-dose treatment volume to the target volume, thus minimizing the dose to the adjacent uninvolved normal structures. This process involves graphic reconstruction of 3-dimentional images from multiple cross-sectional images, beam's-eye-views display, rapid dose calcu-lations and dose display, and the interactive modification of beam parameters to allow target dose coverage and exclude uninvolved tissue. However, the movement of intrathoracic and intraabdominal target during treament still be the major problem for conforming radiation technique. The periodical irradiation with the corresponding of patient's respiratory phase technique for lung metastasis is developed to solved this problem.

[1] Division of Radiation Oncology, Department of Radiology,Faculty of Medicine, Siriraj Hospital, Mahidol Univesity, Bangkok.
[2] Department of Radiology, Srisiam Hospital, Bangkok.

MATERIAL AND METHOD

A 60 years old male patient with carcinoma of rectum was treated with radiation and chemotherapy because of the contra-indication to surgery from cirrhosis of the liver. Metstasis in the right lower lung was detected one year later. The CT scan of the lung was done for evaluation of the metastases and showed only single small lesion in the right lower lung. Because of the same contraindication to surgery, radiation was considered for this condition.

TECHNIQUE

The patient was positioned and immobilized on the CT-scanner couch with the marker wires placed in the midline and lateral of body along the laser beam. This position was set with these markers through out the treatment procedure. Axial CT images, with 0.5 cm slice thickness through the lung were obtianed during full inspiration. The CT images were transfered directly to the treatment planning system : Focus 3D-planning system. The process was done orderly from labelling of the external contour, normal critical organ and normal tissues that effect the inhomogenicity such as bone and air cavity. After that, the treatment volume was defined including the tumor volume and the biological and physical volume. The treatment planning were done according to the shape of tumor and critical organ nearby. Multiple arc rotation beams and static beams of different couch angles were used. The ninety per cent isodose line was encompassed the target while sparing the most of the lung tissue. After the treatment plan was approved, the alignment was transfer to the central level of the treatment field with conventional simulation, while the patient was set in the same position. The simulation film was checked to confirm that the tumor is in the field of treatment.

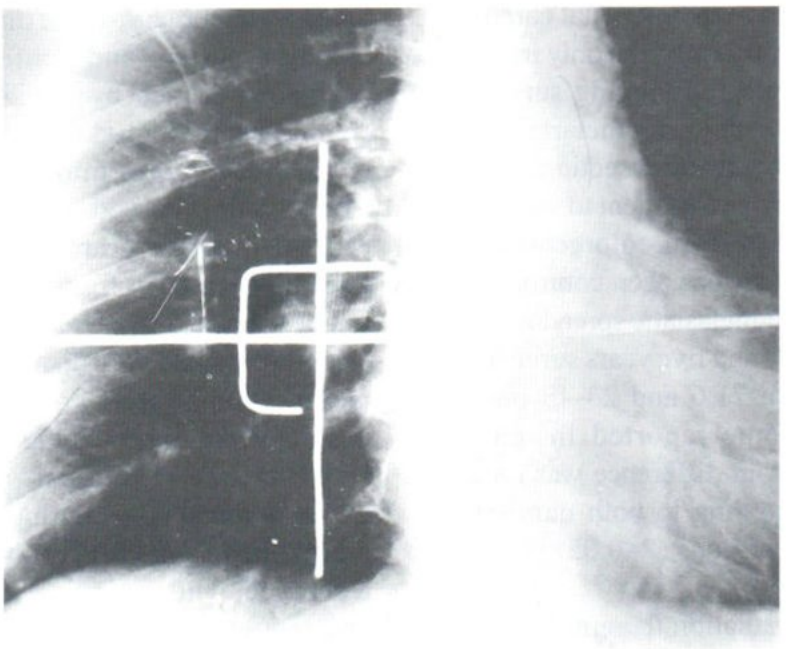

Fig. 1 The simulation film show the correct position of the target in the treatment field in the inspiratory phase.

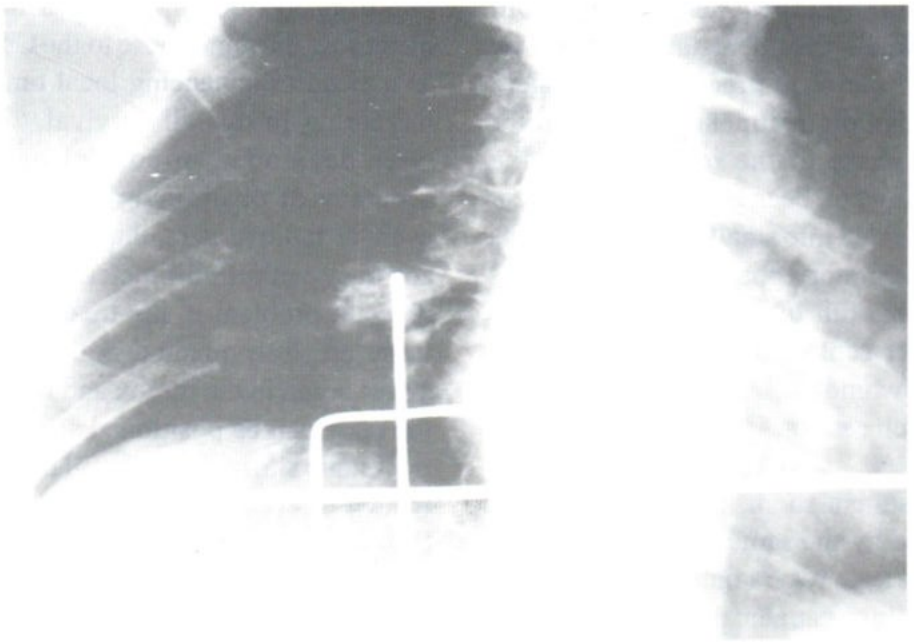

Fig. 2. The simulation film of the expiratory phase showed the error of treatment field due to respiration.

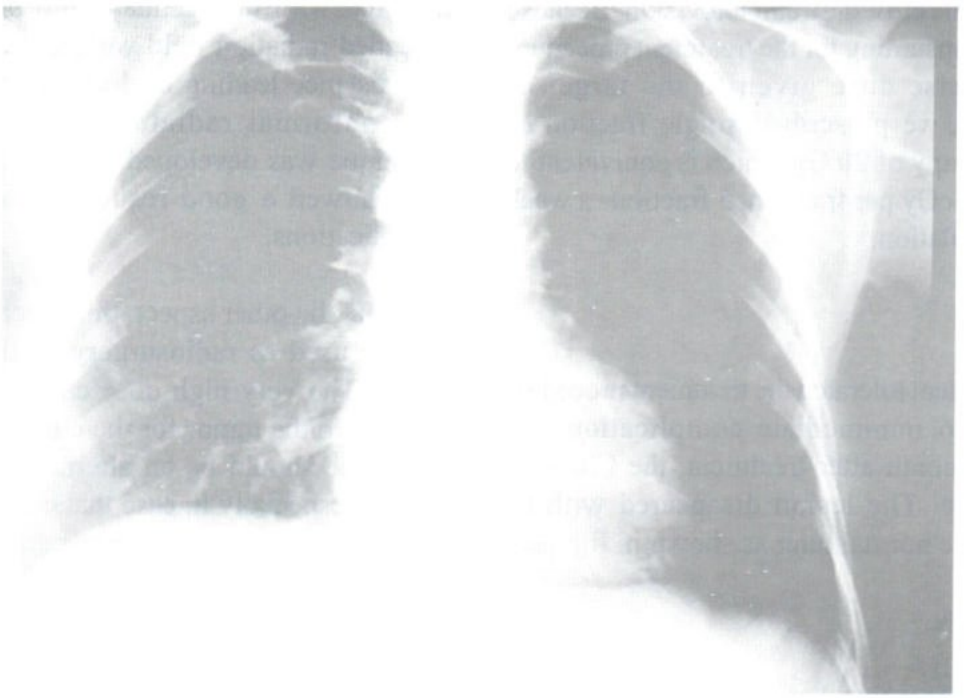

Fig. 3. The chest x-rays film 1 month after treatment showed the disappearance of the lesion.

Because of the chest movement from breathing, the small treatment target would be missed during the period of irradiation as in figure 1 and 2. The radiation treatment was limited for the inspiratory phase of the respiration as the treatment planning had been done. The treatment then had to be divided into small multiple sessions related to the inspiratory phase. The patient was trained to keep his full inspiration as long as he could and 80 per cent of the duration he could hold his breath would be used for the period of irradiation in each session.

In the treatment room, the patient was set and immobilized by the same position as for the CT scanning. At least two radiation technologists were needed for this treatment procedure. The first one worked on the treatment machine while the other controlled the patient respiration during treatment through the intercom, and observed the patient from the closed-circuit television. Because of the time comsuming for the treatment procedure and the precise dose given to the target as radiosurgery, we prescribed single fraction of radiation therapy of 20 Gy which is equivalent to 70 Gy of 200 cGy per fraction, 5 fractions a week by TDF calculation.

RESULT

The patient tolerated the treatment procedure very well, no immmediate complication was found. One month after treatment, the Chest X-ray was done. The lesion disapeared with no reaction of the normal lung as shown in figure 3.

DISCUSSION

The concern that the tumor recieves the dose high enough to achieve a reasonable probability of local control while the radiation dose to normal tissue should be kept low enough to an acceptable complication level was well aware of. Target-specific treatment is particularly desirable if radiosensitive organs are located close to the tumor site. Three dimentional computerized planning system provides a mechanism for increasing the tumor dose to the CT-defined target as a mean of enhancing local tumor control and increasing in overall survival.[6-10] Many system were developed to control or determine the accuracy of positioning and quality assurance even in radiosurgery that was accepted for the accuracy within millimeter.[11-12] One of the most difficult problem in the treatment procedure for these precisely method is the movement of the target organ in the thorax and the abdomen. Even the body can be positioned and immobilized, the metastatic site in the lung still moves up and down related to the cycle of breathing as shown in the figure 1&2. The conventional technique for measuring the motion of an organ is to locate the landmarks in the organ and on the bony anatomy and to compare the distance between these landmarks on subsequent CT scanning. Some invasive techniques using seeds implantation were reported with unacceptable morbidity.[13-14] The extended radiation field were also used to cover this distance leading to decreasing the value of the conformal radiaton technique. So this technique was developed to solved the problem and showed a good result without any acute complications.

In the other aspect, this precised technique can be used as radiosurgery in the movement organ. The very high dose can be given in one fraction to the tumor for the curative intent. This technique should be an alternative treatment to surgery especially in case that contraindicated to surgery. Thus, the 1.4 per cent of operative mortality can also be avoided.[15]

CONCLUSION

Three dimentional computerized planning and periodical irradiation at the corresponding respiratory phase of the patient, is one of the good method for irradiation the moving target such as the lung lesion. This technique should be considered as:

1. An alternative to open surgery for metastectomy in the lung metastasis from the colorectal cancer both for curative or palliative aims.

2. The best method for the new lesion or local recurrent in the previous irradiated lung lesion.

3. Used as the booster technique for delivering the high dose to the well defined volume while sparing the normal surrounding lung tissue.

REFERENCES

1. Shirouzu K, Isomoto H, Hayashi A, et al. Surgical treatment for patients with pulmonary metastases after resection of primary colorectal carcinoma. Cancer 1995;76:393-398.
2. Van Halteren HK, van Geel AN, Hart AA , Zoetmulder FA. Pulmonary resection for metastases of colorectal origin. Chest 1995;-107: 1526-1531.
3. Yano T, Hara N, Ichinose Y, et al. Results of pulmonary resection of metastatic colorectal cancer and its application. J Thorac Cardiovasc Surg 1993;106:875-879.
4. McCormack PM, Burt ME, Bains MS,et al. Lung resection for colorectal metastases, 10-year results. Arch Surg 1992;127:1403-1406.
5. Zapatero J, Flandes J, Lago J, et al. Prognostic factors in pulmonary metastases from colorectal cancer. Respiration 1994;61 :280-282.
6. Ha CS, Kijewski PK, Langer MP. Gain in target dose from using computer controlled radiation therapy (CCRT) in the treatment of non small cell lung cancer. Int J Radiat Oncol Biol Phys 1993;26:335-359.
7. Leibel SA. The biologic basis for conformal three-dimensional radiation therapy. Int J Radiat Oncol Biol Phys 1991;21:805-811.
8. Lichter AS. Three-dimensional conformal radiation therapy : A testable hypothesis. Int J Radiat Oncol Biol Phys 1991;21:853-855.
9. Fuks Z, Leibel SA, Wallner KE, et al. The effect of local control on metastatic dissemination in carcinoma of the prostate : Long term results in patients treated with 125 I implantation. Int J Radiat Oncol Biol Phys 1991;21:537-547.
10. Leibel SA, Scott CB, Mohiuddin M, et al. The effect of local-regional control on distant metastatic dissemination in carcinoma of head and neck : Results of an analysis from the RTOG head and neck database. Int J Radiat Oncol Biol Phys 1991;21:805-811.
11. Menke M, Hirschfeld F, Mack T, et al. Photo grammetric accuracy measurements of Head Holder Systems used for fractionation radiotherapy. Int J Radiat Oncol Biol Phys 1994;29:1147-1155.
12. Drzymala RE, Klein EE. Assurance of high quality Linac-based stereotactic radiosurgery. Int J Radiat Oncol Biol Phys 1994;-30:459-472.
13. Ten Haken RK, Forman JD, Heimburger DK, et al. Treatment planning issues related to prostate movement in response to differential filling of the rectum and bladder. Int J Radiat Oncol Biol Phys 1991;20:1317-1324.
14. Balter JM, Sandler HM, Lam K. Measurement of prostate movement over the course of routine radiotherapy using implanted markers. Int J Radiat Oncol Biol Phys 1995;31:113-118.
15. McAfee MK, Allen MS, Trastek VF, et al. Colorectal lung metastases : Results of surgical excision. Ann Thorac Surg 1992; 53:780-785.

DOSE UNIFORMITY IN ^{60}CO TOTAL BODY IRRADIATION : MULTIPLE FIELD TECHNIQUE

L. TUNTIPUMIAMORN , M.Sc[1] N. DAMRONGKIJUDOM, B.Sc[1]
M. KHANNALAE, B.Sc[2] R. PHUTRAKORNCHAI, B.Sc[2]

ABSTRACT

Study of dose uniformity in total body megavoltage photon irradiation (TBI) from Cobalt-60 teletherapy machine were undertaken by using LiF Thermoluminescent dosimeter (TLD) and Alderson Rando phantom. Halfbody technique with multiple adjacent direct field technique is used in conjuntion with AP/PA position. The prescribed dose at mid plane of the rando phantom is 1200 cGy. From the study, the variation in dose throughout the whole body of phantom ranges from the lowest dose 967.2 cGy on a mediastinal region to the highest of 1337.5 cGy maximum dose to the area of neck. The measured organ doses are 901.5- 945.4 cGy at lens , 723.8- 890.8 cGy at lungs , 1131.2-1154.8 cGy at kidneys, 1144.7-1186.4 cGy at liver and 1135.3-1181.4 cGy at small intestine. The dosimetry revealed that this technique of TBI deliver a uniform dose to the entire body within ± 7.05% of the dose at the prescription point.

INTRODUCTION

Total body irradiation is used in conjunction with high dose chemotherapy to achieve tumour eradication and immunosuppression prior a bone marrow transplantation (BMT).[1,2,3] There is considerable variation in the technique used , depend on the machine availability.[4] For large field radiotherapy, the irradiation method must be produced radiation field large enough to cover the entire target volume adequately. Basic dosimetry should be performed prior the initiation of a magna field treatment technique because of the unusual geometric condition. Dose uniformity should be within ±10 % of the dose at prescription point.[5] The anthromorphic phantom measurement by using TLD is required to verify the technique suitability. In this study , the dose distribution of TBI technique , Halfbody technique with multiple adjacent direct field at Division of Radiation Oncology , Siriraj Hospital was investigated for its suitability by using TLD.

MATERIAL AND METHOD

Due to the limited size of our treatment room (5mx6 m) , TBI was achieved by physical arrangement as in fig.1 and was characterized in Table 1.

[1] Division of Radiation Oncology, Faculty of Medicine, Siriraj Hospital, Mahidol University
[2] Department of Radiation Technology, Faculty of Medical Technology, Mahidol University

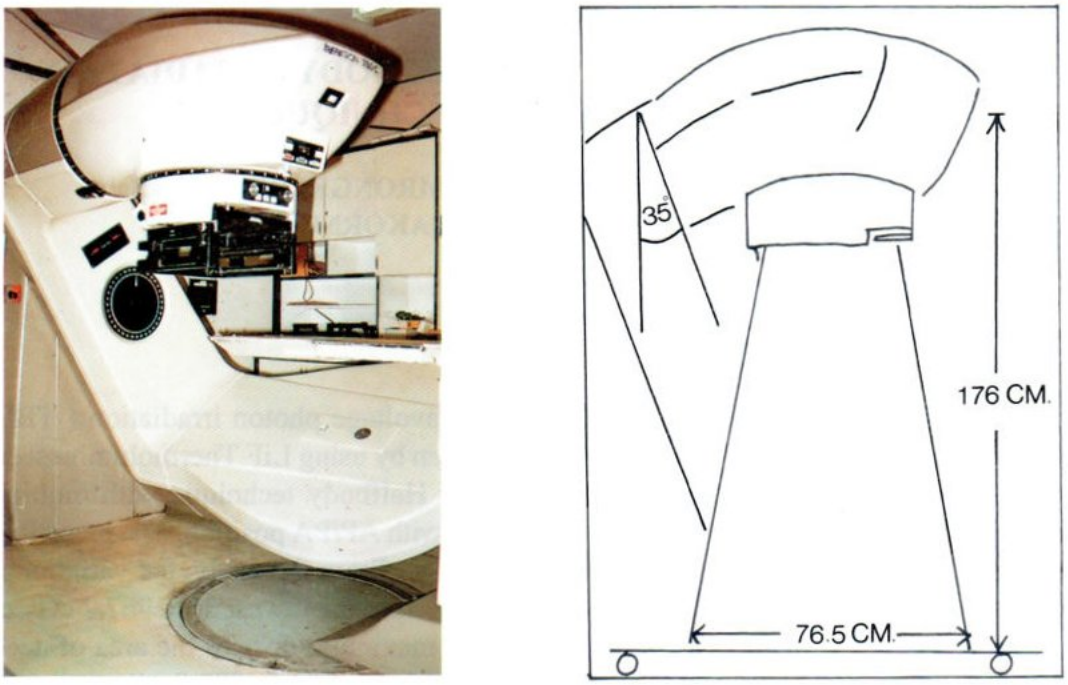

Fig.1 Treatment geometry of Cobalt-60 unit in small therapy room (170 cmSSD)

Table 1. The physical characteristic of ^{60}Co unit for TBI technique

Source	:	^{60}Co gamma-rays
SSD	:	170 cm
Maximum field size	:	76.5 cm x 75.4 cm
Dose rate average	:	40 cGy/min
Patient position	:	supine and prone
Delivery method	:	anterior and posterior
Treatment technique	:	multiple field (half body,adjacent direct field)
Lung shielding	:	1 HVL
Total tumour dose	:	1200 cGy (200 cGy x 6 fractions)

A Rando phantom which is completed with arms and legs made from wax was positioned supine and prone on the special couch on the floor as shown in fig. 2.. Since the maximum field size did not cover the entire body of the phantom, the treatment field was designed to divide into three fields (Fig 3) The mid point of the umbilicus level was chosen to be the reference point and the radiation dose delivered to this point was 1200 cGy to this point. An Lipowitz alloy of 1 HVL lung block thickness was used to reduce lung dose to 50%.

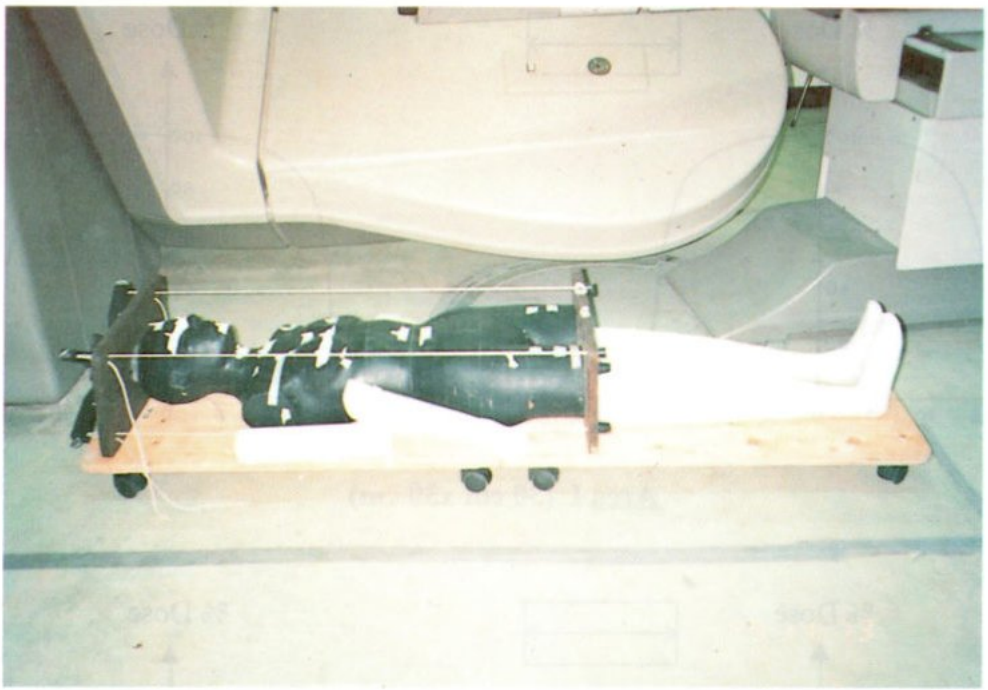

Fig 2. A complete Rando phantom lied on a special couch in treatment geometry.

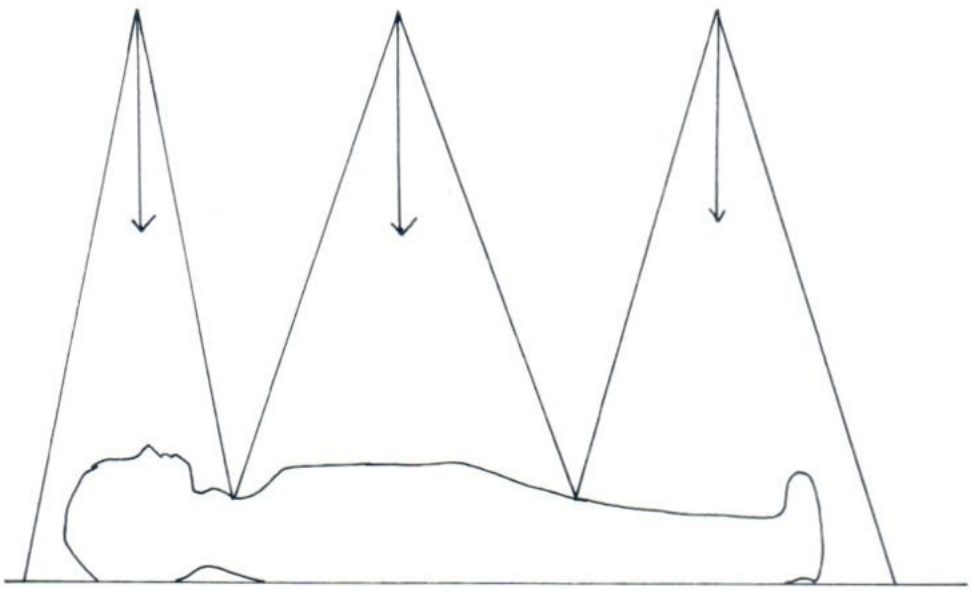

Fig. 3 Irradiation method : multiple field (halfbody, direct adjacent field)

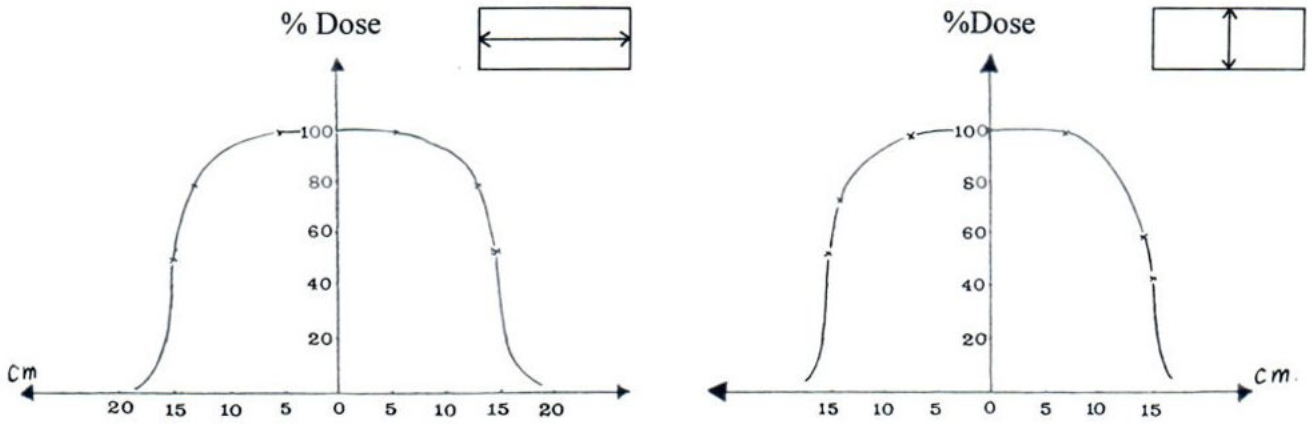

Area I (30 cm x30 cm)

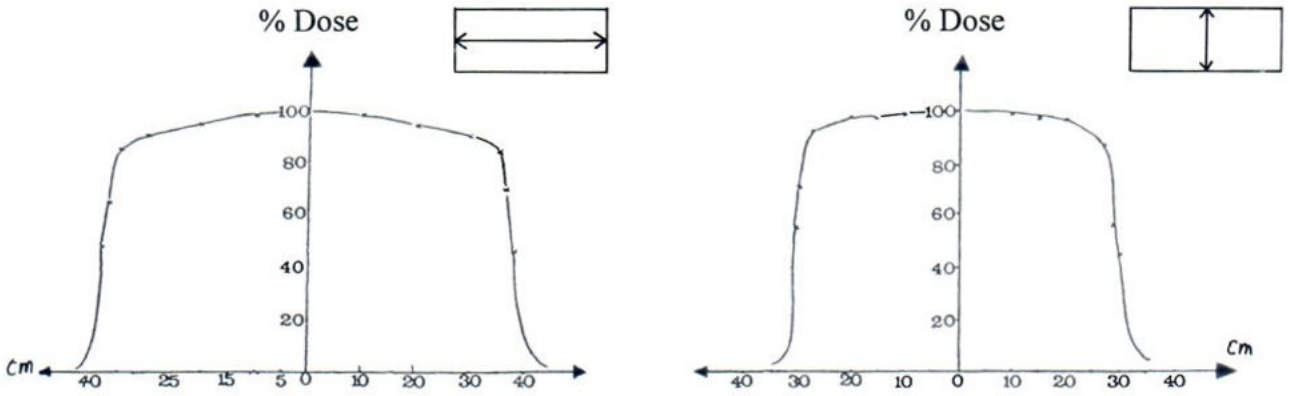

Area II (57 cm x72 cm)

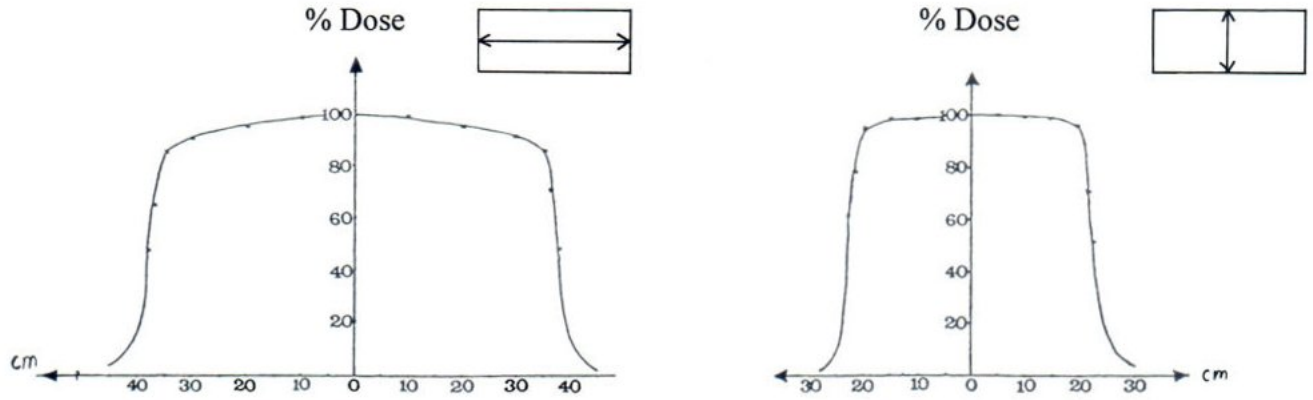

Area III (47 cm x 76.5 cm)

Fig. 4 Beam intensity profile of each treatment field at 170 cm SSD in TBI irradiation

BEAM PROFILE AND OUTPUT MEASUREMENT

The symmetry of the beam intensity across and along the treatment field was measured in air by eight semiconductors (Rainbow type 30-490-80). Output measurement performed in water phantom at the TBI distance of 5 cm depth by the ionization chamber Farmer Dosemeter type 2570/1 NE. The percentage depth dose at TBI distance was converted from the usual 80 cm SSD by Burn's equation.[6]

VERIFICATION DOSIMETRY

Absorbed dose for eleven tranverse sections (brain,neck,mediastinum,abdomen and pelvis region) measured with TLD were accomplished. The surface dose were measured at lens, thighs and legs. The radiation dose was calculated to give 100 cGy to the prescription point for both anterior and posterior port.

RESULT

The results of beam intensity profile for each treatment field was shown in Fig. 4 It can be seen that 80% of field width is fitted in 90% of maximum dose level. Therefore , each treatment field would have a good symmetry. This mean that the most patients whose body width less than 45 cm. can be performed.

Table 2 lists the doses in various sections of the Rando phantom. From the data, it can be seen that the uniformity of dose throughout the whole body of phantom is within ± 7.05% of the dose at the reference point.

Table. 2 The measuring doses as the percentage of dose at reference point in various sections of rando phantom

Sites	Numbers of measuring points	Measuring doses (%)
Brain (Section # 3, 4)	5	90.4-100.00
Neck (Section # 8)	4	99.4-111.5
Chest (Section #15,16,17)	4	80.6-84.6
Abdomen and pelvis (Sec # 23,24,26,29,33)	26	91.3-103.4
Averaged dose	39	96.02±7.05

General agreement with prescribed dose can be seen for most region of the phantom. It is noted there are four measuring points having lower dose comparing to the others

Since the organ dose at the prescribed point from this experiment is set to 200 cGy, therefore, the total organ dose given to reference point can be calculated to 1200 cGy. The dose measured at each organ are summarized in Table 3.

Table 3 The radiation dose to various organs from irradiating 1200 cGy on the prescription point of the Rando phantom

Organs	Radiation dose (cGy)
Lens	901.5-945.4
Lungs	723.8-840.8
Kidneys	1131.2-1154.8
Livers	1144.7-1186.4
Small intestine	1135.3-1181.4
Large intestine	1199.8-1212.5
Rectum	1161.9
Skin (thigh, legs)	1090.6-1146.1

DISCUSSION

Most of the measuring points (35 from 39 points) have a good agreement with the prescribed dose. Except the four points at mediastinum that the dose are quite low (80.4-84.6 % of prescribed dose) when compared to the others. It is found that these four low dose points are the positions of TLD under the perspex shielding tray designed for lung shielding block . Because of the length of this shielding tray is only 1/3 of the treatment field length , the correction factor for tray attenuation (about 7% of primary dose) and PDD for irregular field were not taken into account for dose calculation.

For large-field radiotherapy , the delivery of a uniform dose of radiation over the entire target volume is not a simple task. This report is an attempt to verify the uniformity of the dose delivered to the patients under the unusual geometric condition with the conventional facility. It is found that the thinner perspex sheet or net shielding tray should be replaced the old one and Clarkson' method should be provided in dose calculation for large area blocked treatment field. However, it can be concluded that for the TBI technique, multiple field (halfbody,adjacent direct field) would be given a satisfactorily uniform dose.

REFERENCES

1. Van Dyk J, Galvin JM, Glasgow GP, Podgorsak EB. The physical aspects of total and half body photon irradiation. AAPM., 1986;17:,1-47
2. Barrett A. Totalbody irradiation (TBI) before bone marrow transplant in acute leukemia: a co-operative study from the European group for bone marrow transplantation. BJR., 1982;55:562-567
3. Gale RP , Batturini A, Bortin MM. What does total body irradiation do in bone marrow transplants for leukemia. Int. J. Rad. Biol. Phys., 1991; 20(3): 631-633
4. Van Dyk J. Magna-field irradiation: Physical considerations. Int. J. Rad. Biol. Phys.,1983; 9(12): 1913-1917
5. Van Dyk J. Whole and partial body radiotherapy: physical considerations. In advances in Radiation therapy treatment planning. AAPM Med. Phys., 1983; 9:403-426
6. Bewley DK, BRADSHAW AL, Burns JE, et al. Conversion of percentage depth doses for photon beams from one SSD to another and calculation of TAR, TMR and TPR. In: Central axis depth dose data for use in radiotherapy. BJR supplement No.17.,1983: 115

Foot Note: PDD = Percentage Depth Dose, TAR = Tissue Air Ratio, TMR = Tissue Maximum Ratio, TPR = Tissue Phantom Ratio.

DETECTION OF DEEP VEIN THROMBOSIS BY ^{99m}Tc-SULFUR COLLOID IN 24 CASES

Nisarut RUKSAWIN M.S,[1] Pramot PHORNPHIBULAYA M.D.[2]

ABSTRACT

Scintigrams of the legs were recorded by computed scinticamera after antecubital injection of ^{99m}Tc-sulfur colloid in 24 patients with suspected deep vein thrombosis. Contrast venogram were taken after the scan 1 hour to 1 day. Of 15 patients with confirmed deep venous thrombosis, 11 had positive scans. Of 9 patients with normal venograms, 8 had negative scintigrams. Rate of accuracy read by physician was 79% and rate of accuracy analysed by computer was 83%. The risk and discomfort of contrast studies may be eliminated by the nuclear method.

INTRODUCTION

The uptake of ^{99m}Tc-sulfur colloid by venous thrombosis is well documented.[1-9] Recently Bardfeld et al.[9] have verified that injection of ^{99m}Tc-sulfur colloid into an arm would be a feasible method of detecting deep vein leg thrombosis. Based on reports which suggested that contrast media used for venography might damage the intima of the vein and produce thrombosis,[10-15] we decided to study 24 patients with suspected deep vein thrombosis using Bardfeld's method.

However, we used contrast venography as a standard method. Our experiment was a somewhat more advanced than Bardfeld's series for we compared the result of scintiphotoes as interpreted by a physician in nuclear medicine to more rigid computer analysis and contrast venography.

METHODS

Twenty four patients without varicose veins scheduled for venography were sent to section of Nuclear Medicine by a surgeon. All had normal liver function, otherwise bone marrow uptake might be misleading. Eight mCi (~300 MBq) of ^{99m}Tc-sulfur colloid was injected via an arm vein. Thirty minutes to an hour later scintiphotoes of anterior views from thighs to ankles were obtained with a large field of view gamma camera. We preset 100,000 counts and only two images could cover the area from thighs to ankles. The scintigrams alone were interpreted by a physician in nuclear medicine. The data of both legs were also stored on a computer. Equal areas of interest were selected on left and right legs. If the uptake in one leg was greater than that in another leg by 20% the scan was considered positive. Contrast venograms were obtained 1 hour to 1 day after scintigraphy.

RESULTS

The radionuclide studies which were interpreted by a nuclear medicine physician, by a computer, and contrast venograms were compared

[1] Department of Radiology, Siriraj Hospital, Mahidol University, Bangkok, Thailand.
[2] Department of Surgery, Siriraj Hospital, Mahidol University, Bangkok, Thailand.

DETECTION OF DEEP VEIN THROMBOSIS BY ^{99m}Tc-SULFUR COLLOID IN 24 CASES

Nisarut RUKSAWIN M.S,[1] Pramot PHORNPHIBULAYA M.D.[2]

ABSTRACT

Scintigrams of the legs were recorded by computed scinticamera after antecubital injection of ^{99m}Tc-sulfur colloid in 24 patients with suspected deep vein thrombosis. Contrast venogram were taken after the scan 1 hour to 1 day. Of 15 patients with confirmed deep venous thrombosis, 11 had positive scans. Of 9 patients with normal venograms, 8 had negative scintigrams. Rate of accuracy read by physician was 79% and rate of accuracy analysed by computer was 83%. The risk and discomfort of contrast studies may be eliminated by the nuclear method.

INTRODUCTION

The uptake of ^{99m}Tc-sulfur colloid by venous thrombosis is well documented.[1-9] Recently Bardfeld et al.[9] have verified that injection of ^{99m}Tc-sulfur colloid into an arm would be a feasible method of detecting deep vein leg thrombosis. Based on reports which suggested that contrast media used for venography might damage the intima of the vein and produce thrombosis,[10-15] we decided to study 24 patients with suspected deep vein thrombosis using Bardfeld's method.

However, we used contrast venography as a standard method. Our experiment was a somewhat more advanced than Bardfeld's series for we compared the result of scintiphotoes as interpreted by a physician in nuclear medicine to more rigid computer analysis and contrast venography.

METHODS

Twenty four patients without varicose veins scheduled for venography were sent to section of Nuclear Medicine by a surgeon. All had normal liver function, otherwise bone marrow uptake might be misleading. Eight mCi (~300 MBq) of ^{99m}Tc-sulfur colloid was injected via an arm vein. Thirty minutes to an hour later scintiphotoes of anterior views from thighs to ankles were obtained with a large field of view gamma camera. We preset 100,000 counts and only two images could cover the area from thighs to ankles. The scintigrams alone were interpreted by a physician in nuclear medicine. The data of both legs were also stored on a computer. Equal areas of interest were selected on left and right legs. If the uptake in one leg was greater than that in another leg by 20% the scan was considered positive. Contrast venograms were obtained 1 hour to 1 day after scintigraphy.

RESULTS

The radionuclide studies which were interpreted by a nuclear medicine physician, by a computer, and contrast venograms were compared

[1] Department of Radiology, Siriraj Hospital, Mahidol University, Bangkok, Thailand.
[2] Department of Surgery, Siriraj Hospital, Mahidol University, Bangkok, Thailand.

TABLE 1
Summary of Patient Data

Patient	Age (yr) and sex	Clinical History	Scintigram Read by Physician	Scintigram Read by Computer	Venogram and Final Diagnosis
1. S.S.	56 M	Category ***4, definite positive femoral VT* of the left leg	Increased activity in the left thigh	Positive	Left popliteal VT extending into femoral vein
2. B.P.	58 M	Category 1, equivocal signs, iliofemoral VT of the right leg	Normal	Normal	No evidence of DVT**
3. D.P.	30 F	Category 1, equivocal signs, femoral VT of the right leg	Normal	Normal	No evidence of DVT
4. Y.K.	65 M	Swelling and pain of the left thigh post operation	Increased activity in the left thigh and calf	Positive	DVT in the left thigh and calf
5. A.M.	48 M	Category 1, equivocal signs, femoral VT of the left leg	Normal	Normal	No evidence of DVT
6. L.T.	43 F	Category 1, definite positive femoral VT of the right leg	Thrombosis of the right leg	Positive	Posterior tibial vein thrombosis
7. S.C.	24 F	Inferior vena cava obstruction, middle portion, due to lymphoma	Normal	Normal	No evidence of DVT, lymphatic obstruction
8. K.U.	68 M	Category 5, definite positive, iliofemoral VT of the left leg	Normal	Positive	Extensive DVT
9. C.P.	42 F	Category 1, equivocal signs, femoral VT of the right leg	Normal	Normal	No evidence of DVT
10. L.C.	43 F	Category 1, definite positive, femoral VT of the left leg	Venous thrombosis of the left leg	Positive	Popliteal VT
11. S.T.	26 F	Category 1, equivocal signs, femoral VT of the right leg	Normal	Normal	Occlusion of anterior tibial vein
12. S.P.	30 F	Category 3, equivocal signs, iliofemoral VT of the left leg	Normal	Normal	Iliofemoral VT of the left leg
13. C.L.	62 M	Category 4, equivocal signs, iliofemoral VT of the right leg	Normal	Normal	Iliofemoral VT of the right leg
14. P.C.	64 M	Category 1, equivocal signs, femoral VT of the left leg	Normal	Normal	Normal
15. B.S.	44 M	Category 1, definite signs, iliofemoral VT of the left leg	Probable venous thrombosis of the left lower extrimity	Positive	DVT of the left leg

Patient	Age (yr) and sex	Clinical History	Scintigram Read by Physician	Scintigram Read by Computer	Venogram and Final Diagnosis
16. S.C.	69 M	Category 1, definite signs, iliofemoral VT of the left leg	Positive at the left leg	Positive	DVT of the left leg
17. S.Y.	31 F	Category 1, equivocal signs, femoral VT of the right leg	DVT of the right leg	Positive	DVT of the right leg
18. S.Y.	28 M	Category 1, equivocal signs, iliofemoral VT of the left leg	Probable DVT of the	Positive	Iliofemoral VT of the left leg
19. W.T.	53 F	Category 5, equivocal signs, iliofemoral VT of the left leg	Probable DVT of the left leg	Positive	Normal
20. S.T.	74 F	Category 4, equivocal signs, femoral VT of the left leg	Normal	Normal	No evidence of DVT
21. W.T.	39 M	Category 5, equivocal signs, Cellulitis of the right leg	Normal	Normal	No evidence of DVT
22. B.K.	32 M	Category 1, equivocal signs, femoral VT of the left leg	Evidence of DVT	Positive	Iliofemoral vein of the left leg
23. C.P.	51 M	Category 5, equivocal signs, iliofemoral VT of the right leg	DVT of the right leg	Positive	Right femoral vein thrombosis
24. B.P.	75 M	Category 5, equivocal signs, femoral VT of the right leg	DVT of the right leg	Positive	Thrombosis of posterior tibial vein

VT* = venous thrombosis
DVT** = deep venous thrombosis
Category*** = Categories for patients with clinical diagnosis of deep vein thrombosis
Category 1 : Ambulant patient presenting with pain and/or swelling of calves, without previous illness
Category 2 : Proved or suspected pulmonary embolus
Category 3 : Calf pain or swelling of limb after delivery
Category 4 : Calf pain or swelling of limb after surgery
Category 5 : Calf pain or swelling after rest for medical illness

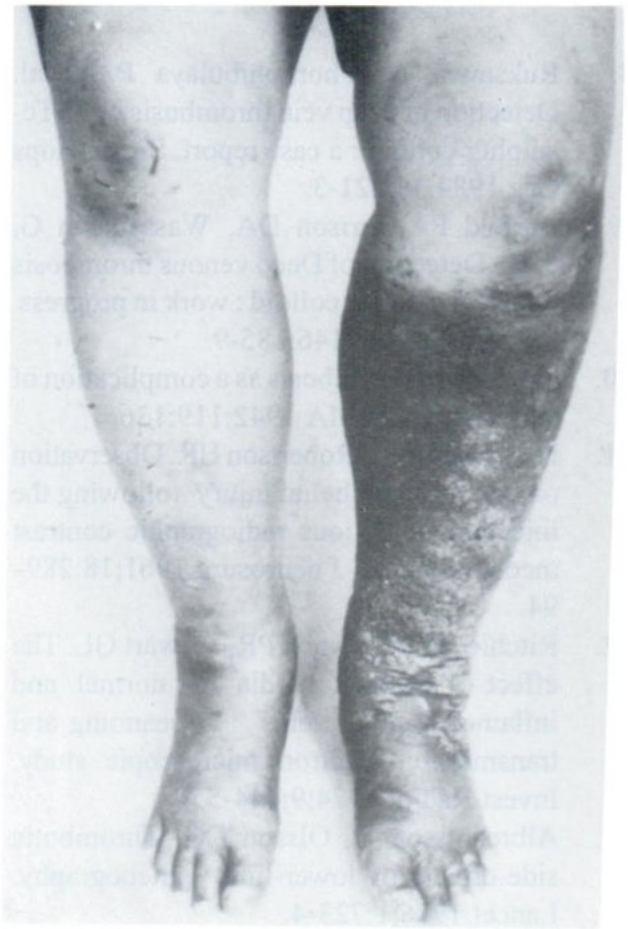

Fig.1 A

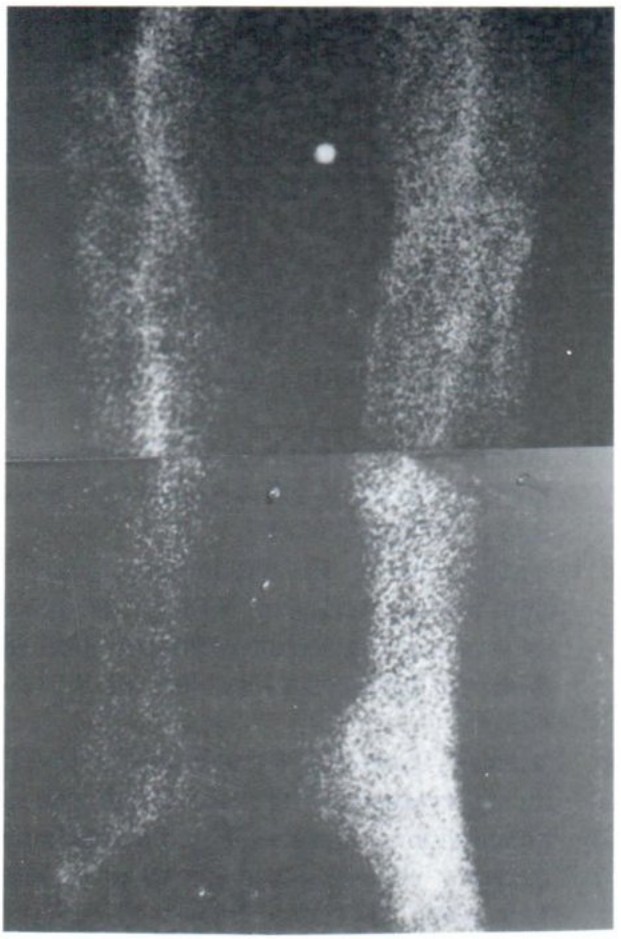

Fig. 1 B

Fig.1.(A) A patient developed swelling and echymosis after the injection of contrast medium at the dorsum of the left foot.

Fig. 1(B) ^{99m}Tc-sulfur colloid scintigrams show higher uptake by the left leg. The bright spot is a marker placed between the knees of the patient. The ratio of the average uptake of ^{99m}Tc-sulfur colloid at the lower part of lt. Leg and foot right foot was 1:1.8

REFERENCES

1. George EA, Codd JE, Newton WT, et al. Further evaluation of ^{99m}Tc sulfur colloid accumulation in rejecting renal transplants in man and a canine model. Radiology 1975; 116:121-6.
2. George EA, Henry RE, Newton WT, et al. Mechanism of ^{99m}Tc sulfur colloid acumulation in canine renal allografts during hyperacute rejection. J Nucl Biol Med 1975;19:213-9.
3. Freeman AH, Wraight EP, Chir B. Uptake of ^{99m}Tc colloid by intravascular clot. Br. J Radiol 1976;49:803-4.
4. Viers F, Barron EL, Preliminary observations on the potential of ^{99m}Tc-sulfur colloid as a radiopharmaceutical for detection of deep vein thrombosis. Radiology 1979;132:-473-4.
5. Vieras F, Barrn EL, Parker GA, et al. Experimental evaluation ^{99m}Tc-sulfur colloid as a potential imaging agent in thromboembolic disease : concise communication. J Nucl Med 1980;21:723-8.
6. Bardfeld PA, Rand J, Coldsmith SJ. The use of ^{99m}Tc-sulfur colloid as a marker for experimental venous thrombosis : concise communication. J Nucl Med 1981;22:598-600.
7. Ruksawin N, Phornphibulaya P, Suwanik R, et al. Uptake of ^{99m}Tc-sulphur colloid by deep vein thrombi : a case report. Nuclear Medicine Communications 1984;5:175-8.
8. Ruksawin N, Phornphibulaya P, et al. Detection of deep vein thrombosis by ^{99m}Tc-sulphur colloid : a case report. Siriraj Hops Gaz 1984;36:221-3.
9. Barfeld PA, arrison DA, Wasserstein G, et al : Detection of Deep venous thrombosis with ^{99m}Tc-sulfur colloid : work in progress. Radiology 1983;146:185-9.
10. Homans J, Thrombosis as a complication of venography. JAMA 1942;119:136.
11. Mersereau WA, Robertson HR. Observation on venous endothelial injury following the injection of various radiographic contrast media in the rat. J neurosurg 1961;18:289-94.
12. Ritchie WGM, Lynch PR, Stewart GL. The effect of contrast media on normal and inflamed canine veins : A scanning and transmission electron microscopic study. Invest Radiol 1974;9:444-55.
13. Albrechtsson U, Olsson CG. Thrombotic side-effects of lower-limb phlebography. Lancet 1976;1:723-4.
14. Albrechtsson U, Olsson CG. Thrombosis after phlebography : a comparison of two contrast media. Cardiovase Radiol 1979;2:9-18.
15. Walters HL, Clemenson J, Browse NL, et al. ^{125}I-fibrinogen uptake following phlebography of the leg : Comparison of ionic and nonionic contrast media. Diagnostic Radiology 1980;135:619-21.

RADIOACTIVE NEEDLE IMPLANT FOR HEAD AND NECK TUMOURS; IS IT A DYING ART?

G.C.C. Lim, F.R.C.R. [1], M.T. Azhar, F.F.R.R.C.S.I. [2]

ABSTRACT

This paper aims to audit the treatment of head and neck tumours with radioactive needle implant techniques in our centre. A retrospective analysis of 50 patients who underwent this procedure from 1986 to 1994 was performed. Cancers of the oral tongue and buccal mucosa were the most common conditions treated, comprising 62% an 26% respectively. Prior external beam radiotherapy was employed in 70%. Implant doses ranged from 20 Gray to 75 Gray. The most frequent toxicity reported was mucositis (10%). While 33% remained free of recurrence, local recurrence was seen in 46%. Crude survival ranged from 1 to 126 months. Results for disease free survival and crude survival were better in the patients with node negative disease. Radioactive needle implants continue to play a significant role in early oral cavity tumours and should be considered in appropriate clinical situations.

INTRODUCTION

The role of primary radiotherapy in head and neck cancer has often been superceded by radical surgery up front although the results of both these modalities in early tumours are comparable. This is partly due to the fact that radioactive implants are less often used nowadays. This paper discusses the merits and problems encountered in this procedure.

As in other radiotherapy centres which practise radioactive needle implants, head and neck cancers form the major bulk of the patients undergoing this procedure. However, the patients must be carefully selected so as to optimize the results. This paper demonstrates that the patients who appear to benefit most in terms of crude survival and disease free interval are those in whom the regional nodes were not clinically involved at presentation.

MATERIALS AND METHODS

A retrospective study was conducted on patients who had undergone radioactive needle implants for head and neck cancer at the Institute of Radiotherapy and Oncology, Kuala Lumpur Hospital. The study population were patients with head and neck cancer who underwent this procedure at this Institute between 1986 and 1994. The radioactive source for the implants needles in our institute was changed from Radium-226 to Caesium-137 in January 1993. The source arrangement and calculation of the prescribed dose adopted the system devised by Paterson and Packer.[1-3] The sample included all patients who met the following inclusion criteria: any primary malignant tumour of the head and neck which had been implanted with radioactive needles, tumours that had been histologically verified. The exclusion criteria applied in this study were: patients whose tumours were not histologically verified and

[1] Institute of Radiotherapy and Oncology, Hospital Kuala Lumpur.
[2] Faculty of Medicine, International Islamic University, Kuala Lumpur.

Correspondance: Dr.Gerard Lim CHIN CHYE, Institute of Radiotherapy and Oncology, Hospital Kuala Lumpur, Jalan Pahang, Malaysia.

patients whose records could not be traced.

The records were retrieved manually, using the list of patients undergoing procedures in the Operating Theatre of the Institute. Records of 50 patients were traced. Data were collected using a check-list questionnaire. Case notes, referral letters, histolopathology reports, laboratory tests, operation findings, radiotherapy records, worksheets for the calculation and prescription of brachytherapy and relevant investigations were reviewed. Information on patient demographic data, tumour characteristics, external beam therapy, brachytherapy, complications of treatment, crude survival, disease free interval and recurrence pattern were retrieved from these notes. Staging was based on the T.N.M. system. The dose prescription for the external beam therapy was based on the International Commission on Radiation Units and Measurements, *Dose specification for reporting external beam therapy with photons and electrons*, I.C.R.U. Report 29[4] and the dose prescription for brachytherapy was based on the system of Paterson and Parker which had been compiled into the Manchester system.[1-3] Crude survival time was calculated from the date of implant to the date of last follow-up or date of death. Relapse-free interval was calculated from the date of implant to the date of first relapse after the implant. Patients who were lost to follow-up had the vital status verified by sending their National Registration Identification Card Numbers to the Director, Identity Card Section, Malaysian National Registration Department to determine the date of notification of death. The status of 3 patients are still unknown as their identity card numbers were not traceable from our records or they were from areas other than Peninsular Malaysia.

RESULTS:

The records of 50 patients were analysed. The male:female ratio was 2 : 3 . The median age was 55 years with a range from 26 to 89 years (Table 1). Indians comprised 46%, Chinese 28%, Malays 22% and other races 4%.

Patients with tumours involving the anterior two thirds of the tongue comprised 62%, while buccal mucosa made up 26%. Other head and neck sites included the lip (2 patients), alveolus (1 patient), frenulum of tongue (1 patient), submandibular region (1 patient) and maxillary region (1 patient). Ninety per cent of the tumours in this series was histologically confirmed to be squamous cell carcinomas. The other histologies included adenocarcinoma (1 patient), non-Hodgkin's lymphoma (2 patients), soft tissue sarcoma (1 patient) and unrecorded in one patient. The grade of these tumours were well differentiated in 36%, moderately well differentiated in 36%, poorly or undifferentiated in 4% and unrecorded in 24%. Only a biopsy was carried out in most of the patients (92%) before the implant procedure. Tumour stage was 28%, 40%, 16%, 14% and 2% for T1, T2, T3 and Tx respectively. Metastases in the cervical lymph nodes was absent in 84%, present in 12% and unrecorded in the rest. None of the patients were known to have distant metastases at the time of the implant. Radioactive needle implants were used for locally recurrent tumours in 2 patients. The WHO/ECOG performance status was 0 in 20%, 1 in 56%, 2 in 16%, and unrecorded in 8%.

Prior to the radioactive needle implant, 70% of the patients received external beam radiation with doses ranging from 27 Gy to 65 Gy. Among the more frequently used dose-fractionation regimens were 50 Gy in 25 fractions (5 patients), 60 Gy in 30 fractions (3 patients), 50 Gy in 20 fractions (2 patients), and 55 Gy in 25 fractions (2 patients). The external beam radiotherapy was delivered by a two-field technique in 23 patients and a single-field technique in 12 patients.

Radioactive needle implants were executed in a single plane in 50%, double plane in 48%, and as a volume implant in one patient with tongue cancer. The prescribed doses for brachytherapy ranged from 20 Gy to 75 Gy. The main morbidities

encountered were mucositis (10%), ulceration (7%) and pain (8%). The other problems encountered were needle dislodgement (8%) and retained needle in one patient when the needles were removed after the end of a tongue implant; an invasive procedure under general anaesthesia was subsequently used to remove it.

The disease free interval ranged from 0 months to 120 months, with a median of 29 months. Thirty four per cent of the patients were free from recurrence, all of whom had clinically negative nodes at presentation. Recurrences involving the local site alone comprised 26% while loco-regional recurrences was found in 20%. The recurrence status of the rest of the patients could not be ascertained. Of the 6 patients who had clinically involved cervical nodes at presentation, at least 4 patients have developed a local or loco-regional recurrence.

The survival status of the patients were as follows: Alive (58%), Dead (36%) and Unknown (6%). The crude survival ranged from 1 month to 126 months, with a median of 22 months. One third of the patients with known regional node positive disease were still alive. In the two patients who underwent radioactive needle implants for locally recurrent tumours, their respective survival was 7 months and 2 months respectively.

The characteristics of the sub-group of 13 patients who survived for at least 60 months after their implants deserve to be highlighted. The age range in this sub-group of 12 patients was 36 years to 76 years. The patients had T1-2 N0M0 squamous cell cancinomas of either the mobile tongue or buccal mucosa. Prior to radiotherapy, all these patients underwent only a biopsy. The external beam radiotherapy dose used in 5 of these patients ranged from 40 Gy to 55 Gy. The brachytherapy dose ranged from 30 Gy to 75 Gy. In patients in whom no external beam was given, the brachytherapy doses ranged from 60 Gy to 75 Gy. A single plane implant was used in nearly 70% of the patients while a double plane technique was used in the remaining patients.

DISCUSSION

Interstitital brachytherapy is often indicated in the management of primary or recurrent head and neck tumours. Radioactive needle implant is an old technique but has been well tried and tested. The principal aims of radiotherapy treatment planning are to achieve a homogenous dose distribution in the target volume, i.e. within and around the tumour, whilst sparing the surrounding normal tissues. Radioactive needle implants can deliver the prescribed radiation dose to the target volume with less radiation to the adjacent normal tissues mainly because of the 'Inverse Square Law' of radiation attenuation. The lower dose-rate of radiation received by the normal tissues during an implant treatment also allows for further sparing of late effects of radiation on such tissues. One of the main advantages of implant treatment over radical surgery in patients who are cured of cancer is the preservation of function of the affected organ, e.g. tongue. The usefulness in the palliative setting has also been suggested by the 7 month survival of one the patients with locally recurrent disease for whom the implant was performed. If some measure of local tumour control could be achieved in these patients in the remainder of their lives resulting in relief of their local symptoms, their quality of life could be improved.

In centres which practise intra-oral needle implants routinely, the single-plane implant is the commonest form of implant used.[5] Radioactive needles have been used, either alone or in combination with external beam, to treat lesions of the tongue and the floor of the mouth.[6] In centres where radioactive needle implants are performed, calculations have been based on the Paterson-Parker system.[1-3] On the other hand, the Paris system[7] is used in centres which practise implants using iridium-192. The disadvantages in using iridium-192 sources include higher operational costs due to the shorter half-life of 74 days and

the potential problems associated with the necessity of regular supplies of this isotope.

Generally, it is not desirable to deliver the whole radiotherapy treatment solely as an implant as the treatment time would be uncomfortably long for the patient. Moreover, the distant areas such as the regional lymph nodes would not be adequately treated by the implant. This has been demonstrated in this study whereby the recurrence rate in patients who had clinically involved cervical nodes at presentation was considerably higher than those patients whose nodes were negative. The course of external beam radiotherapy given before an implant serves to treat both the tumour site as well as the presumed spread in the regional lymphatics.

The results of disease local control in this study suggest that the implants and the subsequent calculations for the prescribed dose had been carried out with acceptable quality. It has been demonstrated by other authors that local recurrence in cancers of the mobile tongue and floor of mouth were significantly related to dose; an increase in local failure was seen when the implant dose was below 62.5 Gy.[8] Typical local control rates of radiotherapy for carcinoma of the tongue and buccal mucosa are in the region of 57% and 75% respectively.[9] Hence the overall local recurrence rate in our centre which was 46% appeared to be within acceptable limits.

The morbidity experienced by patients in this study demonstrated that this procedure was generally well tolerated despite its apparent invasiveness. The only serious complication encountered clinically was a retained needle when the implant was being removed from the tongue. In contrast to another study where necrosis (defined as soft tissue ulceration occurring or persisting longer than 3 months after implantation or osteonecrosis) was seen in 28% at 5 years for mobile tongue and 58% for floor of mouth,[8] late effects appeared to be insignificant in our study. This could be due to the relatively lower implant doses used, differences in techniques employed, incomplete follow-up as well as death occuring before the late effects became evident.

The figures for crude survival, disease free interval and morbidity have to be interpreted with caution as a proportion of the data were censored (excluded due to insufficient follow-up time before the end-point was reached). The main difficulty in defining disease free intervals lies in the fact that time to recurrence is not easy to measure as an end-point. Other limitations were the inability to measure the quality of life in the patients as well as under-reporting of the side effects which can be expected from the retrospective nature of the study.

CONCLUSION

Despite the limitations, this paper has demonstrated the usefulness and practicality of radioactive needle implants for head and neck cancers in the Malaysian setting. The importance of local tumour control in patients was demonstrated in both the curative as well as palliative settings. This treatment is cost-effective and can be recommended for patients with tumours that may otherwise entail extensive and mutilating surgery. In centres which have these radioactive needles, this treatment would be indicated in appropriately selected patients.

ACKNOWLEDGEMENT

The authors wish to thank the staff of the Records Office of the Institute of Radiotherapy and Oncology, Hospital Kuala Lumpur for manually retrieving the patients' records, the staff of the Identity Card Section of the Malaysian National Registration Department for information on patients' survival status, physicists for their technical support and the Director General of Health of Malaysia for permission to publish these data.

REFERENCES

1. Paterson R, Parker HM. A dosage system for gamma ray therapy. Brit J Radiol 1934;-7:592-612.
2. Paterson R, Parker HM. A dosage system for interstitial radium therapy. Brit J Radiol 1938; 252-313.
3. Meredith WJ. Radium dosage: the Manchester system. (2nd ed) Edinburgh: Livingstone, 1967.
4. ICRU (International Commission on Radiation Units and Measurements). Dose Specification for Reporting External Beam Therapy with Photons and Electrons, ICRU Report No. 29, ICRU: Bethesda, 1978
5. Duthie MB, Gupta NK, Pointon RCS. Head and neck. In: Pointon RCS, (ed). The radiotherapy of malignant disease. (2nd ed). London: Springler-Verlag. 1991: 154-9.
6. Delclos L. Interstitial irradiation techniques. In: Levitt SH, Tapley NduV., (eds). Technological basis of radiation therapy: practical clinical applications. Philadelphia: Lea & Febiger, 1984:55-84.
7. Pierquin B, Dutreix A, Paine CH, Chassagne D, Marinello G, Ash D. The Paris system in interstitial radiation therapy. Acta Radiologica Oncology 1978;17:33-47.
8. Mazeron JJ, Simon JM, Le Pechoux C et al. Effect of dose rate on local control and complications in definitive irradiation of T1-2 squamous cell carcinomas of mobile tongue and floor of mouth with interstitial iridium-192. Radiotherapy and Oncology 1991;21:39-47.
9. Henk JM. Cancer of the head and neck. In: Hope-Stone HF (ed). Radiotherapy in clinical practice. Cambridge: Butterworths, 1986: 93-123.

Message from

Prof.Dr. Kawee Tungsubutra

Editor-in-Chief, The Asean Journal of Radiology.

This is the second issue of the Asean Journal of Radiology for the third year which has been kindly supported by the educational grant from Bracco International.

We have been supported by many writers, both from Thailand and from the member countries.

In this issue we also have a paper from Australia, which is from a non-member country of ASEAN.

We welcome writers from all over the world so that it will be an international journal as we have originally aimed.

Thank you again for the writers and the supporters.

Kawee Tungsubutra.

Kawee Tungsubutra
May 1, 1997

In Touch with Tomorrow

TOSHIBA

GLOBAL IMAGING ▪ MEDICAL SYSTEMS

DESTINATION: A NEW CENTURY OF INNOVATION

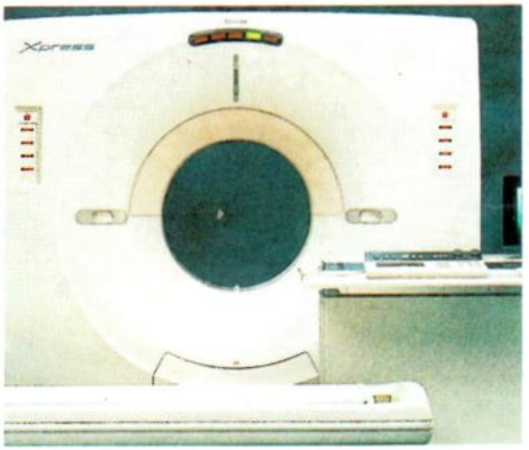

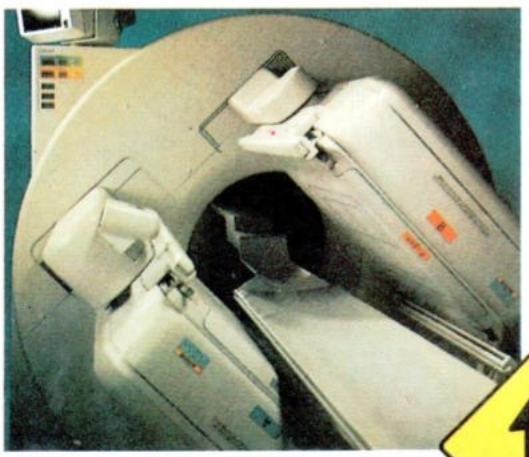

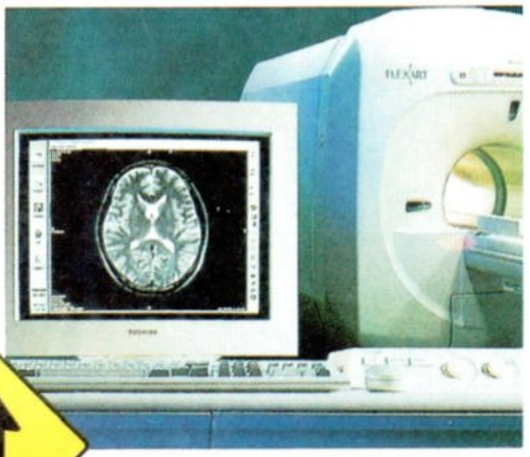

Because we listen carefully to our customers, Toshiba is always focused on providing the medical imaging products that can meet their clinical financial needs.

CMC BIOTECH CO.,LTD.

1433 Soi 3/3 Muban Town-in-Town, Ladphrao 94 Road, Bangkapi, Bangkok 10310
Tel. 530-4995-6, 559-3261-2, 559-3524-5 Fax: (662) 539-6903

Southern Branch 306 Prachayindee Road, Khorhong Haadyai Songkhla 90110 Tel. (074) 356259, Fax: (074) 364-004 Handphone 01-9359703 Pagephone 151, 152 call 341790

North Eastern Branch 301/155 Muban Khon Kaen Villa, Mittrapab Road, Amphur Muang, Khon Kaen 40000
Tel. (043) 246210, 244729 Handphone 01-9283082 Pagephone 151, 152 call 341787